FINAL PROJECT REPORT

Otto – The Wall Driving Platform

Cameron Venancio, Eric Mar, Kelvin Lei
California Polytechnic State University San Luis Obispo
Mechanical Engineering Senior Project
December 2013

STATEMENT OF DISCLAIMER

Since this project is a result of a class assignment, it has been graded and accepted as fulfillment of the course requirements. Acceptance does not imply technical accuracy or reliability. Any use of information in this report is done at the risk of the user. These risks may include catastrophic failure of the device or infringement of patent or copyright laws. California Polytechnic State University at San Luis Obispo and its staff cannot be held liable for any use or misuse of the project.

ACKNOWLEDGEMENTS

A very special thanks to Cody Brown and Skye Jenkins and the rest of Electroimpact for providing the resources and support to make this project possible.

And to our academic advisor Dr. Tom Mackin for his engineering expertise, passion and guidance in our project.

TABLE OF CONTENTS

Abstract ix

1 Introduction 1

1.1 Sponsor Needs and Background 1

1.2 Problem Definition 1

1.3 Design Requirements and Specifications 1

2 Background 2

2.1 International Climbing Machines (ICM) 2

2.2 Caterpillar Tread 3

3 Design Development 3

3.1 Concept Generation 3

3.1.1 Perforated Tread Design 4

3.1.2 Rail Slider 5

3.2 Initial Concept Selection and Testing 6

3.2.1 Concept Revision A – Perforated Tread Design 7

3.2.1 Perforated Tread Testing 9

3.3 Redesign Conceptualization and Analysis 12

3.3.1 Concept Revision B – Sliding Adhesion System 12

3.3.2 Small Scale Prototype Testing 15

3.3.3 Sliding Material Testing 17

4 Final Design 21

4.1 Adhesion Vacuum System 21

4.1.1 Venturi Pumps 21

4.1.2 Suction Cups 22

4.1.3 Normal Force Bias 25

4.1.4 Low Friction Sliding Material 26

4.1.5 Pneumatic Components 27

4.2 Drivetrain System 28
4.2.1 Drive Shaft & Coupler 28
4.2.2 Wheels & Hub 28
4.2.3 Chain & Sprocket 29
4.2.4 Bearings 30
4.3 Motor System 30
4.3.1 Motor Selection 30
4.3.2 Gearbox Selection 32
4.4 Chassis 33
4.4.1 Aluminum Extrusions & Fasteners 33
4.4.2 Suction Cup Mounting Brackets 34
4.4.3 Motor Mounting Plate & Brace 35
4.5 Operation Requirements 35
4.6 Safety Considerations 36
5 Manufacturing 37
5.1 Suction Cup Assembly 37
5.2 Chassis Construction 38
5.3 Drivetrain Components 39
6 Design Verification Testing 40
6.1 Suction Cup Tests 41
6.1.1 Surface Test 41
6.1.2 Suction Cup Force Test 41
6.1.3 Suction Cup Displacement Test 43
6.2 Driving Tests 45
6.2.1 Vertical Driving 46
6.2.2 Inverted Driving 47
6.2.3 System Troubleshooting 48
7 Cost Analysis 49

8 Improvements & Conclusion 51

9 References 52

Appendix A: Test Results 52

Appendix B: Detailed Part Drawings 56

Appendix C: Vendor Component Specifications and Data Sheets 66

Appendix D: Supporting Analysis and Calculations 75

Appendix E: Design Resources 82

LIST OF FIGURES

Figure 1. Electroimpact's current Flex Track system. 1
Figure 2. ICM's climbing robot, with central vacuum adhesion. 2
Figure 3. Caterpillar Tread design, with mechanical valve suction actuator. 3
Figure 4. CAD renders of the initial Perforated Tread design and other variations. 4
Figure 5. CAD render of Rail Slider design. 5
Figure 6. Rail Slider concept movement pattern. 6
Figure 7. CAD model of Concept Revision A – Perforated Tread Design. 7
Figure 8. Underside of custom vacuum platform, showing cup compartments and with PTFE screen. 8
Figure 9. The perforated tread design, with holes that allow for the vacuum force to contact the driving surface. 8
Figure 10. Drive system and perforated tread exploded assembly view. 9
Figure 11. Attempting to move the polycarbonate platform with a handle (Left), handle breaks off before platform moves (Right). 10
Figure 12. Perforated tread stretches a large amount as it is pulled against the suction cup and polycarbonate. 11
Figure 13. FBD and MAD showing the design for Otto accelerating on a vertical surface. 12
Figure 14. An example of common suction cup usage. 13
Figure 15. Initial Lego prototype, with four wheels and complicated gear system – did not work. 15
Figure 16. Small scale Lego prototype successfully driving on vertical and inverted orientations. 16
Figure 17. Small scale prototype rubber pad modified with dust for low friction. 17
Figure 18. All sample materials cut to size and labeled for testing. 18
Figure 19. Material test set up: pull-off force test and friction force test. 19
Figure 20. CAD model of the complete final design, Otto. 21
Figure 21. Visual representation of the internal mechanism of a venturi pump. 22
Figure 22. Close up view of the actual venturi pump used in the final assembly. 22
Figure 23. Top and bottom views of a nitrile 1.5 bellow suction cups. 23
Figure 24. Test setup used for preliminary tests of the 2.07" bellow suction cup. 24
Figure 25. The bellow suction cups are capable of staying adhered to the surface without having the wheels touch the surface. 25
Figure 26. Suction Cup assembly mounted onto the frame. 26
Figure 27. Bellow suction cups modified with PTFE sheets, adhered with 3M industrial strength adhesive. 27
Figure 28. Layout of pneumatic lines - all venturi pumps are attached for parallel performance. 27

Figure 29. AndyMark "HiGrip" thermoplastic polyurethane tread wheels. 29
Figure 30. The 1:1 driving ration sprocket and #35 medium grade chain. 29
Figure 31. FANUC βiS 0.5 AC servo motor. 31
Figure 32. CAD model of the initial custom gearbox design. 32
Figure 33. Thomson XTRUE Planetary Gearhead with a RediMount system attached (Left), with motor (right). 33
Figure 34. Otto's bare chassis, made of T-slotted aluminum extrusions. 34
Figure 35. Custom machined aluminum suction cup mounting brackets, 12 total. 34
Figure 36. Custom machined aluminum motor mounting plates. 35
Figure 37. The PLC and pendant used to control Otto, supplied by Electroimpact. 36
Figure 38. Part of the manufacturing process for Otto. 37
Figure 39. Close-up view of the T-shaped push connectors used in the suction cup assembly (Left), completed single suction cup sub-assembly (Right). 38
Figure 40. Aluminum extrusion assembly and reinforcement bracket attachment. 38
Figure 41. Aluminum plate attached to gearhead as primary drivetrain support (Left) and steel sheet metal bracket mounted as secondary support (Right). 39
Figure 42. Wheel, hubs, bearings, sprocket, bushings and lock collar sub-assembly. 40
Figure 43. Mounted wheel sub-assembly, connected to gearhead with spider coupler (Left), underside of Otto – showing the layout of the suction cup sub-assemblies (Right). 40
Figure 44. Test stand used for bellow cup tests - vacuum gauge (left) and pressure gauge (right). 42
Figure 45. Weights are added to the carry tray in order test bellow suction cup performances. 43
Figure 46. Bellow cup under linear displacement (Left), bellow cup under exponential displacement (Right). 44
Figure 47. CAD model of suction cup assembly and mounting bracket. 45
Figure 48. Otto proving its capabilities by carrying a load of 70 lb, for a total weight of 100 lb. 46
Figure 49. Otto performing all the driving maneuvers with a payload: 70 lb payload (Left), and a human payload of 160 lb (Right). 47
Figure 50. Venturi pumps, removed from their housing, are covered with residue from the air supply lines. 48
Figure 51. Maximum cup holding force vs. supplied inlet positive pressure. 52
Figure 52. Negative pressure generated by suction cup assembly vs. inlet positive pressure. 52
Figure 53. Bellow suction cup displacement test at 50 psig. 53
Figure 54. Bellow suction cup displacement test at 60 psig. 54
Figure 55. Bellow suction cup displacement test at 70 psig. 55
Figure 56. Side CAD view, showing basic important dimensions. 56

Figure 57. Top CAD view, showing basic important dimensions. 56
Figure 58. Front CAD view, showing basic important dimensions. 57
Figure 59. Piab Venturi Pump detailed drawings. 57
Figure 60. Von Mises stress analysis on the bracket. 78
Figure 61. Displacement analysis on the bracket. 78
Figure 62. Loads and fixtures of the drive shaft. 79
Figure 63. Von Mises stress analysis on the drive shaft. 80
Figure 64. Displacement analysis on the drive shaft. 80
Figure 65. Drive shaft SimulationXpress results. 81
Figure 66. Quality Function Deployment chart. 82

LIST OF TABLES

Table 1. Decision Matrix used to optimize initial concept designs. 7
Table 2. Material testing pull-off force and coefficient of friction results. 20
Table 3. Bill of Materials. 50
Table 4. Data collected from bellow suction cup displacement test at 50 psig. 53
Table 5. Data collected from bellow suction cup displacement test at 60 psig. 54
Table 6. Data collected from bellow suction cup displacement test at 70 psig. 55

ABSTRACT

Electroimpact is currently a world leader in the aerospace industry with state of the art aerospace tooling and automation design. One of their most successful machines, the Flex Track, is used to assemble airplane fuselages – drilling holes and installing rivets while traveling circumferentially around the fuselage on suctioned tracks. Currently, this track method is limited in travel, as the machine can only access locations where the tracks have been placed. For a Senior Project in the Mechanical Engineering department at California Polytechnic University San Luis Obispo, Electroimpact has expressed its interest in sponsoring a proof-of-concept prototype design for a robotic wall driving unit. Aimed at eventually replacing Electroimpact's suction track system, this wall driving unit is designed to meet all of the project specifications, while remaining within the allocated budget of $2500.

Otto, the wall driving unit, works on the principle of vacuum-adhesion, utilizing twelve suction cups on its underside to stick to vertical and horizontal surfaces as it drives. The bottom of each suction cup is fitted with a low friction, polytetraflouroethylene sheet, which is the main contact point with the driving surface. The low friction material allows the suction cups to slide along the surface it is traveling on, reducing the load on the drive motors and increasing the carrying efficiency of the system. The driving system onboard consists of two high torque AC motors attached to gear reduction units, and then to high traction rubber wheels. The vacuum and battery power, as well as the motor controller, will be attached to the driving platform via an umbilical cord connected to the ground.

Otto's final design is fully conceptualized, developed, built and tested in this report; with every component specified and analyzed, after many design iterations. Thorough calculations, analysis, and testing support the machine design and provide numerical justification for the parts/materials chosen. Test results, detailed drawings for custom parts, and supporting analysis are supplied in the Appendix.

1 INTRODUCTION

1.1 SPONSOR NEEDS AND BACKGROUND

The sponsor for this project is Electroimpact (Mukilteo, Washington), a company that specializes, among other automated processes, in automated aircraft fuselage and wing panel splicing. Their current process consists of a robotic system, called the Flex Track; which performs the drilling part of the splicing process. It does so by traveling along and around the body of an aircraft using a suction-mounted, track system. Electroimpact is sponsoring this senior project team to develop a mobile base prototype that is aimed at replacing their current track system. The mobile base must be capable of adhering to, and navigating, the entire external surface of the aircraft while carrying a substantial payload. Eliminating the suction mounted tracks would facilitate portability and simplicity while it would also reduce set-up times and the associated costs. The goal for this project is to develop a working proof-of-concept model of this track-less design.

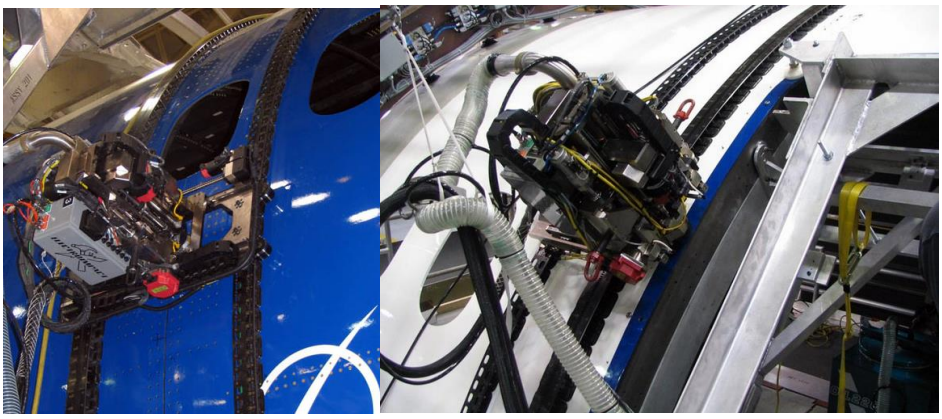

Figure 1. Electroimpact's current Flex Track system.

1.2 PROBLEM DEFINITION

The final design of the driving platform needs to be capable of traversing the entire circumference of a convex airplane fuselage, in two axes without the aforementioned tracks– that is, the robot will be able to move about the circumference, as well as along the length of the fuselage. The design needs be able to carry a reasonable payload while recognizing stability and safety as its two priorities during operation. The prototype will be designed to be attached to an umbilical cord for power, control, and air supply.

1.3 DESIGN REQUIREMENTS AND SPECIFICATIONS

The scope of this project is ultimately to produce a proof-of-concept model, as functionality is the reigning priority over traditional performance-based specifications. After the above-mentioned functionality

requirements are met, additional features such as air supply failure or leakage prevention, operating speed, ease of deployment and robotic control are some detailed parameters that will be considered during the analysis phase of the design. Some additional design requirements for this project are:

- Capable of carrying a load of 25 lb.
- Top speed of at least 3.5 MPH – average human walking speed.
- Acceleration of at least 8 ft/s^2.
- Overall design should not exceed the dimensional size of 30” x 30” x 12”.

2 BACKGROUND

Background research shows that stable wall driving systems are relatively un-explored, aside from small school projects with low budgets and no published analysis or data to support the manufacturability of these machines.

2.1 INTERNATIONAL CLIMBING MACHINES (ICM)

International Climbing Machines has developed a wall crawler that covers a wide variety of applications. This wall crawler can scale almost any surface, and utilizes a single central vacuum pump as its adhesion force. The new technology that ICM has created involves a rolling seal, or a seal for the vacuum chamber that moves while also maintaining the low pressure suction within the chamber. The driving mechanism treads are made of a malleable sponge-like material, allowing it to transverse small obstacles such as rivets, bumps and ridges, while still maintaining its vacuum seal and adhesion to the surface. These climbers are portable, easy to deploy, and have a pull off strength of over 200 pounds. This design works because of one central vacuum, making it prone to failing. It should be noted that ICM often includes a fail-safe rope attached to the top of the object/wall it is scaling. Also, the carrying capacity of this machine is unknown.

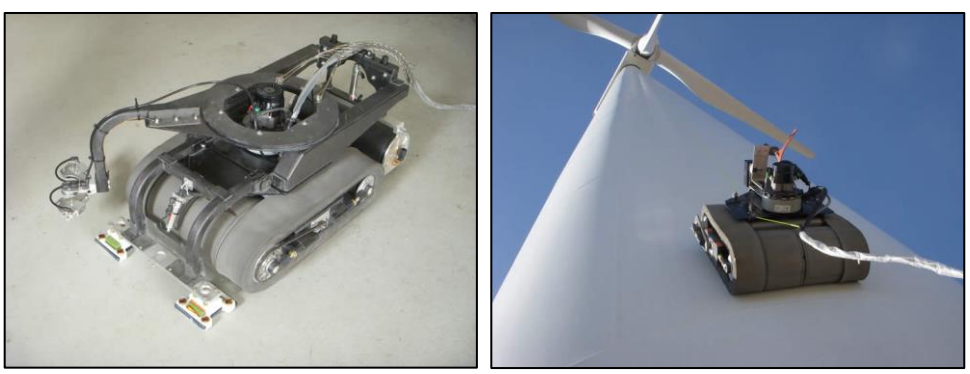

Figure 2. ICM’s climbing robot, with central vacuum adhesion.

2.2 CATERPILLAR TREAD

A research group at Seoul National University designed a vacuum caterpillar tread robot, as pictured in Figure 3. This design employs two vacuum caterpillar tread wheels, with a vacuum pump positioned in the middle of the robot. It utilizes 24 suction cups, 12 on each tread, with mechanical valves opening and closing vacuum air flow to each suction cup, along with a rotary joint in the middle of the tread to keep the pneumatic tubes from twisting. The unique aspect of this design resides in the suction tread system, which allows the robot to scale a vertical surface without slipping or falling off the wall, though turning does not seem plausible due to a slip condition. The timing of the suction cups on the treads relies on mechanical spring valves that are activated by a ball bearing on top of the valve. With the valves open, free flow positive vacuum suction is allowed to flow to the suction cups, and the suction is activated in order for the climber to stick to the wall.

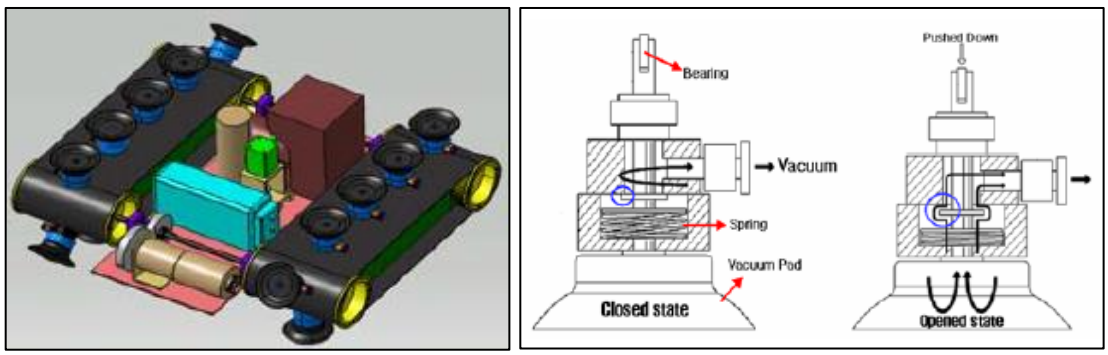

Figure 3. Caterpillar Tread design, with mechanical valve suction actuator.

3 DESIGN DEVELOPMENT

Design development consists of the initial concepts generated for this project, as well as the testing and procedures conducted to verify the feasibility of these concepts. Concept revisions and decisions made prior to the final design are outlined below.

3.1 CONCEPT GENERATION

The initial concept generation phase consisted of developing a simple idea of a working wall driving mechanism that could support its own weight and a small load, while traversing a working surface both vertically and horizontally. Two key drive mechanisms were conceptualized and modeled with mobility in the XY plane in mind.

3.1.1 PERFORATED TREAD DESIGN

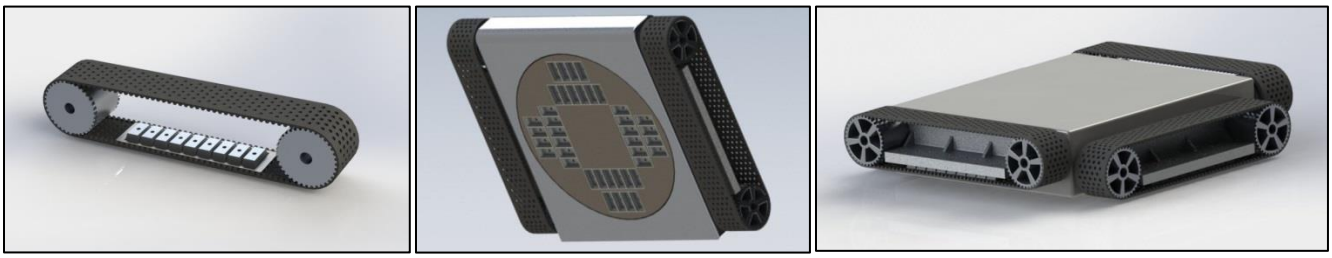

Figure 4. CAD renders of the initial Perforated Tread design and other variations.

One of the first ideas conceptualized was the Perforated Tread concept – which embeds a vacuum platform into the treads of a continuous track system. The track is made of rubber with a multitude of holes punched into it. When the holes pass between the vacuum plate and the contact surface, they allow for transfer of vacuum, which effectively applies suction force onto the working surface. The benefit of this method allows the tank-like system to turn as it would normally slide on the ground, but without shearing off. It provides the robot with the perpetual motion benefits of a continuous track, and solves the problem of breaking the seal of a suction cup when turning and sliding. This concept was thought to excel because of its simple nature – requiring only two driving wheels, and no need for a pneumatically controlled (dis)engagement system.

The static friction force between the continuous track and the working surface is what allows the robot to propel itself linearly. When turning, however, this static friction will have to be overcome in order effectively turn the platform via traditional tank skid-steering. During this turning sequence, kinetic friction will be responsible for holding the vehicle to the surface, and maintaining its general position, yet allowing it to slip for turning.

Two variations of the perforated tread design were also developed, as a pre-caution in case the robot experienced a hard time with turning and changing direction. The Perforated Tread design can be modified into a Dual Tread (basic design), Four Tread and Rotating Tread design.

FOUR TREAD

The Four Tread design is an alternative solution to the Dual Tread design. This design would have been considered if the Dual Tread design proved to be incapable of tread-steering while adhering to a vertical wall. The Four Tread design differs from the Dual Tread design in that it has two pairs of treads rather than just one. By having two pairs of treads, the locomotion system is capable of traveling in two orthogonal directions, eliminating the need for turning altogether. This allows the system to traverse effectively on an XY-plane.

ROTATING TREAD

The Rotating Tread design is another alternative solution and is based on the Dual Tread design. The key difference between this design and the Dual Tread design is the addition of the center column and its underside vacuum cups, which will be powered by venturi pumps. This design is developed to provide the locomotion system with an effective method for steering that is different from the Dual Tread and Four Tread. Unlike the Dual Tread design which steers by the inefficient method of slippage, the steering mechanism of the Rotating Tread operates by activating the center vacuums and rotating the rectangular base about the center column.

This design will be capable of traveling in the XY-plane of a vertical wall and any sections of an airplane fuselage with ease and at any angle because of the center column. Also, the addition of the center column and its vacuums allows the system to be a lot more stable than the Dual Tread design when in the stationary position.

3.1.2 Rail Slider

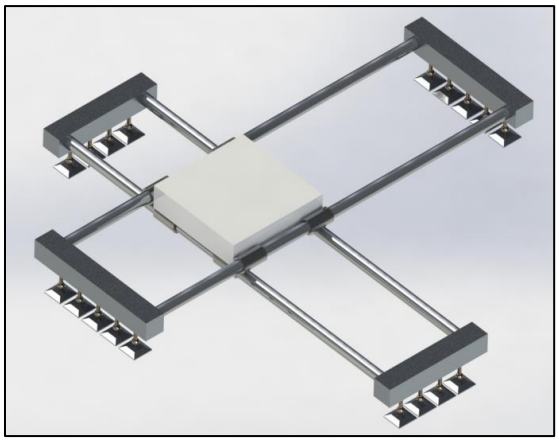

Figure 5. CAD render of Rail Slider design.

The Rail Slider design relies on rails that the machine “slides” on, with motion provided by threads, gears or pneumatics. The main concept is that the robot maintains suction in one axis while the rails in the other axis slide. Working in conjunction with each other, the rails allow for a quick and easy change of direction on the X-Y axes, though it is limited to movements only along these axes (no turning).

For example, moving in the horizontal X-axis *(note that yellow represents suction engaged)*:

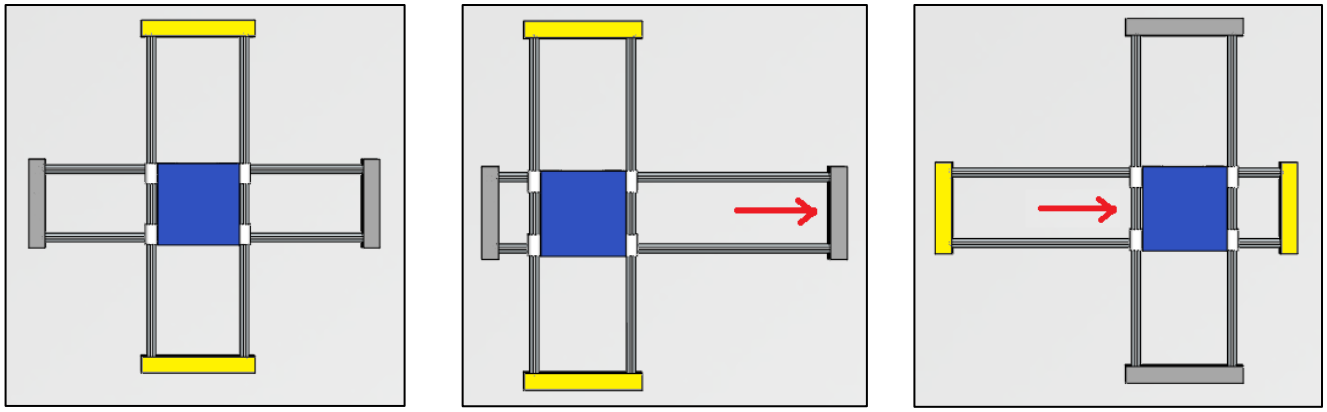

[1] [2] [3]

Figure 6. Rail Slider concept movement pattern.

[1] The suction in the vertical Y-axis engage, keeping the robot stable and in place. [2] The rails in the X-axis slide past the robot. [3] The suction in the X-axis engage and the suction in the Y-axis disengage, as the robot pulls itself along the X-axis, creating a displacement. This process is repeated in an “inch-worm” effect, until the robot reaches its destination. Changing directions requires similar movement, but instead, the robot would switch to the other axis and push and pull itself along this axis instead.

Suction cups are attached at the ends of each rail element. In order to account for the curvature of a fuselage, the suction cups would be mounted on pivot joints that allow the Rail Slider to adjust for uneven surfaces while keeping the body straight, relative to the surface.

The Rail Slider has the potential to be a very stable machine, while also being very accurate in finding its exact destination; as it cannot alter its course with different angles, given its XY-axis limitations. For maximum stationary stability, all suction from both rails would engage with the contact surface, creating a large coverage area for the robot and machine stability. Though its movement may be methodical and its maneuverability a slight issue, the stability and reliability of this machine are its selling points, especially in an application that does not require speed or flexibility as a main specification.

3.2 Initial Concept Selection and Testing

Initially, a combination of a Decision Matrix and a QFD, as seen in Table 1 and Appendix E, were used to optimize the results and select the best candidate for the project requirements. Design considerations included manufacturability, speed, maneuverability, scalability, load capacity, and stability, with each concept being scored relative to the other designs on a scale from 1-5.

All design aspects considered, the Perforated Dual Tread system was thought to have the best maneuverability, and perceived to be the most feasible to design, build, and implement. Conceptually, it was the most innovative and ground-breaking design, as it offered the ability to turn and drive like a standard tracked vehicle, while providing intuitive feel for the user.

Table 1. Decision Matrix used to optimize initial concept designs.

Concept	Type of Score	Design Requirements						Total Weighted Score
		Manufacturing [4]	Speed [2]	Manuverablility [2]	Scalability [4]	Load Capacity [4]	Stability [4]	
Four Tread	Raw	2	4	3.5	3	4	3.5	
	Weighted	8	8	7	12	16	14	**65**
Dual Tread	Raw	3	4	5	3	4	3	
	Weighted	12	8	10	12	16	12	**70**
Rotating Tread	Raw	2	4	3.5	3	4	4	
	Weighted	8	8	7	12	16	16	**67**
Rail Slider	Raw	4	2	3.5	4	2.5	4	
	Weighted	16	4	7	16	10	16	**69**

3.2.1 Concept Revision A – Perforated Tread Design

The initial design chosen for this project was the Perforated Dual Tread system. This unit was designed around a rubber tread with perforated holes and the corresponding vacuum platform powered by venturi pumps. The tread would act as a gasket for the vacuum platform, where the holes channel the vacuum to the driving surface. The driving unit would run on two high powered AC motors, allowing for steering and speed control while it scaled vertical walls and ceilings in any orientation.

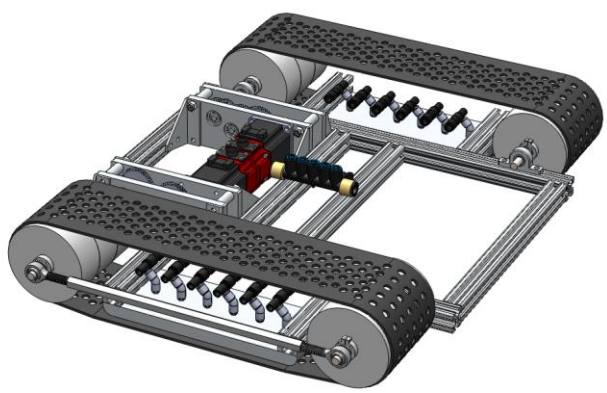

Figure 7. CAD model of Concept Revision A – Perforated Tread Design.

Adhesion System

The main component of the system relied on the suction power that allows the driving unit to adhere to the wall, and maintain adhesion while traversing on a vertical or inverted surface. The suction power for adhesion is supplied by individual venturi pumps.

This design would require a custom machined aluminum vacuum plate, which would house multiple suction cup cavities. Venturi pumps would be attached on top of the plate and would create vacuum pressure in the cavity sections. This custom plate would be designed to have the tread slide underneath it, as this action transferred the vacuum pressure to the driving surface through the holes in the tread. In order to avoid the deformation of the tread into the suction cup's cavity, a perforated screen is attached to the underside of the suction plate. This plate consists of a large array of small slots milled into a sheet of PTFE in order to reduce the friction between the tread and the suction plate.

Figure 8. Underside of custom vacuum platform, showing cup compartments and with PTFE screen.

PERFORATED TREAD

The perforated tread was designed to be the mechanical interface between the wall and the driving unit. Small holes in the tread act as mini 'suction cups', providing a sealed area in which the pressure can be lowered. The tread was chosen to be made of nitrile rubber, so that it would be durable yet stretch when it would need to. With a continuous track of perforated holes, the vacuum plate will never lose contact with the driving surface, as the hole-pattern allows for continuous driving. In order for the robot to move, the tread must slide underneath the vacuum plate, pulled by the high torque motors and large wheels.

In order to maintain the position of the driving unit securely on a vertical surface, the static friction between the driving surface and tread must be high enough to prevent the robot from sliding. The friction force generated by the tread on the wall will be an important force to help maintain position while driving and while at a standstill. Conversely, the friction on the inside of the belt (in contact with the vacuum plate) will need to be low, to allow the tread to slide easily past the vacuum platform when driving.

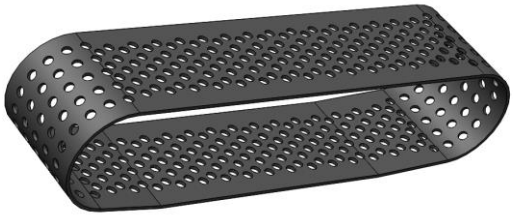

Figure 9. The perforated tread design, with holes that allow for the vacuum force to contact the driving surface.

DRIVE SYSTEM

The drive system for the wall driving robot will consist of four custom wheels, with the tread looped around two of them per side of the robot. Each wheel will have its own shaft and bearings, allowing for speed differences on each side of the climber. One idler wheel and one drive wheel will be located on each side of the driving unit. The drive wheels were positioned at the rear of the drive unit, in order to pull the tread from underneath the vacuum plate when driving forward as opposed to pulling the tread from the top side. The front of the robot will have the two idler wheels, which create tension in the belt and allow the drive motors to effectively move the system.

The stepped drive shaft will be connected to the body with two bearings, one on the wheel end, and one attached to the body of the robot. The bearing on the wheel end will be attached to a push rod. The push rod helps to carry the load created by the belt tension and minimize the amount of moment applied onto the inner bearings. The pillow block bearings chosen were low cost, self-aligning medium load bearings that would theoretically withstand the projected loads and maintain a low profile on the chassis. They are pillow base mount ball bearings, and they will be press fit onto the shafts, up to the first step.

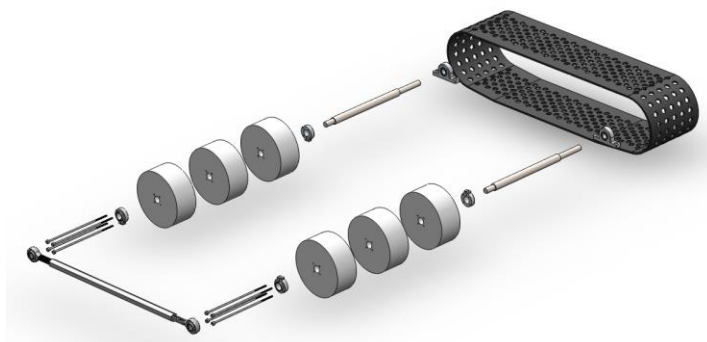

Figure 10. Drive system and perforated tread exploded assembly view.

CHASSIS

The body of the robot will be structured upon the vacuum platforms, as this is the component with the most structural dependence. Built around the vacuums, the body of the driving unit will attach to a frame connecting the vacuum plates together. Here, the bearings, drive shafts, motors, and pneumatics will attach to the body frame. Lightweight aluminum T-slotted frames were chosen to make up the majority of the Perforated Tread design's structural body.

3.2.1 PERFORATED TREAD TESTING

A series of tests with the proposed rubber tread material was performed to validate the engineering intuitions assumed in the mechanical operation of the tread motions. In these tests, the analysis was primarily focused on

the performance of the rubber on different driving surfaces as well as the performance associated with sliding against an intermediate material of polycarbonate, which was used to simulate the vacuum platform. These tests helped to demonstrate the operation of the tread.

In these tests, a 4” x 12” x ⅛” nitrile butadiene rubber (NBR) tread material perforated with ⅜” holes spaced ⅓” apart was used, along with EI’s suction cup, EI’s venturi pump and a 4” x 4”- $^{1}/_{10}$” thick polycarbonate platform with a 3” x 3½” square cut out. The polycarbonate platform was used because it was inexpensive, required minimal machining work, and was assumed to have similar friction characteristics as aluminum.

The first test performed on the tread was to simulate the tread being pulled from underneath the vacuum platform by the wheels. The perforated tread was placed on a driving surface, on top of the tread was the polycarbonate platform and on top of that was the suction cup. The suction cup was attached with a venturi pump and then to a compressed air supply (100 psig), which generated suction through the holes in the tread. The tread was held in place as the polycarbonate and suction cup were attempted to be pulled along the tread. This simulated the driving action of the tread system, and helped with analyzing the sliding friction between the custom vacuum platform and the perforated tread, see Figure 11.

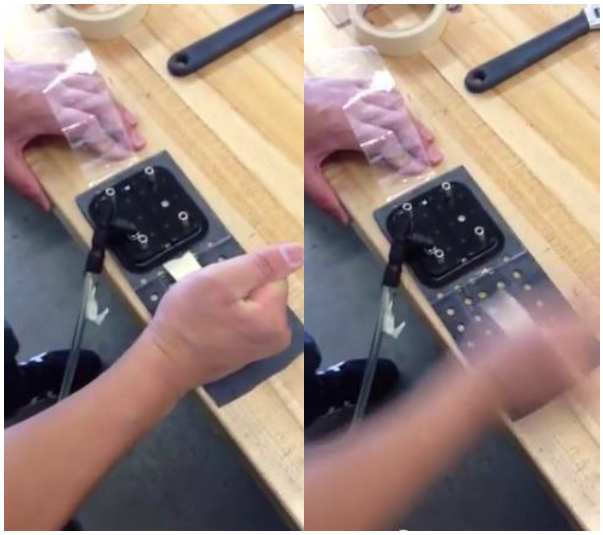

Figure 11. Attempting to move the polycarbonate platform with a handle (Left), handle breaks off before platform moves (Right).

As a result of this first test, it was shown that the vacuum platform had a very difficult time sliding against the perforated tread. Due to the high normal force of the suction cup with vacuum adhesion, the polycarbonate platform required a large lateral force before movement was achieved, if at all. The high friction characteristics of the NBR also attributed to the difficulty in sliding, which could potentially be solved by using another intermediate low friction material in between the tread and the custom platform. This test also revealed that

the friction between the tread and the driving surface was less than the friction between the custom platform and the tread. A similar test was performed with the same suction load, but this time without holding the tread stationary to the driving surface. When the polycarbonate platform was pulled, it maintained its position on the tread, but the tread broke its static friction from the driving surface very easily. Because the entire test system moved easily along the driving surface while still maintaining strong adhesion, it showed that utilization of the NBR's sliding performance could potentially be an alternate to the tread concept.

Another unanticipated consequence of these tests showed that the tread material elongated much more than expected, even under relatively small loads. After seeing the results from the test that revealed the relative ease of sliding the tread against the driving surface, another test was performed - this time the tread itself was pulled. Surprisingly, the tread stretched a large amount before breaking the static friction force - somewhere near 20% elongation, which is very high for this application, see Figure 12. Looking forward, this stretch would result in drastically changing belt lengths, under varied loading. For example, when there is high tension in the belt during turning, the material would stretch, and some tension force would be lost. Potential remedies for this problem may involve a composite tread material or a dynamic belt tensioning device, which would add complicated subsystems and expensive components.

Figure 12. Perforated tread stretches a large amount as it is pulled against the suction cup and polycarbonate.

Another effect that was noticed during testing was the relative ease of dislocating the vacuum platform from the tread. If any torque, twisting or peeling force was placed on the perforated tread, the vacuum platform and suction tended to lose suction easily, and dislodge from the tread and driving surface simultaneously. Because the platform is a rigid plate and does not allow for flexion, a slight peel-off of the tread produces catastrophic results. If one edge or side of the platform is lifted, it automatically loses its seal with the surface. This is because

the rigidity of the material instantly removes the entire platform from the surface, as air leakages rush in and equalize the vacuum pressure created by the seal. There is no forgiveness in the rigid plate, as any small leakage can result in the removal of the entire plate from the tread.

3.3 Redesign Conceptualization and Analysis

Due to the complications and issues involved with the perforated tread model as discussed in *Section 3.2.2 Perforated Tread Testing*, a decision was made to pursue a redesign of the project. The redesigned system, called Otto, no longer utilizes a perforated tread drive system. Instead, Otto is based on a sliding suction cup mechanism, as seen in the diagrams of Figure 13. Some of the benefits of pursuing this redesign include improvements in the following areas: reduced number of components, unrestricted suction placement, and improved skid steering performance.

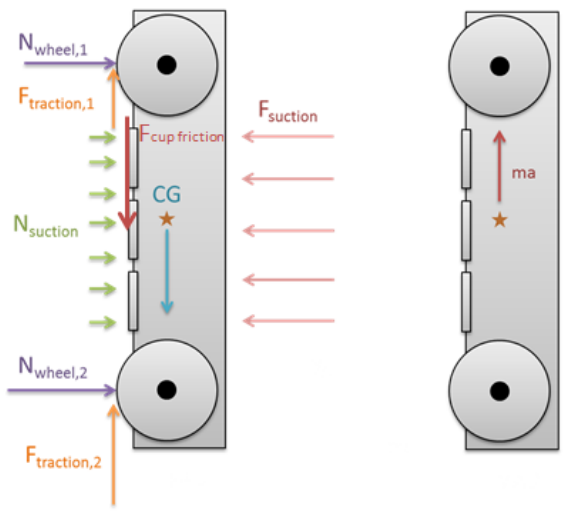

Figure 13. FBD and MAD showing the design for Otto accelerating on a vertical surface.

3.3.1 Concept Revision B – Sliding Adhesion System

Redesigning the tread system to a sliding system means that there is no longer a need for a perforated belt tread, a belt tread tensioner nor the enlarged drive pulleys used for driving the belt. This reduction in components helps to remove approximately 20% of the system's overall weight. It also simplifies the adhesion and drive system, as there is no longer the need to design and develop a complicated subsystem that combined both aspects into one. With the new design, the drive system and adhesion system are separate, making their individual design more concrete and specific. The placement of the suction sources is also no longer constrained to a specific location and there is no longer a restriction on how many suction sources can be used with the new design.

The philosophy behind the design of Otto is to have its adhesion assembly slide along the driving surface while still how maintaining a strong and reliable adhesion force. From there, the adhesion forces will cause reactive normal forces to be applied about the suction cup assembly and most importantly, the drive wheels. Adjustments of how the normal force is to be distributed between these two components are tuned to maximize the traction forces on the wheels while minimizing the frictional forces associated with the sliding suction assembly. The value of this adjustment is termed as the Normal Force Bias (NFB). In contrast to common usages, such as in Figure 14, the suction assembly will not be directly responsible for keeping the system adhered to its drive surfaces. Instead, the drive wheels and motors are the main components which operate to maintain Otto's position on any surface. For example, when the system needs to remain stationary on a vertical surface, the motors will apply a constant torque output to the drive wheels, which prevents any rotational movement by the wheels and keeps the system statically adhered - assuming that the wheels do not slip on the driving surface. For these reasons, the normal forces and frictional forces associated with the drive wheels are very critical, along with the torque outputs delivered by the motors and drive system.

Figure 14. An example of common suction cup usage.

Analysis of the overall system was performed with Engineering Equation Solver (EES), as shown in Appendix D. The analysis primarily helped with determining the normal forces about the wheels and suction cups, an appropriate gearbox ratio, and the safety factors associated with the system. Only one of the drive orientations was analyzed with EES: straight vertical climb along a flat surface. This orientation was chosen because it is the most strenuous for the motors and it relied most heavily on the normal and traction forces on the wheel. In addition, the safety factors of the overall drive system are at its lowest in the vertical climb. The analysis starts by having assumed values for the system's total suction force and its normal force bias (NFB) constant. The assumed frictional forces which are associated with the system are the kinetic friction between the suctions cups and the driving surface (0.1) and the static friction between the wheels and the driving surface (0.95). From

there, the necessary traction forces associated with constant velocity and accelerated driving are determined - max acceleration used in the analysis was 8 ft/s^2 or approximately $^1/_4$ g's. Adjustments to the values of the total suction force and the NFB are then made to minimize the "necessary traction forces" on the wheels (helps to minimize the torque demands from the motor) and to maximize the "possible traction forces" on the wheels (increases safety factor based on wheel slippage).

The second portion of the analysis involves determining the torque loads required by the motor, under available gearbox ratios. This portion also validates the decision of using the FANUC AC servo motors provided by Electroimpact. These AC motors have a normal operating torque of 0.5 N·m, a max intermittent torque output of 2.5 N·m and a top motor speed of 6000 rpm – see Appendix C for the FANUC FANUC βiS 0.5 motor datasheet. The normal operating torque was analyzed for constant velocity drive and the intermittent torque was analyzed for linear acceleration and skid steer maneuvers. Using these values, a gear reduction ratio of 20:1 was determined by analysis as the optimal reduction value. This gear ratio allows for the system to have a constant velocity drive of approximately 5.9 ft/s or 3.5 MPH (average human walking speed) along a vertical smooth surface while carrying a 25 lb load, for a total system weight of about 55 lb. Acceleration with this gear reduction ratio meets the requirement of a minimal acceleration value of 8 ft/s^2 as well.

The two main safety factors concerned with the design are the slippage of the wheels and the slippage of the motor. Assuming the NFB to be 0.75 (75% of the total suction forces is converted into reactive normal forces seen in the wheels) and the total suction force to be 300 lb, the safety factor for wheel slippage is approximately 3.2. The safety factor of the motor is approximately 1.43 - this value is determined by comparing the "normal motor torque output" with the "necessary drive torque" for constant velocity drive. Therefore, the bottleneck components of the design in the vertical climb orientation are the AC motors and drivetrain. One solution for increasing the safety factor for motor slippage is to increase the gear-reduction ratio of 20:1 to a larger reduction ratio. This option was considered but was not chosen because it would have lowered the system's top speed to less than the desired value of 3.5 MPH. Also, a larger reduction ratio creates a risk in overheating the motors because it would demand the motors to operate at speeds that are close to its max range of 6000 rpm. In contrast, when the system is under acceleration, the safety factor of the motor is increased from 1.43 to 5.9, which is a sufficient amount of a torque for our application.

The inverted driving orientation was not considered in the analysis because it is less critical than the vertical driving orientation - due to its lower risk of failure. During a vertical climb, factors that can contribute to failure include wheel slippage, insufficient motor torque and disengagement of the suction cups or wheels. In comparison, the only factor which can cause a failure in the inverted orientation is if the suction cups fail. For example, in the inverted orientation, if the wheels or motor slip, Otto will still stay adhered statically in its position because of the suction cups' adhesion forces - the same cannot be said about the vertical climb. In

addition, the torque necessary for constant velocity driving and acceleration in the inverted orientation is significantly less than the vertical climb because the motors and drivetrain do not work against gravity.

3.3.2 Small Scale Prototype Testing

After initiation of the redesign phase, a miniature prototype was constructed in order to reinforce that the concept of a sliding suction cup was a possible solution to this project. The prototype was created solely to prove that the concept could work at a larger scale, and that some early troubleshooting problems could be solved early on with this model. Also, similar forces and stress locations were analyzed on the prototype, though at a smaller scale.

The small scale prototype chassis was constructed mainly out of Lego Technics because of their ease-of-use, complex modularity, and scale factor. Some screws and hot glue were used as added fastening strength, as well as some modified Lego Technic pieces. The Lego Technics and hot glue allowed for many variations to be tried and tested, before finally settling on a design that worked, see Figure 15. Attached to the Lego Technic chassis was one miniature DC motor, which was hot glued to the side, and connected to a single drive wheel via Lego gears. The DC motor was supplied with 7.5 V and 0.8 A and provided the necessary torque and speed to drive the prototype. Also attached to the chassis via four screws was one low-profile suction cup and venturi pump provided by Electroimpact. This single suction cup was placed on top of a $^{1}/_{16}$" thick rubber pad with a square hole in the middle, which acted as the sliding material for the prototype, see Figure 17. The single low-profile suction cup, when connected to the venturi pump and compressed air, provided more than enough suction force to adhere the light-weight prototype to the testing surface. The design of the prototype featured one rear drive wheel, in order to simplify the mechanism and limit the number of Lego parts and gears used. Initially, a design with two rear drive wheels was built, but the stiffness of the plastic Lego gears were not as reliable under load as was originally thought. By limiting the number of gears in the prototype, the drive train meshed tightly and had more success driving smoothly.

Figure 15. Initial Lego prototype, with four wheels and complicated gear system – did not work.

There were many important discoveries that were learned just from building and running the Lego prototype alone. First is that the sliding suction adhesion system was successful in driving up a wall and on an inverted upside-down surface, as shown in Figure 16. Designing the prototype to be successful was an accomplishment in itself - proving that the redesigned sliding suction system was a very feasible solution to the wall driving robot project, as well as potentially scalable. Second, it was discovered that low-profile, shallow suction cups did not work well with the wall driving robot. The shallow lip of the suction cup allowed for very limited adjustability when attempting to relieve some of the normal force from the suction cup and transfer it to the wheels. When fully compressed, the stoppers inside the suction cup would contact the driving surface, creating more friction and making it more difficult to drive. Ideally, the suction cup should only be touching the sliding rubber pad with the lip edge, and not be fully compressed so that the stoppers touch the driving surface. Here, the height of the suction cup needed to be adjusted relative to the chassis so the wheels would prevent the suction cup stoppers from reaching the driving surface. The travel of the lip, or the suction cup's height adjustability when attached to the surface was small and difficult to work with. When designing a larger scale model, a suction cup with a larger lip was chosen because it offered more room for adjusting cup height.

Figure 16. Small scale Lego prototype successfully driving on vertical and inverted orientations.

Another key design consideration learned from the prototype was the importance of a rigid chassis. The plastic Lego Technic parts were not very rigid under any sort of load, and the structural integrity of the body was compromised once the suction cup adhered to the driving surface, bending the Lego pieces and not transferring the normal force to the wheels as intended. Due to the lack of rigidity in the Lego pieces, the plastic gears would often un-mesh themselves and grind endlessly. Though this problem was solved with new rigid materials for the large scale prototype (aluminum extrusions), to fix this problem on the Lego prototype, many reinforcements and hot glue were used to stabilize the chassis and limit the deformation under load. This was an important factor to consider because the normal force from the suction cups was being transferred to the chassis frame rather than the wheels, which made driving very difficult at first.

Continuing along the lines of transferring the normal force to the wheels, it was also important to note that the Lego Technic wheels had to be modified to be able to withstand the increased normal force from the suction cup. The wheels are made to be very deformable, and offer no resistance to any load placed on them. As a solution, tape was wrapped around the inside hub of the wheel, in order to make the wheels the wheel thicker and firmer. The firmer wheels did not deform under load, which was a key component that was included in Otto's design - firm yet high friction driving wheels.

The final important design consideration was the effectiveness of the $^{1}/_{16}$" thick rubber sliding pad. The rubber used was not a low-friction material, and offered unwanted resistance to the prototype when driving up a wall. During the testing, the rubber pad was modified by adding dust to the contact surface of the rubber in order to reduce sliding friction, see Figure 17. Also, the thickness allowed too much compression in the material, creating problems with the fickle height adjustments that were already meticulous to begin with. A thinner and lower friction material was implemented into the design of Otto, as building the Lego prototype helped identify this key design factor.

Figure 17. Small scale prototype rubber pad modified with dust for low friction.

3.3.3 Sliding Material Testing

In order to determine the best option for the intermediate sliding material in between the suction cup and the driving surface, research was conducted to identify potential materials. After the chosen materials were ordered, tests were performed to analyze the sealing properties and coefficient of kinetic friction for each material option.

Many different materials were researched for the series of tests, with the main characteristics of the material needing to be: slightly deformable/malleable for pneumatic sealing, low friction for sliding, and relatively thin

for low profile geometry. Overall, there were nine material samples that were chosen to be tested: $^{1}/_{16}$" Polyvinyl Chloride (PVC), $^{1}/_{16}$" Delrin, $^{1}/_{16}$" Polyethylene (PE), $^{1}/_{16}$" Polycarbonate, $^{1}/_{16}$" Polyurethane, $^{1}/_{64}$" Polytetraflouroethylene (PTFE), $^{1}/_{10}$" PVC cutting mat, ⅛" Nitrile Butadiene Rubber (NBR), and a $^{1}/_{16}$" Unknown Rubber.

Figure 18. All sample materials cut to size and labeled for testing.

The coefficient of friction tests performed on each material was conducted using EI's custom suction cup, a venturi pump, compressed air, and a spring tension gauge. The spring tension gauge had a maximum reading of 15 lb and had a resolution of 1 lb, which gives an uncertainty of about ±0.5 lb. There were two steps to determining the coefficient of friction of each material, the first was to measure the sealing properties of each material by a normal pull-off force test, and then to measure the force required to laterally slide the material while under suction. The first step was set up by cutting each material to a square with a square hole so that the material only contacted the outer edge of EI's square suction cup. Next, the material was placed between a tabletop surface and the suction cup venturi assembly; a laminate tabletop was chosen to roughly represent the laminate texture of an aircraft's exterior surface. As the venturi assembly was supplied with 33 psig of compressed air, the suction cup fully engaged onto the test material and a spring tension gauge was attached to the top of the suction cup and pulled upward in the normal direction, as shown in Figure 19. With the measured force slowly incrementing, the measurement on the tension gauge right before the suction cup failed was recorded in lbs. For each material, three readings were taken, and averaged. Right away, this initial test separated certain materials that had sealing problems from those that excelled, as there were large discrepancies in adhesion strength, as seen in Table 2. As expected, some of the stiffer, more rigid materials disengaged from the surface very easily, as leakages appeared often and resulted in weak sealing properties. Some materials such as Delrin and PVC were ruled incapable right away, as they failed to seal the vacuum

pressure from the start. The most outstanding materials in this first test were ⅛" NBR, $^{1}/_{16}$" Unknown Rubber, PTFE, Polyurethane and Polycarbonate - they all recorded an average pull-off force larger than 10 lb.

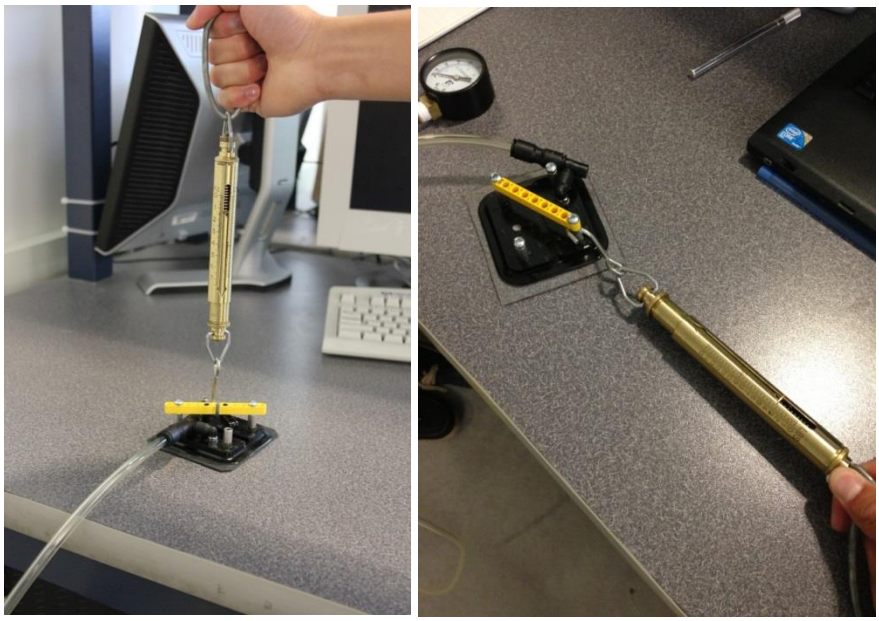

Figure 19. Material test set up: pull-off force test and friction force test.

The second part of the material test consisted of a similar set up to the first step, with each material placed on a tabletop surface and the suction assembly adhered on top. Instead of the tension gauge being attached to the top of the suction cup, the gauge was attached parallel to the table, so that the force would pull the material and suction cup laterally, measuring the static and kinetic friction force. For each material, the static friction force was measured by slowing incrementing the force of the gauge against the stationary suction cup until the moment right before the suction cup starts to move. Here the static friction force is keeping the suction cup stationary until the lateral force becomes too large, and the static friction force is broken. Each material was tested 3-4 times and the values were averaged. To measure the kinetic friction force, each material was pulled with the tension gauge until the static friction was broken, and then continually pulled by hand with a constant velocity. After the static friction is broken and the tension gauge "recoils" to the lower kinetic friction force equilibrium state, the value of the constant force is taken and averaged with 3-4 other readings on the same material. The coefficient of static and kinetic friction was determined by dividing the average respective friction force by that material's average normal pull-off force. The coefficient of friction equation outlines this effect: $\mu = \frac{F}{N}$, where is the μ coefficient of friction, F is the friction force and N is the normal force. As seen in Table 2, the material that had the best performance was by far the PTFE sheet. It had one of the strongest adhesion forces, while also being the easiest to slide due to its low coefficient of friction (approx. 0.1). Other materials excelled in one aspect, but failed to excel in the other tests, such as NBR, which had the strongest sealing

capabilities but also maintained high, unwanted friction characteristics. Another important result to note is that PTFE had static and kinetic coefficients of friction that were nearly identical, which is important for start-then-stop movements.

Table 2. Material testing pull-off force and coefficient of friction results.

Material	Pull-off force (lb)	Sliding Force - Static (lb)	Sliding Force - Kinetic (lb)	CoF (static)	CoF (kinetic)
NBR (1/8")	11.25	6.5	6.75	0.65	0.52
	11.25	7.5	5.5		
	11.5	8	5.5		
			6.5		
	avg: 11.33	avg: 7.33	avg: 6.06		
Unknown rubber (1/16")	12	9	7.5	0.75	0.69
	11.75	8.5	8		
	11.75	8.5	9		
		9.5	9		
	avg: 11.83	avg: 8.88	avg: 8.38		
PTFE (1/64")	10.75	2	1.25	**0.15**	**0.10**
	11.25	1.5	1.25		
	11.5	1.5	1		
	avg: 11.17	avg: 1.67	avg: 1.17		
Delrin (1/16") *	3	1.25	1	0.42	0.33
Polyethelene (1/16") *	2.5	1	1	0.40	0.40
Polycarbonate (1/16")	10	3.75	3	0.36	0.30
	10	3.5	3		
	avg: 10.00	avg: 3.625	avg: 3.00		
Polyurethane (1/16") *	16.5	5.5	5	0.33	0.30
	16.5	Inconsistent			
	avg: 16.5				
PVC (1/16") *	0.5	0.5	0.5	1	1
Cutting mat (1/10") *	2	1	0.75	0.5	0.375

**Denotes that full testing was not conducted on these materials due to their inability to create an effective vacuum seal.*

4 FINAL DESIGN

This section highlights the major components which make up Otto, the wall-driving platform. Details about the engineering decisions and analysis which went into selecting these components will be addressed along with their functions and operational limits. Otto weighs approximately 30 lb and its dimensions are approximately 23”L x 22”W x 6”H.

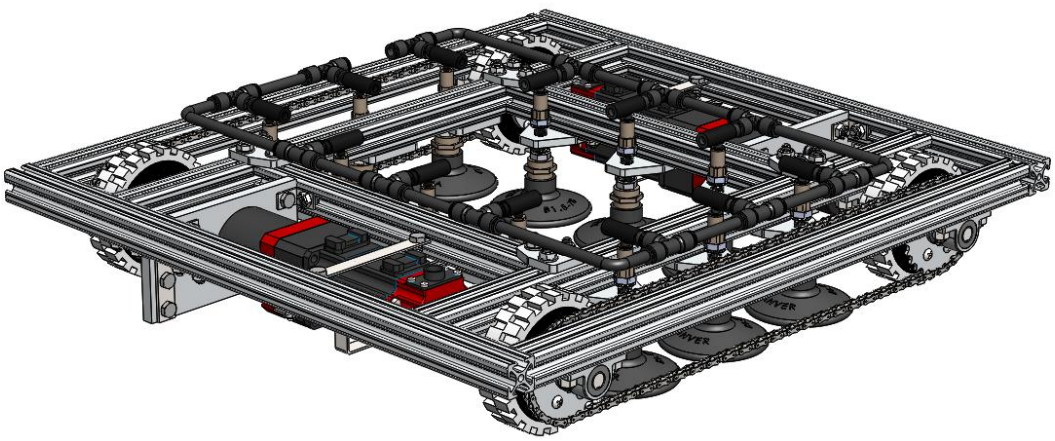

Figure 20. CAD model of the complete final design, Otto.

4.1 ADHESION VACUUM SYSTEM

4.1.1 VENTURI PUMPS

Otto utilizes a suction mechanism to adhere to the wall and maintain adhesion while traversing on a vertical or inverted surface. Venturi pumps were chosen as the ideal vacuum generators because they are currently being used by Electroimpact’s Flex Track rail system, and are easily assembled and fitted for this application.

Venturi pumps are aptly named, because they make use of the Venturi Effect, derived from the Bernoulli Principle. When positively pressured air is forced through a constriction, as in a nozzle, its velocity must increase to satisfy the principle of continuity. Furthermore, in accordance with conservation of energy, this increase in kinetic energy must be balanced by a decrease in pressure, see Figure 21 for a visual representation. Thus, by supplying a flow of positive-pressure flowing air, a negative pressure can be attained.

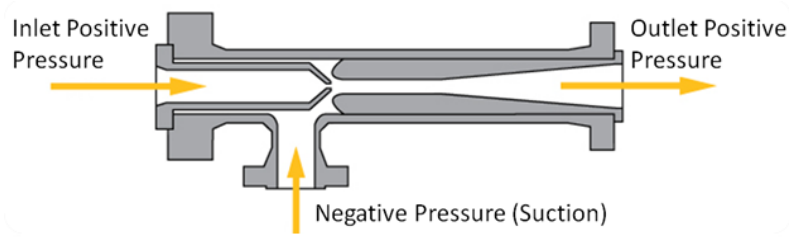

Figure 21. Visual representation of the internal mechanism of a venturi pump.

Venturi pumps allow for minimal footprint, and for some leeway in terms of failure. Working in unison, the venturi pumps are the most feasible option when dealing with size, safety, and assembly. Additionally, since the robot is tethered to a ground compressed air generator, carrying the weight of a vacuum generator is eliminated with these small pumps, as all that is needed onboard the driving unit are a pneumatic connectors, lightweight pneumatic tubing, and the venturi pumps, see Figure 22 of the actual venturi pump used. The high pressure air will be appropriated onboard the robot, and distributed to the venturi pumps individually – atop each suction cup. This plumbing organization allows each pump to work in parallel with each other, so if one of the suction cups or pumps fail, it will not detrimentally affect the rest of the system, and the system will still be functional.

Figure 22. Close up view of the actual venturi pump used in the final assembly.

Based on the performance characteristics, form factors, and popularity in industry, the venturi pump chosen for the Otto's vacuum platform is the Piab Xi2.5-2 two-stage venturi cartridge. A total of twelve venturi pumps will be integrated into the custom housing (one for each bellow suction cup) and supplied by the sponsor, Electroimpact. This pump achieves deep vacuum levels with relatively low intake air consumption, in a package that is lightweight and small. The maximum negative pressure obtained through testing is approximately -12.8 psig when a positive pressure of 100 psig is supplied to the venturi pump and the air consumption per unit is approximately 0.03 SCFM. Also, considering that the cost of an individual intricate pump is relatively high, using pumps supplied by the sponsor is a very feasible option in the overall scope of the project.

4.1.2 Suction Cups

After realizing that the low-profile suction cup provided by Electroimpact was not an ideal candidate for sliding purposes (refer to *Section 3.3.2 Small Scale Prototype Testing*), the design required some research upon

different suction cup sizes and geometries from other manufacturers. Prior to determining the type of suction cup, the geometry of the driving surface must first be considered. Because it is necessary for the platform to drive on the dynamically-convex shape of an aircraft fuselage, variation of the driving surface's height must be compensated in order to maintain a proper seal. Therefore, the suction cup characteristics required for this design must include the capability of actuating generously (about .1 in to .25 in) in the normal direction of the mounting surface and the capability of handling lateral loads caused by sliding friction. In addition, a very critical requirement for the suction cup is that it must be capable of being loaded by a substantial pull-off force (in a range that is equivalent to at most 60% to 80% of the total suction force) and still maintain a very reliable seal. This is of utmost importance because this pull-off force governs the amount of normal forces the drive wheels will experience.

Some examples of potential suction cup designs include suction cups with elongated skirts, ones with mechanical springs, ones with swivels joints, and bellow suction cups. After considering all these possibilities and analyzing their properties, the bellow suction cup design was chosen as the most appropriate suction cup, see Figure 23 for an example. The accordion-styling of the bellow cups allow for both compression and extension, as well as drive orientation changes. An initial concern was that the bellows may be distorted when loaded laterally, but after further testing of different sliding materials (refer to Section 3.3.3 Material Testing), the range of lateral forces seen by the bellows will only be within the range of 1 to 3 lb, which is not enough to cause any irregularities upon the bellow shape.

Figure 23. Top and bottom views of a nitrile 1.5 bellow suction cups.

To verify these performance traits in the bellow cups, a series of visual tests were performed with a 2.07" diameter 1.5 bellow suction cup, see Figure 24 for test setup. In the figure, a venturi pump is attached to the top of the cup and is used to generate the vacuum pressure within the bellow. The paracord attached with a tension gauge is used to apply a pull-off force onto the bellow cup. Since the tension gauge has a measuring limit of 15 lb, the bellow cup was tested at a suction force that is less than the actual forces seen on the final design. It can be assumed that the characteristics seen at the lowered suction forces are proportionally similar to the ones

seen at higher suction forces. During the tests, the vacuum pressure was adjusted so that the bellow cup would fail at a pull-off force of 8.25 lb. The bellow cup was then loaded with different pull-off forces between 0 and 8 lb (0% to 90% range of max suction force) and it proved to maintain a very reliable vacuum seal. The bellow cup showed signs of slight actuation when loaded with different pull-off forces and it also verified the assumption that the bellows can be actuated while keep a relatively constant internal vacuum pressure. In addition, sliding of the bellow cup while it was loaded with the pull-off forces did not affect the vacuum's seal nor did it lower the max pull-off forces. These visual results verified that the bellow cup design meets all of the suction cup requirements, as previously stated.

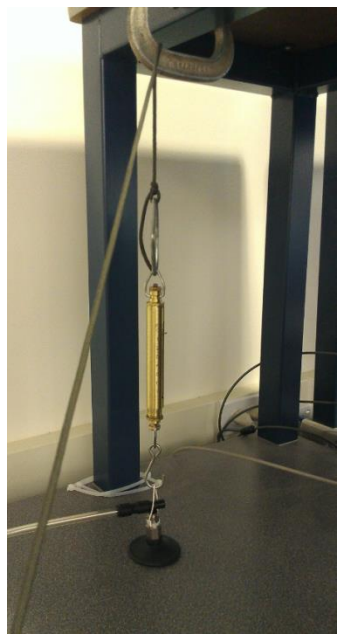

Figure 24. Test setup used for preliminary tests of the 2.07" bellow suction cup.

Because of the positive test results with the 2.07" suction cup, the final design consists of twelve 3.07" bellow suction cups (model no. B1.5-78-NBR), which were purchased from Anver – a leading manufacturer of suction cups. The larger diameter cups allow for a greater max adhesion force in combination with the low friction material attached. Each suction cup will be operating at a max suction force of approximately 25 lb while the venturi pumps are fed with an inlet positive pressure of 60 psig. By having a total of 12 bellow cups, the design mitigates the chances for failure. The system (with a total weight of 55 lb) is still capable of staying adhered to a vertical or an inverted surface if 7 of the suction cups fail due to vacuum leakages - although it will not be capable of driving.

Lastly, it may appear that the system will be relatively easy to detach from its driving surface if it has a total suction force of 300 lb with a derived normal force of 225 lb about the wheels (0.75 NFB). But if an additional

pull-off force of 75 lb is applied to the system, the system will not detach; instead, the normal forces which are applied to the wheels will be lowered to 150 lb. Therefore, in order for the system to be completely detached, a minimum pull-off force of 300 lb is needed. This is a result of the bellow suction cups having an actuation range that extends past the bottom edge of the wheel, see Figure 25.

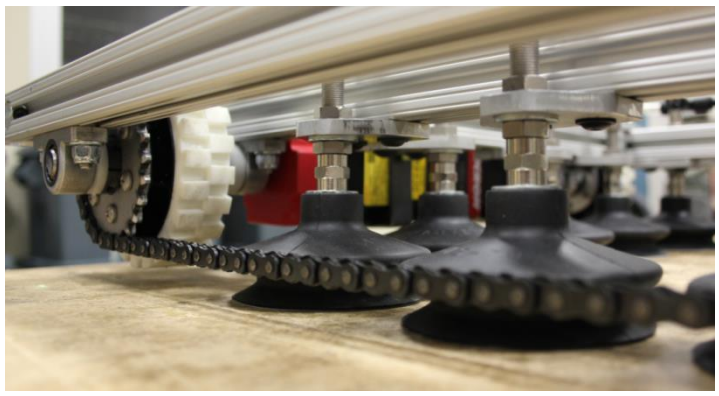

Figure 25. The bellow suction cups are capable of staying adhered to the surface without having the wheels touch the surface.

4.1.3 Normal Force Bias

By changing the relative height of the cups, the total suction forces generated by the cups can be "distributed" rationally as normal forces to both the drive wheels and the suction cup boots (as previously mentioned in Section 3.3.1 Conceptualization and Analysis). The assembly of the bellow suction cup in conjunction with the venturi pump housing is shown in Figure 26. The threaded stud has a through hole along its center axis to allow air flow between the suction cup and venturi pump. The stud is placed through the mounting plate and the two nuts and washers are used to set the relative height of the bellow cup. The ideal height is determined from the tests outlined in Section 6.1.1 Suction Cup Force Test and 6.1.2 Suction Cup Deflection Tests. This value is set to 5.60 mm in order to achieve an ideal NFB value of 0.75. This correlates to approximately a total of 225 lb of normal force about the wheels and approximately 75 lb of normal force about the suction cups when the total suction force is set to 300 lb. This NFB value of 0.75 is used for both the vertical and inverted drive orientations. In addition to flat surfaces, this value should also be sufficient for driving on curved surfaces which have a large radius of curvature. For a better performance for driving on curved surfaces, the cups may be adjusted to achieve a non-flat profile about the bottom of all the suction cups, where the middle cups are set for a slightly smaller height to accommodate the curved contours.

Figure 26. Suction Cup assembly mounted onto the frame.

4.1.4 Low Friction Sliding Material

Hard plastics are capable of forming a sufficient seal as long as the vacuum source provides a large enough suction flow rate. This was discovered unintentionally, after initially using EI's rectangular suction cups and a polycarbonate medium between the cup and the drive surface. This discovery led to research into other similar plastics, one of which being polytetrafluoroethylene (PTFE).

In order to allow the suction cups to slide on the driving surface, a low-friction material must be applied to the entire bottom of the suction cup. After testing different materials (*Section 3.3.3 Material Testing*), PTFE was chosen as the best-suited material. Not only does it have a low coefficient of friction, its kinetic and static coefficients of friction are similar. As stated previously in *Section 3.3.3*, the PTFE was tested to have a coefficient of friction of 0.1 on smooth surfaces. This low coefficient eliminates any dynamic involved with starting and stopping. Because it is not very rigid and slightly deformable, PTFE altered the suction cup's sealing performance by only 90% in terms of suction strength, refer to *Section 6.1.2* and *6.1.3* for more details regarding the suction cup's performances. Sheets of $^{1}/_{64}$" thick PTFE material were bonded with 3M's (model no. 9474LE 300LSE) double-sided adhesive sheets, and laser-cut into circular shapes, to match the footprint of the suction cups.

This proof-of-concept method of doctoring the suction cups sufficed, but, as noted in the *Section 8 Conclusion and Improvements*, custom manufactured cups with embedded PTFE would be a more elegant and robust solution.

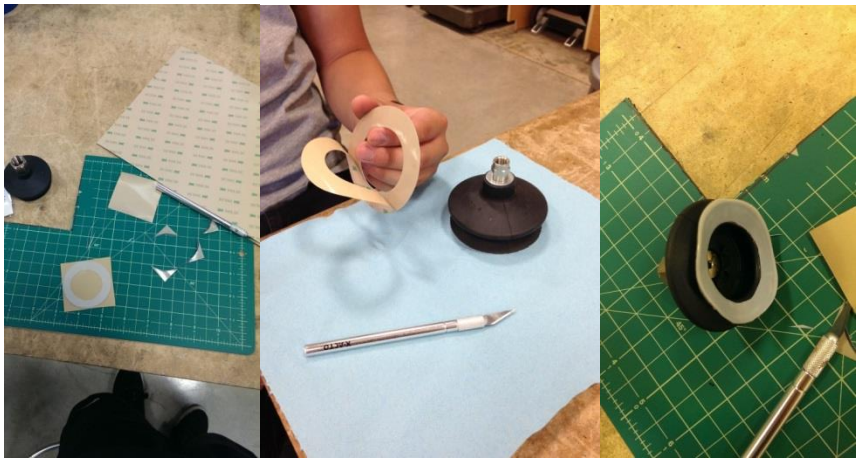

Figure 27. Bellow suction cups modified with PTFE sheets, adhered with 3M industrial strength adhesive.

4.1.5 Pneumatic Components

Along with having an umbilical cord attached to Otto for motor control and power, an air supply hose is used to deliver compressed air from the wall outlet to Otto's pneumatic assembly. This compressed air source is ideal because it is treated as an infinite supply source, which can deliver high flow rates at any pressure up to 100 psig.

In selecting the pneumatic hose, it was important to consider a hose with a pressure rating that was compatible with at least 100 psig (which is the max rating for the venturi pumps), have an 8 mm outside diameter, and have the relative flexibility to fit the contours of Otto's pneumatic plumbing design. Many short tubes were cut and installed in between the venturi pumps, linking them in parallel, see Figure 28 for the pneumatic setup. The inlet hose is 50 feet long, and connects the one end of the pneumatic line on Otto with the compressed air coming from the building compressor.

Figure 28. Layout of pneumatic lines - all venturi pumps are attached for parallel performance.

4.2 DRIVETRAIN SYSTEM

4.2.1 DRIVE SHAFT & COUPLER

The drive shaft is responsible for transmitting torque and rotation from the motor source to the driving wheels. Carbon steel drive shafts connect the motor and gearbox output to the wheels. For a secure hold in high torque driving situations, these shafts are outfitted with an AISI keyway.

The drive shaft chosen is 6" long, and 0.5" in diameter with a $^{1}/_{8}$" keyway. The drive shaft connects to the gearhead's output shaft via the coupler, and is held in place with two aluminum pillow block sleeve bearings. In between the bearings is the wheel, the aluminum attachment hub, the sprocket and Delrin spacers. The drive components are held in place with a $^{1}/_{8}$" key that is slotted in between the slot in the drive shaft and the slot on the wheel hub.

Stress analysis was performed on the drive shaft to make sure it could withstand the expected loads that were calculated previously in EES. The most important analysis was to verify that there would be no deformation or deflection on the shaft when heavily loaded. The stress simulation was performed with SimulationXpress on Solidworks, using a normal force of 85 lb_f, a friction force of 35 lb_f, and a chain load of 72 lb_f. Based on the displacement and Von Mises Stress analyses, the maximum displacement that should be seen by the steel shaft is 0.000243", along with a minimum factor of safety of 5.491. Both the factor of safety and maximum displacement values are more than acceptable for this application. Furthermore, the simulated loads and forces used in the analysis are conservative to begin with. The real-life prototype shaft should only be experiencing a normal force of about 57 lb_f under normal operating conditions. Simulation results are shown in Appendix D.

A spider coupler mates the drive shaft to the gearhead output shaft. Due to the different sized diameters of the two shafts, two different size C couplers (one with a 14mm bore and one with a ½" bore) are used.

4.2.2 WHEELS & HUB

Otto utilizes four wheels as its main contact with the driving surface. These wheels transmit the speed and torque from the motors to the driving surface, allowing the Otto to move. The wheels also act as a counter-force to the increased normal force from the suction cups. Mentioned previously, as the vacuum pressure in the suction cups increase and the cups compress, the chassis will lower toward the driving surface. The wheels keep the chassis at a stable position as the suction cups compress, absorbing the increased normal force, and distributing it evenly to each wheel. The difficulty with selecting a wheel for this application resides within the material selection rather than the size. Wheels come in standard sizes, and the 4-in diameter wheel was chosen specifically to fit with the size constraints of Otto.

Because Otto utilizes high friction to maintain its position on the driving surface as well as rigidness to withstand the increased normal force, the ideal wheel material for this application is one that has high friction, but is not easily deformable. Wheel material selection was a difficult task because high friction materials are generally rubber and non-stiff, while firm materials tend to have low friction characteristics. After researching and analyzing many options, it was decided that Otto would use polycarbonate wheels outfitted with thermoplastic polyurethane “HiGrip” tread. The thermoplastic tread on these wheels allows for high friction on the driving surface and are rated to have a coefficient of friction of 1.2 on carpet due to its toothed/tracked outer tread. Because the tread is made from polyurethane, they have relatively low deformation, remaining rigid as the normal force on the wheels is increased by the suction cups. These light-weight (0.31 lb) wheels are sold and distributed by AndyMark, and are shown in Figure 29.

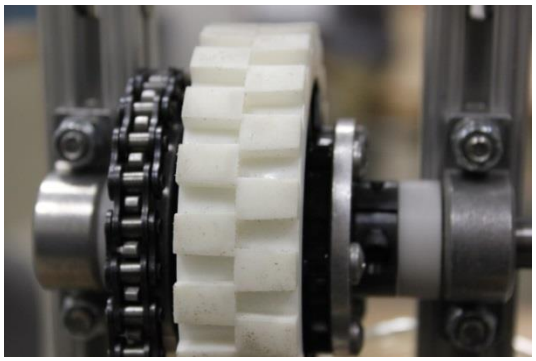

Figure 29. AndyMark "HiGrip" thermoplastic polyurethane tread wheels.

4.2.3 Chain & Sprocket

For Otto, it was decided that all-wheel drive would be the ideal driving condition - as all-wheel drive increases driving efficiency while also limiting the chances of wheel slip, compared to a two-wheel drive system. All-wheel drive is the most practical driving method because it utilizes all of the normal forces that are loaded onto each wheel. In order to achieve all-wheel drive with only two motors, the wheels are connected with a chain and sprocket. The motors and gearboxes are connected to two of the four wheels, and thus the sprocket and chain effectively transmit the motor output to the parallel wheels, see Figure 30.

Figure 30. The 1:1 driving ration sprocket and #35 medium grade chain.

The four aluminum sprockets all have an outer diameter of 3.075” with 24 teeth, resulting in a 1:1 driving ratio between the wheels. The size was chosen to be the maximum standard diameter that does not exceed the diameter of the wheel. In other words, the chain, when tensioned properly, will not drag along the surface when driving. A larger sprocket is ideal because it requires fewer loads on the chain when running as compared with a smaller sprocket.

The chain connecting the sprockets is a #35 medium grade chain, which is commonly found in go-cart drive systems. The sturdy chain ensures that it can handle all the driving loads and torques without any inconsistencies or link failures.

A chain and sprocket subsystem was selected over a pulley-belt system because of its robust mechanical characteristics, as well as its reliability in high torque scenarios. Pulley-belt systems perform better in high speed, low torque applications, which is not suitable for this design.

4.2.4 Bearings

The drive shafts that carry the wheels are connected to Otto with 0.5” high load roller sleeve bearings. One bearing is mounted onto each side of the shaft, so that the force on the driving wheels is evenly distributed to the chassis. The bearings chosen are mounted via aluminum pillow block casings, and are equipped with two base mounting points. Mounted on the underside of the chassis for assembly geometry and support, these bearings are also self-aligning and adjustable along the aluminum extrusion chassis - and must be installed perfectly parallel to each other in order to create a straight driving path.

Brief analysis using predicted bearing loads and speeds showed that the bearings chosen will work in this application. In addition to the type of load and size of the bearing, the load value (*P*), velocity (*V*), and load at velocity (*PV*) had to be calculated in order to choose the correct bearing on McMaster-Carr’s online catalogue. Using 69 lb as the bearing load and the top speed of 5.9 ft/s converted to 338 shaft rpm, the P and V values were determined, where *P = Bearing Load / (Shaft Dia. x Bearing Lg.)*, and *V = Shaft Velocity x 0.262 x Shaft Dia.*. The pillow block sleeve bearings chosen carry a maximum *P* value of 2000, a maximum *V* value of 1200 and a maximum *PV* value of 25000. The maximum values calculated for Otto’s operation well precedes McMaster-carr’s rated maximum loads, with values of *P* = 220.8, *V* = 44.3 and *PV* = 9776 - providing a suitable bearing for the shaft size and expected operation parameters.

4.3 Motor System

4.3.1 Motor Selection

Two electric motors are utilized in Otto’s drive system, and are powered by the umbilical cord (eliminating the need for a carry-on energy source, such as a battery). This also means that motor efficiency is not a critical factor

when choosing a motor. When performing a skid-steering turn, it is necessary that the two drive sets and their respective motors operate independently of each other. The torque delivered to the driving wheels will need to be large enough to overcome frictional forces between the suction assembly and the driving surface, as well as the friction forces between the wheel and the driving surface during skid steers. To achieve the necessary high output torques, a speed reduction assembly will be attached to the motors.

The selection of the motors was initially based on the analysis of different driving orientations and scenarios, as mentioned in *Section 3.3.1 Concept Revision B – Sliding Adhesion System*. A variety of motors were considered during the selection process, including: AC motors, DC motors, stepper motors, standalone motors and motors with built-in gearheads. DC motors were chosen as the best motor option because of their power-to-cost ratio and linear performance curves. In addition, the team has had prior experiences working with DC motors. After analyzing the cost of purchasing DC motors, respective gearheads, power supplies and motor control units, the total cost exceeded the initial budget for motor selection.

As an alternative motor option, Electroimpact was able to provide two of their FANUC AC servomotors for the design, see Figure 31. The initial options for these motors were the βiS 0.3/5000 and the βiS 0.5/6000 - the βiS 0.5/6000 motor was chosen for its higher torque and speed outputs. The smaller βiS 0.3 motors would have required a larger speed reduction ratio and would not have been able to meet the performance requirements of driving at average human walking speed and carrying large loads simultaneously. The βiS 0.5 motors have a continuous operational output torque of 0.5 N*m and an intermittent output torque of 2.25 N*m. The continuous output is used for straight-line maneuvers whereas the intermittent output is used for short-term maneuvers which demand a higher torque output such as acceleration and skid-steering. Refer to Appendix C for performance datasheets of this motor.

Figure 31. FANUC βiS 0.5 AC servo motor.

An additional benefit of using the FANUC motors is that Electroimpact was able to provide a FANUC programmable logic controller (PLC). The controller is a standalone unit which takes user inputs and controls the

drive of the FANUC motors accordingly. By using the motors and PLC's provided by Electroimpact, the project budget was held to a minimum of costs.

4.3.2 GEARBOX SELECTION

Based on the torque and speed output of the supplied FANUC βiS 0.5 AC servo motor, as well as the desired speed and load of the robot, a gear ratio of 20:1 was necessary (for detailed analysis regarding the reduction ratio, refer to *Section 3.3.1 Concept Revision B – Sliding Adhesion System*). Initial plans for achieving the desired gear reduction included pulleys and belt drive systems, a custom gearbox or a standard gearbox with a custom fitting. These options were considered primarily for their inexpensive costs, which was within the range of $200 to $300. See Figure 32 for a model of the custom gearbox.

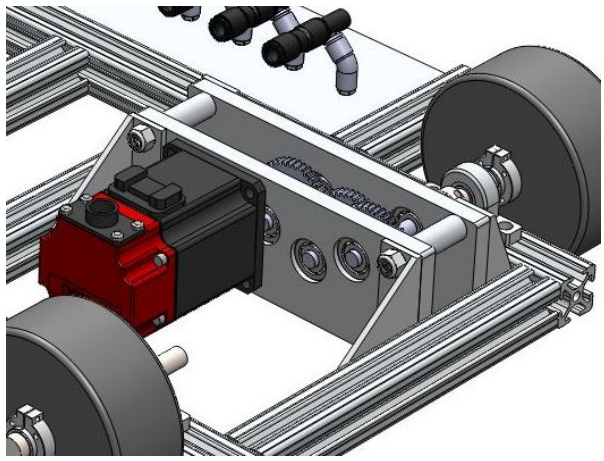

Figure 32. CAD model of the initial custom gearbox design.

Eventually, a decision was made to move forward with an industrial gearhead. The final design is equipped with two Thomson XTRUE planetary gearheads, one for each side of the drive sets. The model number for the gearhead is XT060-020 and along with each gearhead is a RediMount system, model number RM060-16. The RediMount system allows for a perfect fit between the FANUC motors and the gearheads. The cost of each gearhead assembly is $485.00 per unit, which accommodated the project budget as well. These industrial gearheads have rotational accuracies and torsional strengths that are well beyond any of the custom options previously mentioned. The XTRUE gearheads have a peak torque output or 48 N*m which are rated for shock and intermittent loadings. Since the AC motors have a max torque output close to 2.5 N*m, the gearboxes are minutely within the rated operational range. Based on the total system load of 55 lb, the motor outputs are never required to have an output that is near its max torque. Instead the motor will only need to output 0.45 N*m to accelerate the system at a rate of 8 ft/s^2. Refer to Appendix C for the performance datasheet of the Thomson gearhead. Therefore, the relatively low torque output of the motors during acceleration is suitable for the use of the Thomson gearheads.

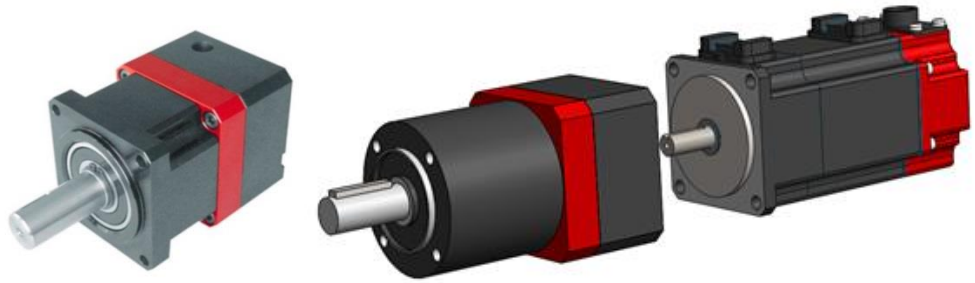

Figure 33. Thomson XTRUE Planetary Gearhead with a RediMount system attached (Left), with motor (right).

4.4 CHASSIS

4.4.1 ALUMINUM EXTRUSIONS & FASTENERS

The structural frame of Otto is made from custom length T-slotted aluminum extrusions manufactured by 80/20 Inc. Many different geometries and materials were researched before selecting aluminum extrusions. These include plastic molded members, steel bars and sheet metal – but these options did not meet Otto's strength and weight requirements for the chassis. Aluminum extrusions are used because they are easily modified, strong, relatively lightweight, and cost effective. They allow for custom positioning of the robot's sub-components, while providing sturdy joints and connections. As the main structural support of Otto, the 80/20 aluminum extrusions are custom cut and sized accurately to match the conceptual design dimensions.

Using 80/20's detailed equations in their online catalog, preliminary analysis for stress and deflection on the aluminum extrusions were performed. These calculations verified that the extrusions could withstand the expected loads without any deformation or damage. Also, calculations were performed in order to determine which fasteners to use, so that the joints would not fail during operational loads.

The 1010 (1" x 1") series is used because it is the smallest size offered, as well as the lightest. All of the components mounted onto the chassis are small enough to fit while using the 1010 series without any problems, which didn't warrant a need for the larger, heavier, 1515 extrusion series. All of the fasteners and carriage bolts were sized to fit with the 1010 series.

Adjustable 90° joint fasteners hold the aluminum extrusions together. They were chosen because of their reliability and strength under high load and torque stress on the chassis joints. Basic analysis was performed on each joint to make sure the rated loads on 80/20's catalog exceeded the expected loads on Otto. Certain joints on the chassis are reinforced with added fasteners and brackets, as these were installed as a precaution to the joint locations expected to see the highest load, see Figure 34 for the chassis design.

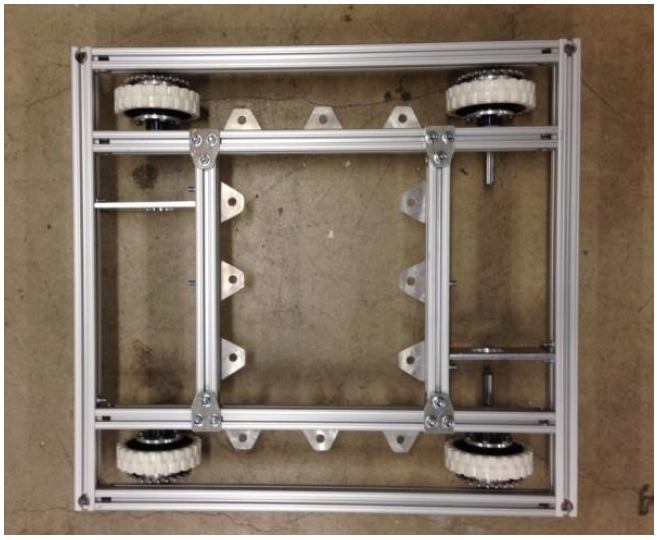

Figure 34. Otto's bare chassis, made of T-slotted aluminum extrusions.

4.4.2 Suction Cup Mounting Brackets

Due to available design spacing and unique suction cup positions, it was determined that the mounting brackets for the suction cups would be custom machined. Brackets that could have been purchased from an online vendor were found to be either too expensive or not the correct size.

The brackets are used to mount the threaded stud of the suction cup assembly to the inner section of the chassis. The brackets are fastened to the chassis with 80/20 “drop-in” fasteners, which easily slide into the T-slot and under the bracket, bolting them together with a screw. There are two fastener holes per bracket, and one ⅜” hole for the threaded rod. The threaded rod is positioned with a combination of washers and nuts, allowing for easy suction cup height adjustments.

The custom machined mounting brackets are cut from a 2 ft x 1 ft 6061 Aluminum Alloy plate. There are twelve individually machined brackets, one for each suction cup.

Figure 35. Custom machined aluminum suction cup mounting brackets, 12 total.

4.4.3 Motor Mounting Plate & Brace

In order to hold the motor and gearhead in place for Otto, a custom machined mounting plate had to be designed. The mounting plate is made from the same 6061 aluminum that the suction cup mounting brackets are made from. The mounting plate is a custom piece, cut and drilled to fit exactly with the geometry of Otto and the surrounding components with a tolerance of at most ± 0.010”. The mounting plate connects at the front of the gearhead, as a large circular cut-out positions the gearhead and the four mounting screws attach it to the plate.

The mounting plate measures 3.0 in. tall and 5.68 in. wide, fitting tightly between the inner and outer aluminum extrusions, and below the chassis – in line with the wheels. There are three attaching points for the mounting plate to ensure a secure connection to the chassis.

At the rear, a brace supports the motor by clamping onto the cantilevered motor system. In order to avoid over constraining the motor and gearbox with this additional mount (which would make three mounting points in total), the brace is padded with foam and is clamped with a conservative force. Instead of a mount, the brace primarily acts as a vibration damper and keeps the cantilevered motor steady when driving. This damping brace is made from custom cut 0.100” steel sheet metal, and bent into shape. Mounting holes have been drilled on the ends to allow for a bolt and nut clamping system.

Figure 36. Custom machined aluminum motor mounting plates.

4.5 Operation Requirements

To operate the equipment, the electronics panel (PLC) must be must have a power input of 208 to 220 VAC, 3-phase power, as well as power to the computer terminal. Prior to powering on the electronics, however, the motors need to be attached to their respective power lines and control wires. Once the PC is booted along with the electronics panel, the two units then recognize each other and are ready for operation. The pneumatic assembly is to be fed with a controlled air pressure input of 60 psig - for operation with a total load of 55 lb. The

air pressure is controlled by a regulator attached with a pressure gauge in series. Once the electronic and pneumatic systems are turned on, Otto can be placed and adhered onto a smooth surface. At this point, Otto is ready for operation and its motors may be controlled from the attached pendant for regular driving maneuvers. Also, the air pressure can be adjusted in order to increase or decrease the max load carrying capacity (see *Section 6.1 Suction Cup Tests* for examples).

Figure 37. The PLC and pendant used to control Otto, supplied by Electroimpact.

4.6 SAFETY CONSIDERATIONS

In considering safety, it is important to classify the modes of failure associated with the design. Otto is a proof-of-concept design which has scalable potential of carrying loads up to 200 lb or more, and detachment from its driving surface is considered the worst-case scenario of all failures. Because this type of failure may cause harm to the machinery or any personnel within the vicinity of the device, this failure mode must be avoided at all costs.

The first step in avoiding catastrophic failure is to mitigate and to localize all suction failures. In the case that a suction cup loses suction, the overall capacity of the robot decreases by the amount of suction force the cup had. Therefore, many cups with smaller suction capacities can better compartmentalize losses than a singular cell that carries the entire load. Furthermore, should one pump or cup be compromised, the system should not fail either, so redundancies were added to reduce the risks of detachment failure. This results in a design “safety factor” that provides the platform with more suction than is needed for just adhesion, though all working suction cups are required for driving operations. As mentioned in *Section 4.1.2 Suction Cups*, when the system is at a total weight of 55 lb, the system can stay adhered to the drive surface if up to 7 of the suction cups manage to fail.

In addition, the robotic platform was designed to stop driving before it detaches from the surface in the occurrence of multiple suction cup failures. This creates a premature, but less dangerous failure mode in

comparison to the worst-case failure of detachment. An example of this specific failure is if a load that is larger than the rated capacity is placed upon Otto during its inverted driving operations. Refer to *Section 4.1.2 Suction Cups* and *Section 6.2.2 Inverted Driving* for details of this failure mode.

5 MANUFACTURING

This section outlines the manufacturing and assembly process that was used to create Otto. It outlines the critical measurements and adjustments that were made in order to create a functioning drive unit.

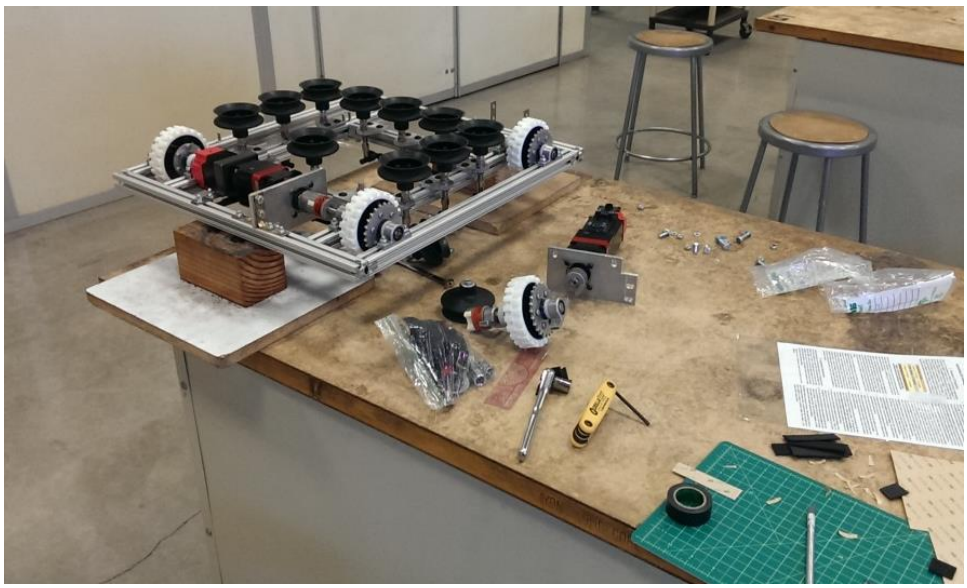

Figure 38. Part of the manufacturing process for Otto.

5.1 SUCTION CUP ASSEMBLY

In order to mount the rubber suction cups to the rigid body, mounting hardware from Anver was used. A threaded stud and a coupler piece are fitted to the top of the bellow suction cups, which exposed a BSPP (British Standard Pipe Parallel) pipe thread on the other end for mounting. The external threads on the stud allowed for securing of the assembly onto the mounting brackets, which extended from the T-slotted framing. Finally, the assembly was finished with a BSPP to push-to-connect coupler used for adapting the 6 mm inlet of the venturi pump housing. At every interface between pneumatic tubing and/or venturi pumps, push-to-connect fittings were used. This type of coupler is ideal because it allows for very easy assembly and disassembly of the pneumatic lines, see Figure 39.

Figure 39. Close-up view of the T-shaped push connectors used in the suction cup assembly (Left), completed single suction cup sub-assembly (Right).

The overall layout of the suction cup assemblies was chosen primarily for its symmetry. This symmetry allows for a relatively even distribution of loads about the cups and the drive wheels. Also, by having the suction cups placed on the inner locations of the chassis, their components are protected by the aluminum framing if Otto was to detach and collide with the ground.

5.2 Chassis Construction

Otto's frame is comprised entirely of T-slotted aluminum extrusions, attached with fasteners made specifically for this type of framing. Each segment was cut to length using a mill, to ensure accuracy and consistency. Variations in length could potentially cause uneven loading about the wheels, which could ultimately cause slippage failure, or, at the very least, stability issues. During the assembly of the aluminum segments, there were no fixed mounting datums in most cases, so the positions of the framing were measured then securely mounted in the appropriate position with multiple joint fasteners. In addition to the aluminum framing, the joint locations deemed with the highest stress were reinforced with custom brackets secured on the top side with carriage bolts. See Figure 40 for pictures of the frame during assembly.

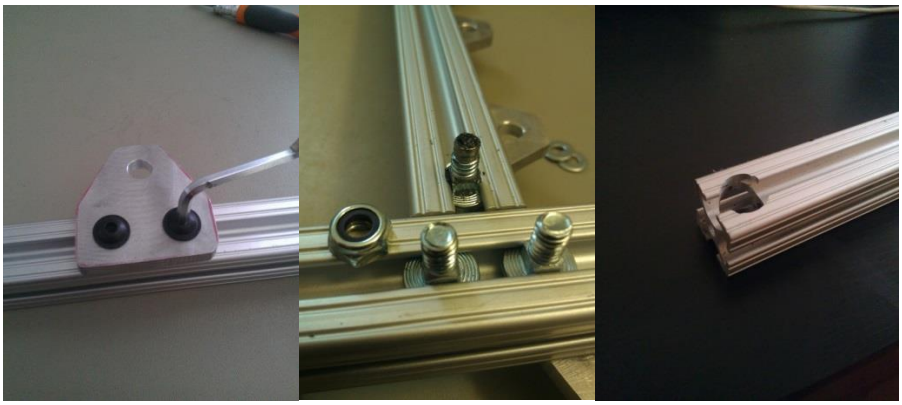

Figure 40. Aluminum extrusion assembly and reinforcement bracket attachment.

5.3 DRIVETRAIN COMPONENTS

The motor was attached to the frame by two brackets - one attached to the gearbox's mounting holes, and the other cradling the rear portion of the motor. The former is the major load-bearing attachment point, and was milled from an aluminum plate; while the latter was created from bent sheet metal, and supplemented with foam padding to provide additional support and dampen any vibrations from an otherwise cantilevered servomotor. See Figure 41 for images of these two mounting components.

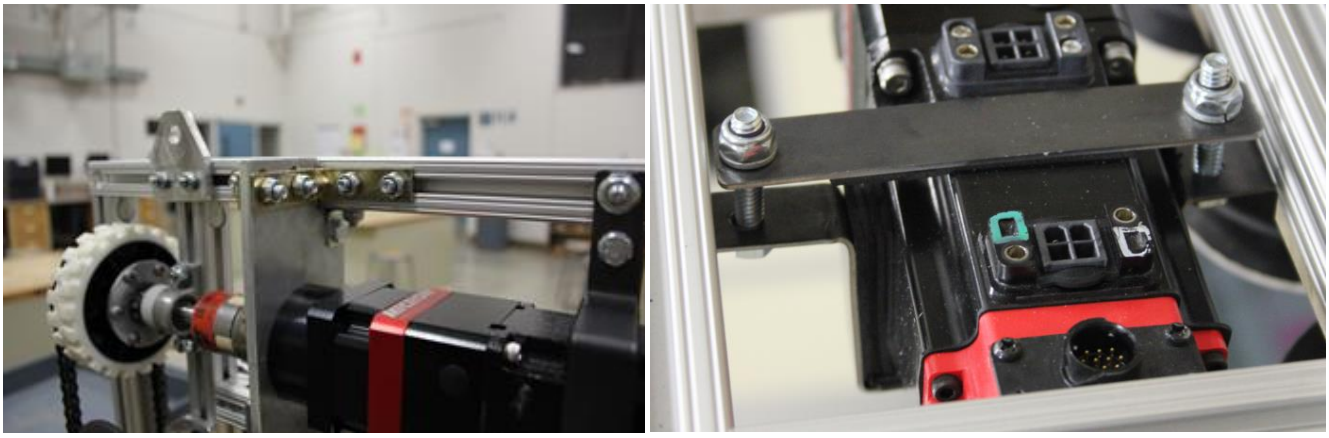

Figure 41. Aluminum plate attached to gearhead as primary drivetrain support (Left) and steel sheet metal bracket mounted as secondary support (Right).

A shaft, which extends from the motor-gearbox assembly via Thomson's RediMount system, mates with the output shaft through the use of a spider coupler. Both of these shafts are securely held to the coupler using a keyway and a setscrew. The spider couple servers as the interface between the motor unit and the drivetrain.

The output shaft end of the spider coupler is the keyed steel drive shaft which connects to the wheel-sprocket sub-assembly. This wheel-sprocket sub-assembly was built and assembled four times, once for each wheel. Each sub-assembly was pieced together onto the custom cut drive shaft before connecting it the coupler and fastening it to the chassis, see Figure 42. The wheel was fitted onto the drive shaft via two keyed hubs that were mated end to end with each other. One of the wheel hubs had to be slightly machined, so that when mated, the wheel would fit perfectly. The hubs ordered from AndyMark are only designed to fit one per wheel, but for this project, the use of two hubs was deemed a more conservative option. Once the hubs and wheel were fastened together onto the drive shaft, the sprocket, Delrin bushings and lock collar were placed onto the shaft. The sprocket was positioned to face the outer edge of the chassis, so that the chain would not interfere with the pneumatic tubing and suction cups positioned on the inner sections of the chassis. The Delrin bushings were cut to a custom size so that the spacing in between the bearings would be exactly the same for all shafts and fit perfectly with the spacing allowed by the chassis.

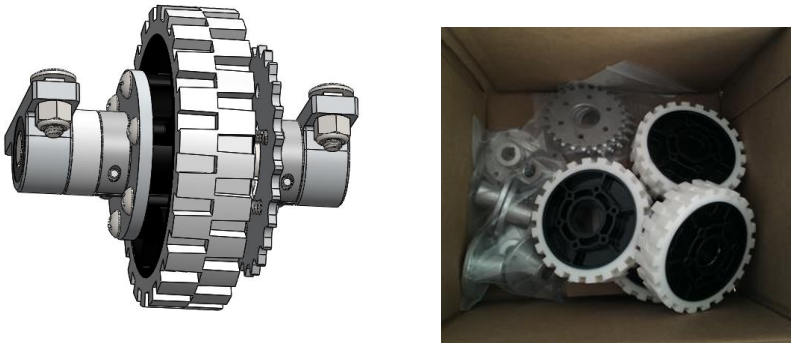

Figure 42. Wheel, hubs, bearings, sprocket, bushings and lock collar sub-assembly.

Because the bearings are sleeve bearings, no press fitting procedures were needed. Instead, shaft collars and spacers were mounted near the middle of the shaft to hold the position of the wheel and the bearings. To finish off the assembly process, the bearings were fastened to the chassis and spaced evenly from the end of the extrusion. At the same time, the drive shaft was carefully aligned with the spider coupler and connected, using set screws. Because there are only two motors, only the two drive shafts on opposite ends needed to be connected to spider couplers. The motors were placed on opposite ends to create symmetry and balance the weight of the system evenly.

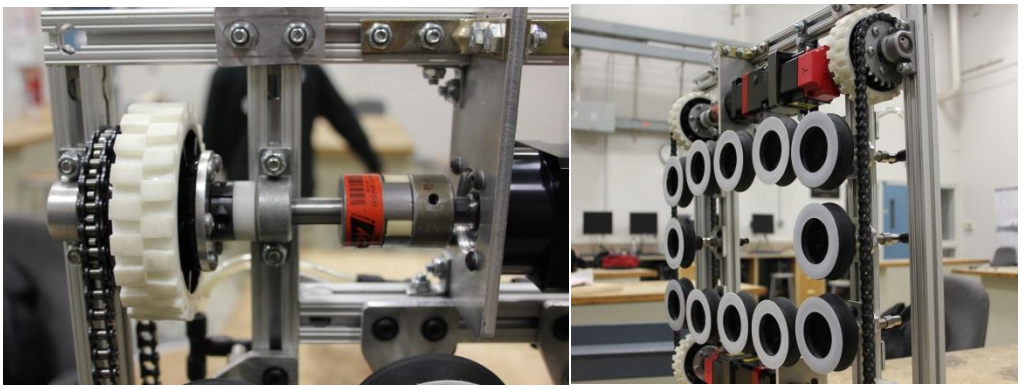

Figure 43. Mounted wheel sub-assembly, connected to gearhead with spider coupler (Left), underside of Otto – showing the layout of the suction cup sub-assemblies (Right).

6 DESIGN VERIFICATION TESTING

This section describes the detailed tests that were conducted on the design and on some specific components. Each test is outlined below, along with their results, which can be found in the following figures or in the Appendix at the end of the report. These tests verify a complete working prototype and that the requirements outlined at the beginning of the project have been met or exceeded.

6.1 SUCTION CUP TESTS

6.1.1 SURFACE TEST

The goal of the surface test was to determine which surfaces the modified suction cups can adhere to effectively. Without the PTFE modification, the regular bellow suction cups are capable of adhering onto uneven contours and surfaces with relatively rough finishes, such as drywall. With the addition of the PTFE sheet, the bellow suction cup's abilities of conforming onto rough surfaces are reduced and are thus limited to fewer surface types.

Since Electroimpact will be using Otto primarily for driving on the outer surfaces of aircraft fuselages, the PTFE modified suction cups need to be capable of adhering onto surfaces with a similar finish and smoothness. The surface that was used for the majority of the tests was a laminated tabletop. The surface of the tabletop has a laminated finish which somewhat represented the slick gloss coating of an aircraft fuselage though it has slightly more grit. Since the tabletop surface was used in both the Force and Deflection tests (*Section 6.2.1* and *6.2.2*) and proved to be an excellent mating surface for the suction cups, it can be justified that the modified cups will be just as effective, if not more, when used on an actual aircraft fuselage surface. Therefore, for the driving tests performed in S*ection 6.2*, a large tabletop surface was also utilized.

6.1.2 SUCTION CUP FORCE TEST

Because the 1.5 bellow suction cups are modified with the addition of the PTFE sheets, their adhesion performances have been altered. Therefore, the supplier's rated performance datasheets for these cups can no longer be used and testing was necessary to determine the modified cups' performances. These results are especially critical for setting the system's NFB value and determining the minimum necessary inlet air supply pressure.

The focus of this test is to load the suction cups while setting the venturi pumps at various inlet pressures and then to determine when the cups fail, i.e., the max adhesion force. The test setup, shown in Figure 44, consisted of the test stand, a sample of the driving surface (5" x 5" cut-out of a laminate tabletop) attached with a weight-carrying tray, an assortment of various weights, a pressure regulator, a 100 psig gauge, and a PTFE modified 3.07" 1.5 bellow suction cup attached with a venturi pump. The suction cup was securely mounted into a center hole located on the test stand. A venturi vacuum pump was attached to the top of the suction cup and supplied with compressed air from a wall outlet. Between the vacuum pump and the wall outlet were the pressure regulator and pressure gauge. Once the vacuum pump was pressurized, the surface sample adhered to the bottom of the suction cup.

Figure 44. Test stand used for bellow cup tests - vacuum gauge (left) and pressure gauge (right).

The test begins by loading the carry tray with an assortment of weights until the cups detaches. After running several sample tests, it was very noticeable that the suction cup behaved as a first-order response system - a time delay is apparent before the suction cup reaches a steady-state vacuum pressure within its bellows. This response was significantly noticeable in the following two scenarios: “initial suction cup adhesion to the surface sample” and “loading of weights onto the carry tray.” During the initial cup adhesion scenario, the time delay is related to the flow rate of the vacuum pump and the micro leaks between the PTFE sheet and the surface sample. The micro leaks prevent the cups from reaching its internal vacuum pressures instantly. During the loading of weights scenario, the act of loading weights onto the tray causes a slight acceleration of the tray and allows the micro leaks between the surface sample and the PTFE sheet to increase in flow rate for a short period of time. Once the suction cups reach a steady state vacuum pressure, the micro leaks are no longer apparent or significant and the cups behave normally.

Figure 45. Weights are added to the carry tray in order test bellow suction cup performances.

To prevent the time delays of the suction cups from affecting the test results, a waiting period was used during the initial adhesion of the cups and the loading of the weights. For the initial adhesion setup, 20 seconds of wait-time was given before any weights were to be loaded onto the carry tray. Also, a wait-time of 10 seconds was given after every incremental loading of the weights onto the carry tray. These wait-times allowed the suction cup to reach a steady-state after every transition of the test.

The results of the test show that the cup's detachment load is linear with respect to the inlet pressures supplied to the venturi pumps. The range of pressures tested was from 20 psig to 100 psig. This is true since it reflects the linear relationship of the equation *Force = Pressure x Area*, where the area of the cup is constant. Also, the result shows that the suction cup is stable through the range of inlet pressures, even though they are modified with the PTFE sheet. See Appendix A for test results.

6.1.3 Suction Cup Displacement Test

There were two distinct methods which could have been used for setting the normal force bias of the suction cups.

The first method involves setting up a fixture which measures the distribution of normal forces across the wheel. This method requires the placement of load cells or weight scales under the wheels. A foreseen complication with this method is that load cells generally have an operational range of a few hundred pounds to several thousand pounds. Since the magnitude of the loads which are applied to Otto's wheels should be within the

range of 80 to 100 lb per wheel, these load cells are not suitable for measuring the wheel loads. In addition, the use of weight scales would cause deflection issues. Since weight scales generally use a deflection mechanism to measure its loads, it would be very difficult to measure the wheel loads while keeping the surfaces of the suctions cups and the wheels aligned along the same plane. This is critical because a slight difference in the surfaces' alignment would skew the ratio of normal forces (NFB) between the wheels and the suction cups.

The second method involves parameterizing the suction cup's performance in relation to its bellow stretch or displacement. The test setup for this method is very similar to the setup and fixture used in *Section 6.1.2 Suction Cup Force Test*. Essentially, this test involves placing incremental weights on the carry tray and then measuring the displacement of the cup's bellow. This test was performed for three different inlet pressures: 50, 60 and 70 psig. The test results can be viewed in Appendix A.

The displacement measurements were taken between the underside of the test stand and the top of the surface sample. Note that for the test setup, a lock washer and a nut were placed between the suction cup and the test stand - the displacements of these two objects need to be accounted for when using the test data to set the NFB value. In the final setup of Otto, the lock washer, which had an approximate thickness of 0.05 cm was removed from the assembly of the final design. Therefore, the values of the suction cup displacements should be interpreted as 0.05 cm less than the actual value when viewing the test results.

Based on the test results, the cups generally have a stretch performance that is linear in relation to the incremental weights are placed upon it. This linear performance is consistent until the weighted load reaches approximately 90% of the cups max holding load. At the last 10% of the total weight, the bellow cups tend to have an exponential stretch and are very susceptible to detachment failure. See Figure 46 to view the difference between normal operational stretch exponential stretch of the cup.

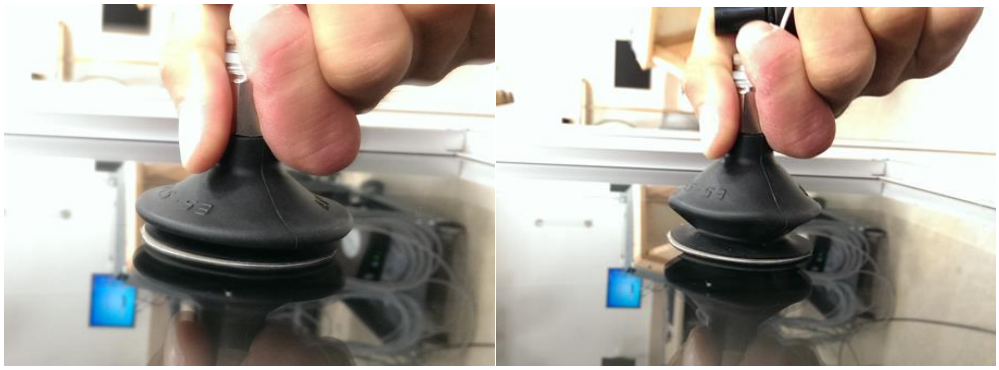

Figure 46. Bellow cup under linear displacement (Left), bellow cup under exponential displacement (Right).

The graphical plots of the final test results are used as a tool for the setting the NFB value of the system, see Appendix A. The y-axis on the right side (shown as the red plot) represents the percentage of the load that is

applied to the suction cup in relation to the maximum suction cup load, this value is also interpreted as the NFB value. The y-axis on the left side (shown as the blue plot) represents the displacement of the suction cup in relation to the test stand. Lastly, the x-axis represents the incremental weights that are placed onto the carry tray.

After reviewing the results of the tests for the three different inlet pressures, 60 psig was rated as the optimal inlet pressure to be fed to the venturi pumps. This pressure supplied the best balance between having a sufficient safety factor for both wheel and motor slippage: 2.84 and 1.43, respectively. In addition, Otto needs to have an NFB value within the range of 0.70 to 0.80; in other words, the suction cups are to be loaded within the range of 70% to 80% of their maximum suction load. From the plots, it can be determined that the cup needs to be have a displacement of 5.65 cm in order to achieve a 0.75 NFB value. Because the lock washer (0.05 cm) is no longer used in the final assembly, that displacement value is to be interpreted as 5.60 cm. Also, the distance between the bottom of the suction cup mounting plate and the bottom edge of the drive wheels is 5.80 cm. Therefore, a 0.20 cm washer is placed between the nut of the suction cup assembly and the mounting plate to achieve a final cup displacement of 5.60 cm. See Figure 47 for a layout of the bellow cup adjustments.

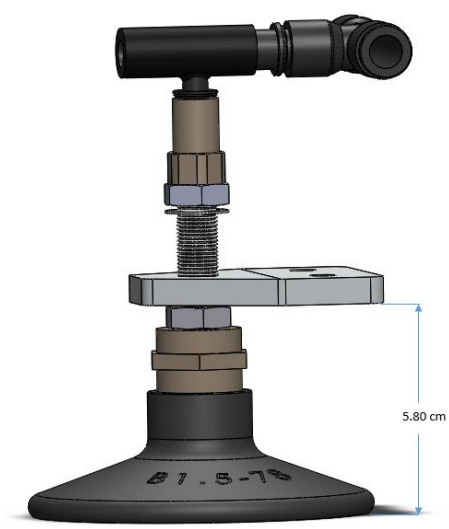

Figure 47. CAD model of suction cup assembly and mounting bracket.

6.2 Driving Tests

As stated earlier, the two most important scenarios for this wall-driving platform are the vertical and inverted drive. The test results associated with these driving orientations will be discussed below. The testing surface was a 2” thick repurposed wood tabletop, with a smooth-finish laminate. In all of the tests, a rope or stainless steel

braided wire was attached to the robot, in case of an unexpected failure. Once Otto was attached to the driving surface, standard barbell weights were attached with paracord for payload testing.

6.2.1 Vertical Driving

The vertical climb was theoretically determined to be the most strenuous case. Motor torque, and subsequent body stresses are at their highest because the motors must drive the entire weight of the system against gravity. For these reasons, this scenario is the case that limits the overall weight capacity of the robot, and is used to define the system.

Testing at normal operating pressure (60 psig) resulted in successful vertical driving at any speed up to the desired speed of 5.9 ft/s or 3.5 mph. At this input pressure, vertical driving was also successful with a 25 lb additional payload. Otto was able to accelerate upward, accelerate downward, turn 360 degrees with and without the payload attached. It should be noted that during a skid-steer maneuver, there is a slight drop in height of the robot, due to the static friction force on the wheels being converted to kinetic friction as it slips and turns. Once the skid-steer is completed however, the wheels quickly re-engage with static friction to maintain its position on the driving surface.

In order to test the maximum payload capacity of Otto, the normal operating pressure was increased to the maximum in-house pressure available, approximately 100 psig. This increased operating pressure resulted in the platform being able to successfully carry 70 lb of additional payload up the wall, Figure 48. It was also able to turn (although with slight slippage), as well as successfully drive downward. Including the body weight of Otto, this resulted in a total weight of about 100 lb. It should be noted, however, that the torque output of the motors to accomplish this exceeded the “continuous operation” specifications, and extended operation in this region is not recommended.

Figure 48. Otto proving its capabilities by carrying a load of 70 lb, for a total weight of 100 lb.

6.2.2 *Inverted Driving*

The same test surface that was used in the vertical test, was re-oriented to mimic a ceiling for inverted testing. Load testing, in this orientation, resulted in an expected higher load capacity, without experiencing any type of failure.

At the normal operating pressure of 60 psig, Otto was able to successfully drive on an inverted surface; turning, accelerating, and maintaining its position at any location while carrying a payload of 25 lb. When the operating pressure was increased to the maximum 100 psig, Otto was able to perform normal operating functions with an additional 70 lb payload attached via paracord, see Figure 49. There were no noticeable declines in performance while driving with the 70 lb payload. Because inverted driving was theoretically less critical than vertical driving, extra testing was conducted while carrying a human payload (160 lb), at 100 psig. While carrying a human, maximum driving speed could not be achieved, as the wheels would tend to slip and dis-engage from the driving surface at high velocities. In the inverted orientation, the large payload acted as an opposing normal force, relieving the normal force between the wheels and the driving surface. This meant that the force required to break the static friction force on the wheels was also lowered, and therefore Otto was more susceptible to slippage during this specific test. Thus, the maximum achievable speed while carrying a large, 160 lb payload was approximately 2 ft/s. Successfully carrying a human while driving was an impressive feat, something not demonstrated by any other similar wall-driving robots. This maximum payload testing verifies that the vertical driving scenario is the more critical driving orientation, as the inverted driving orientation was more successful with more than twice the amount of additional payloads attached.

Figure 49. Otto performing all the driving maneuvers with a payload: 70 lb payload (Left), and a human payload of 160 lb (Right).

6.2.3 System Troubleshooting

During operational testing, a few system issues interfered with the performance of Otto. It was beneficial to note these issues so that further testing could be done and future problems could be avoided.

After testing Otto for approximately 3-4 hours of continuous operation, it was noticed that suction power was low on a few suction cups and very low on a few others. When attempting to drive at normal operating pressure (60 psig) on a vertical surface, the wheels would slip very easily on the sides with low suction, yet the platform would maintain its position. After inspecting the seals and the suction cups for wear or leakages, and rotating the suction cups to different positions, the Piab venturi pumps were instead found to be the cause of the issues. Removing the venturi pumps and disassembling them revealed that dust particles had become prevalent within the pump filters, restricting airflow and reducing the output suction power, see Figure 50. Because the venturi pumps produce a very minimal amount of suction airflow, the dust was determined to be due to the residues found in the compressed air supply, and not from the external environment. It was unknown if the in-house compressed air supply used for operation was continuously filtered for dust, so this was a plausible cause for having clogged venturi pumps. Once the venturi pumps were thoroughly cleaned, re-assembled, and re-installed, they performed as expected and suction power to each suction cup was restored. This system failure demonstrates that even if some of the suction cups leak or lose suction, the system will still maintain its position, though it may not be able to move. The multiple suction cups and venturi pumps installed in parallel make sure that total failure does not happen as a result of a few small individual failures.

Figure 50. Venturi pumps, removed from their housing, are covered with residue from the air supply lines.

During one vertical drive test, the safety rope became intertwined with the air supply while attempting a 360 degree maneuver, in such a way that it choked the input flow of air to the venturi pumps. Consequentially, this caused complete failure and detachment of the robot from the driving surface. Fortunately, the safety rope which caused the event to happen prevented Otto from hitting the ground. This was the only complete failure

experienced during testing, and the safety rope used in future tests was changed to be safer and less obstructive to the robot during operation.

Lastly, since Otto's adhesion relies on a sliding mechanism and its turning method is of a skid steering maneuver, it is expected that a certain amount of surface wear will be apparent on the PTFE and wheel materials. Although there were no controlled tests for these wear performances, a visual inspection of the components showed that a fair amount of wear occurred on the wheels during skid steer maneuvers and a very light amount of wear on the PTFE. The wheels tend to leave traces of white residue onto the drive surface after a series of successive skid steer maneuvers, whereas the PTFE did not show signs of significant wear on its surfaces.

7 COST ANALYSIS

This section gives a detailed description of the costs associated with this project, and a cost breakdown of each subgroup. The amount of money spent was thoroughly considered before each purchase to make sure that the parts ordered were correct and essential to the completion of the project.

Table 3 shows a complete bill of materials, broken down into subsections labeled Suction Cup Assembly, Drivetrain, Motor and Gearhead, and Chassis. The most expensive sub-system is the Motor and Gearhead, mostly in part due to the two Thomson XTRUE gearheads at $485.00 each. If Electroimpact had not provided the Piab venturi pumps, FANUC β iS 0.5 motors and the motor controller, the project budget of $2500 would have been well surpassed. As seen at the bottom of Table 3, the total cost of purchased hardware for Otto was $1944.73, which was under budget.

Table 3. Bill of Materials.

No.	Parts	Part Description	ID #	Vendor	Price Per Item	QTY	Cost
			Suction Cup Assembly				
1	Bellow Suction Cup	3.07" 1.5 Bellow Cup	B1.5-78-NBR	Anver	$13.89	12	$166.68
2	Fitting	G 1/8" Male	HS18G	Anver	$5.48	12	$65.76
3	Fitting	G 1/8" Female to Female	HS18-18F-G	Anver	$4.25	12	$51.00
4	Mount Rod	M5 Female to G 1/8" Male, Mount Rod SLSA-1, 2.00 in.	VX18M5-200-51	Anver	$4.50	12	$54.00
5	Press-fit Adapter	6mm Tube OD x G 1/8" Female	5225K604	McMaster	$5.28	12	$63.36
7	Cup Mounting Plate	6061 Alloy Aluminum 2'x 1'	---	---	$0.00	1	$0.00
8	Double Fastener	Double End-Feed Fasteners, Cup Mount Plate 4/pack	47065T147	McMaster	$4.29	3	$12.87
9	Adhesive	3M industrial adhesive sheet 12"x12"	9474LE 300LSE	Amazon	$13.95	3	$41.85
10	Low Friction Material	PTFE 12"x12"	---	Amazon	$10.93	3	$32.79
11	Pneumatic Hose	8 mm clear hoses	---	Electroimpact	$0.00	2	$0.00
12	Hose Connectors	T shaped push connectors	---	Electroimpact	$0.00	12	$0.00
13	Venturi Pumps	Piab venturi pumps	---	Electroimpact	$0.00	12	$0.00
					Subgroup Total:	**$488.31**	
			DriveTrain				
14	Shaft Collar	Black-Oxide 1/2" Shaft Collar	6435K14	McMaster	$1.97	8	$15.76
15	Drive Shafts	1/2" Keyed Shafts, 24" Long	1497K31	McMaster	$29.37	1	$29.37
16	Key	1/8" x 1/8" x 12" steel key	98535A130	McMaster	$2.07	1	$2.07
17	Wheel Screws	10-24 x 3/4" thread-forming screw, 50/pack	98273A260	McMaster	$7.08	1	$7.08
18	Locking Fastener Nut	Thin Nylon-Insert Hex Locknut, 100/pack, 1/4"-20	90566A029	McMaster	$3.65	1	$3.65
19	Wheel Bushing Mat'l	White Delrin rod 1ft.	8572K22	McMaster	$6.32	1	$6.32
20	Bearing	Aluminum-Mounted Bronze Bearing (SAE 840 Bronze)	5912K4	McMaster	$11.11	8	$88.88
21	Bearing Fastener	Round Head Square Neck Bolts, 1/4"-20	---	---	$0.00	8	$0.00
22	Wheel	4" diameter HiGrip wheel	am-2256	AndyMark	$6.00	4	$24.00
23	Wheel hub	500 Key Hub, 6061 Aluminum	am-0077	AndyMark	$10.00	8	$80.00
24	Sprocket	Aluminum Sprocket, #35, 24 Teeth, 3.075 OD	am-0119	AndyMark	$5.50	4	$22.00
25	Chain	#35 Chain, 10 feet long	am-0367	AndyMark	$10.00	1	$10.00
26	Coupler Hub A	Coupler Hub #1, 1/2", Drive Shaft, size C	6408K12	McMaster	$5.61	2	$11.22
27	Coupler Hub B	Coupler Hub #2, 14 mm , Gearhead, size C	6413K12	McMaster	$5.61	2	$11.22
28	Coupler Spider	Coupling Spider, size C, Hytrel	6408K93	McMaster	$11.12	2	$22.24
					Subgroup Total:	**$333.81**	
			Motor and Gearhead				
29	Gearhead and coupler	Thomson Industries - Xtrue Gearhead (20:1) and Redimount Motor Mount Coupling System	XT060-030-0 RM060-16	Thomson Industries	$485.00	2	$970.00
30	Motor Mounting Plate	6061 Alloy Aluminum, 6" X 3" Plate	---	---	$0.00	1	$0.00
31	Motor Mount Bracket 1	Large Angle Brackets	---	---	$0.35	4	$1.40
32	Motor Mount Bracket 2	Small Angle Brackets	---	---	$0.15	8	$1.20
33	Motor Rear Mount	Steel sheet metal	---	---	$0.00	2	$0.00
34	Carriage bolts	Square neck bolts 1/4" - 20 thread, 1/2" long	---	Ace Hardware	$0.20	24	$4.80
35	Hex bolts	Cap screw, 1/4" - 20 thread, 3/4" long	---	Ace Hardware	$0.20	4	$0.80
36	Hex bolts	Cap screw, 1/4" - 20 thread, 1" long	---	Ace Hardware	$0.25	4	$1.00
37	Drive Motors	FANUC Beta iS 0.5/6000 Motor	-	Electroimpact	$0.00	2	$0.00
38	Motor Controller	Motor Controller	-	Electroimpact	$0.00	1	$0.00
					Subgroup Total:	**$979.20**	
			Chassis				
39	Framing	1" x 1" T-Slot Stock Frame, 2 ft.	47065T101	McMaster	$8.35	7	$58.45
40	T-style connector plates	Aluminum mounting plates	---	---	$0.00	4	$0.00
41	Carriage bolts	Square neck bolts 1/4" - 20 thread, 3/4" long	---	Ace Hardware	$0.20	12	$2.40
42	Washer	M7 ID steel washer	---	Ace Hardware	$0.10	12	$1.20
43	Joint Fastener	Adjustable 90 fastener	47065T153	McMaster	$3.39	24	$81.36
					Subgroup Total:	**$143.41**	
					Total Cost	***$1,994.73***	

8 IMPROVEMENTS & CONCLUSION

Because this prototype was a proof-of-concept, using T-slotted aluminum framing was very beneficial because it was easy to work with and modular. In the future, however, navigating away from this would be beneficial to weight savings, and potentially structural integrity. A more realized vision may have a simpler frame with specific mounting points instead of a modular frame.

Another improvement could be made to the PTFE modified suction cups. In one instance, the PTFE material separated from the rubber suction cup, when it slid over a surface irregularity. It may be more appropriate to mold the suction cups with the PTFE portion embedded onto the rubber bellows. This would create a continuous part, and eliminate the problem of material separation.

Off-the shelf thermoplastic polyurethane wheels, with deep cogs were used because of its stiffness and high friction characteristics. The tread in this iteration of the wheel was optimized for motion on non-smooth surface, like carpet. Overall, this style of wheel worked very well, but using a full surfaced wheel would allow for less slippage and less wheel wear, and potentially higher carrying capacity.

Finally, it should be important to note that Otto is a scaled down proof-of-concept wall driving unit. In the future, when this is scaled up, the forces will be as well, and appropriate roller bearing, and similar components should be used in lieu of the ones selected for this relatively mild and inexpensive case. Future iterations or scaled up versions should be able to support tools, machinery, or any attachments which can utilize the full range of Otto's capabilities.

9 REFERENCES

APPENDIX A: TEST RESULTS

SUCTION CUP FORCE TEST

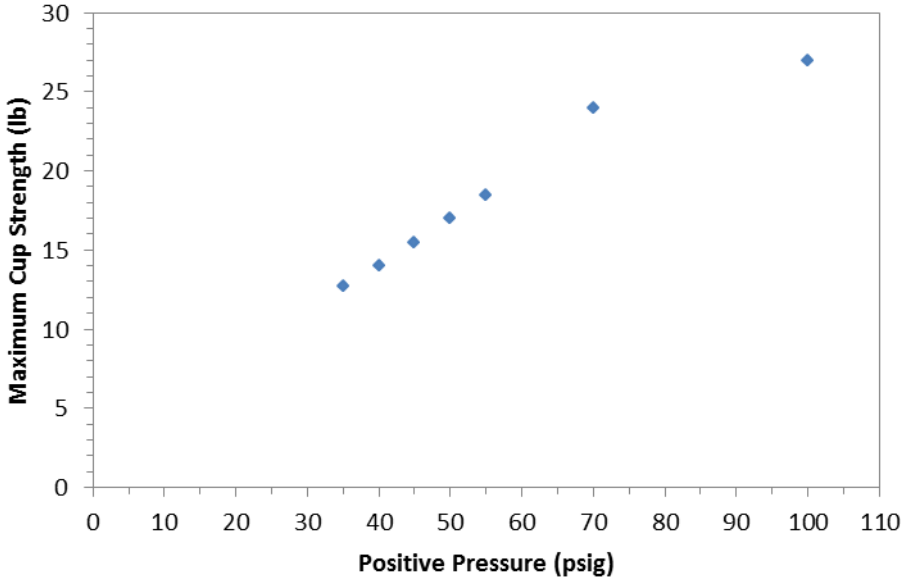

Figure 51. Maximum cup holding force vs. supplied inlet positive pressure.

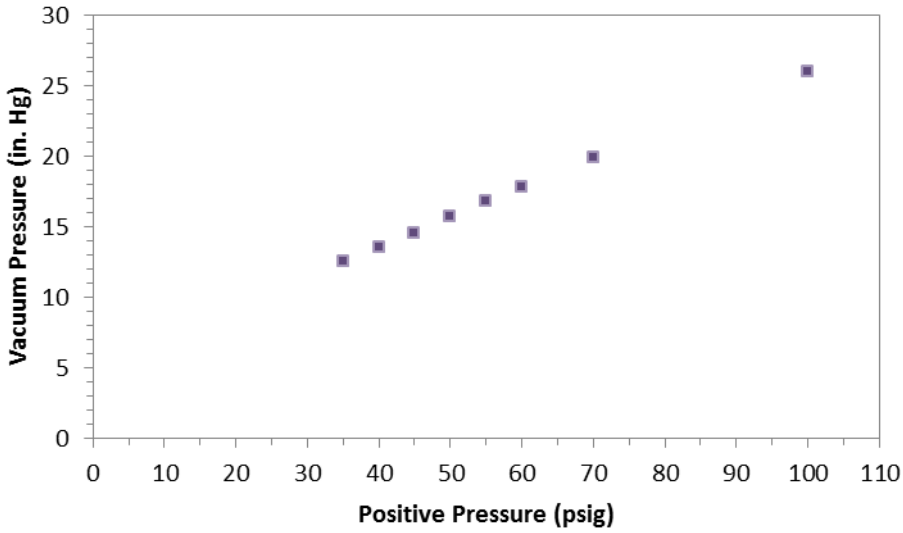

Figure 52. Negative pressure generated by suction cup assembly vs. inlet positive pressure.

SUCTION CUP DISPLACEMENT TEST

Table 4. Data collected from bellow suction cup displacement test at 50 psig.

Weight (g)	% of Total Weight	Edge Location Displacement (cm)				Average Displacement (cm)
		A	B	C	D	
3765	43	5.40	5.40	5.40	5.40	5.40
5765	66	5.50	5.60	5.50	5.50	5.53
6465	74	5.55	5.65	5.60	5.55	5.59
7246	82	5.65	5.75	5.65	5.65	5.68
8046	91	5.70	5.80	5.80	5.70	5.75
8500	97	6.15	6.00	5.95	6.05	6.04
8795	100	6.40	6.30	6.30	6.35	6.34
Total: 19.4 (lb)						

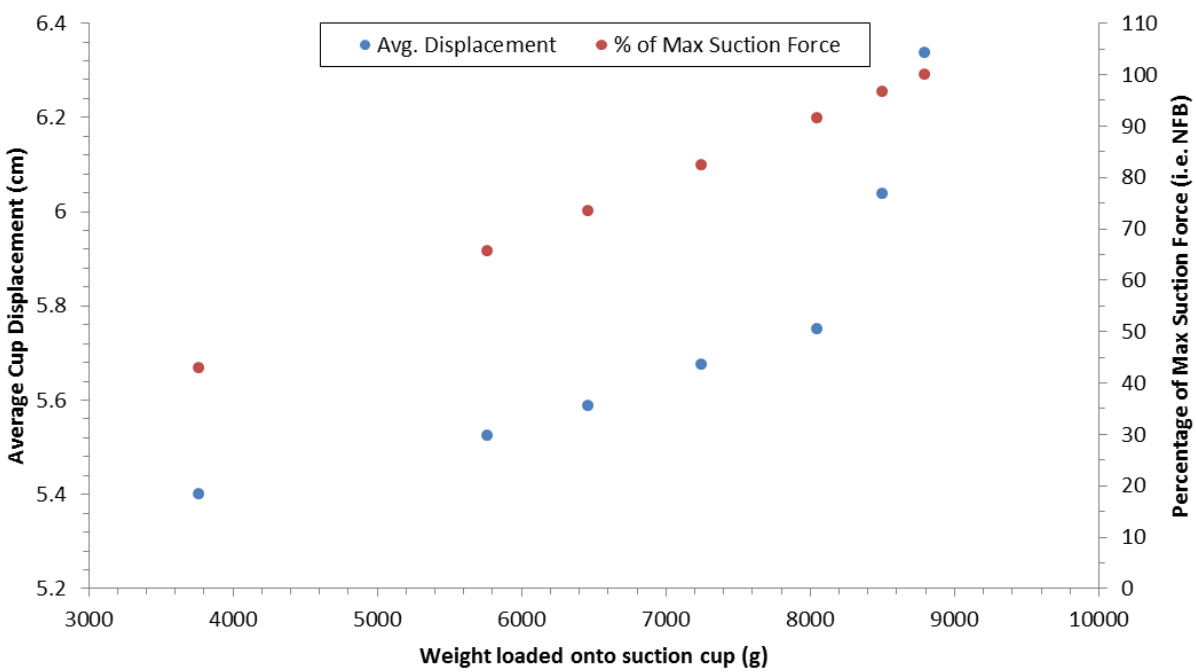

Figure 53. Bellow suction cup displacement test at 50 psig.

Table 5. Data collected from bellow suction cup displacement test at 60 psig.

Weight (g)	% of Total Weight	Edge Location Displacement (cm)				Average Displacement (cm)
		A	B	C	D	
3765	35	5.30	5.30	5.30	5.35	5.31
6715	63	5.50	5.60	5.60	5.50	5.55
7010	66	5.50	5.60	5.60	5.50	5.55
7810	73	5.65	5.70	5.60	5.55	5.63
8591	81	5.70	5.75	5.60	5.65	5.68
9291	87	5.80	5.85	5.70	5.65	5.75
9586	90	5.80	5.90	5.80	5.70	5.80
9881	93	6.25	6.15	5.95	6.05	6.10
10176	96	6.50	6.30	6.30	6.20	6.33
10276	97	6.55	6.40	6.40	6.30	6.41
10376	98	6.60	6.50	6.50	6.35	6.49
10476	99	6.70	6.55	6.55	6.45	6.56
10635	100					
Total: 23.4 (lb)						

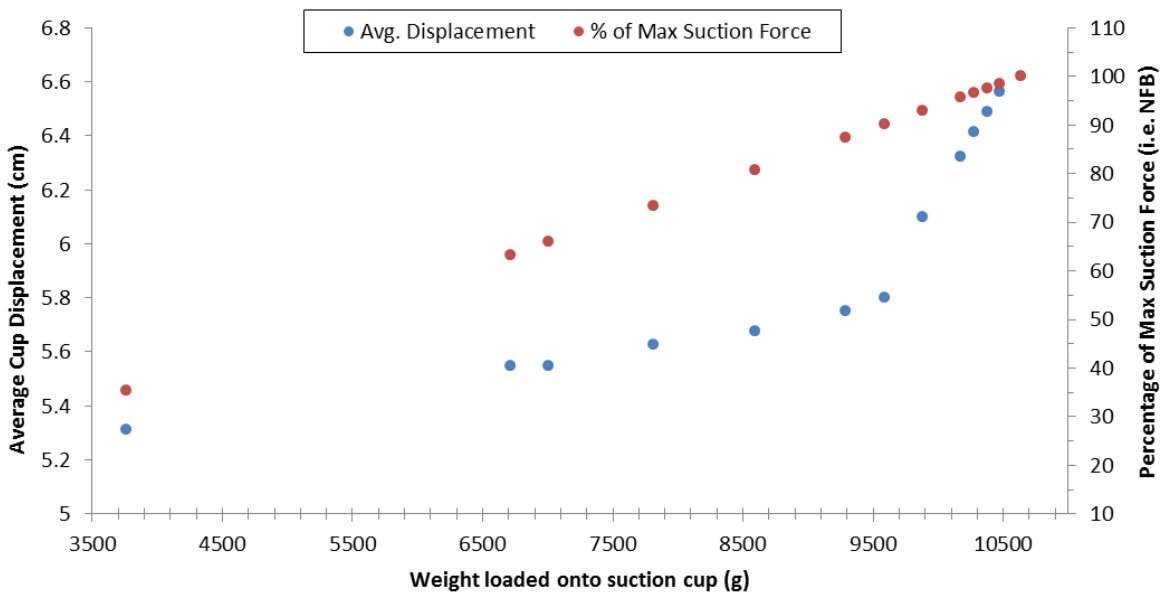

Figure 54. Bellow suction cup displacement test at 60 psig.

Table 6. Data collected from bellow suction cup displacement test at 70 psig.

Weight (g)	% of Total Weight	Edge Location Displacement (cm)				Average Displacement (cm)
		A	B	C	D	
3765	31	5.20	5.30	5.30	5.40	5.27
4565	38	5.25	5.40	5.35	5.40	5.33
5019	42	5.30	5.40	5.35	5.40	5.35
6019	50	5.40	5.50	5.40	5.35	5.43
7219	60	5.60	5.50	5.45	5.40	5.52
8019	67	5.65	5.55	5.55	5.50	5.58
8315	69	5.70	5.60	5.55	5.50	5.62
9915	82	5.85	5.75	5.70	5.60	5.77
10696	89	6.00	5.85	5.80	5.70	5.88
10991	91	6.00	5.90	5.85	5.75	5.92
11286	94	6.10	5.95	5.95	5.80	6.00
11740	98	6.45	6.20	6.25	6.15	6.30
12035	100	6.80	6.50	6.65	6.45	6.65
Total: 26.5 (lb)						

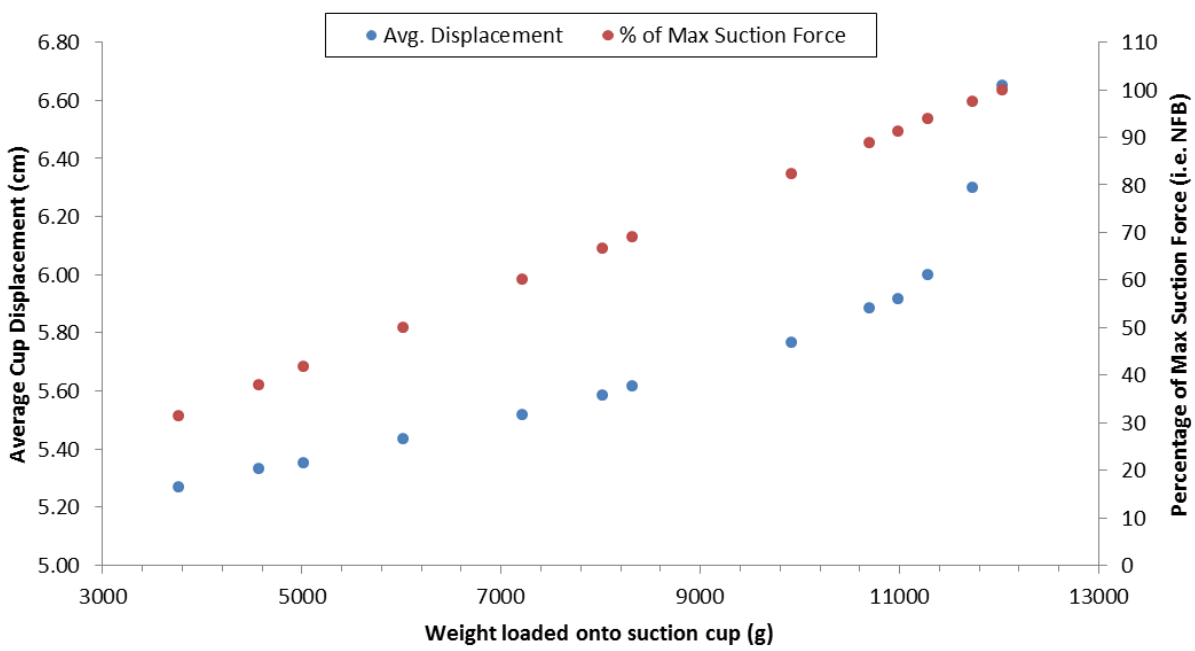

Figure 55. Bellow suction cup displacement test at 70 psig.

APPENDIX B: DETAILED PART DRAWINGS

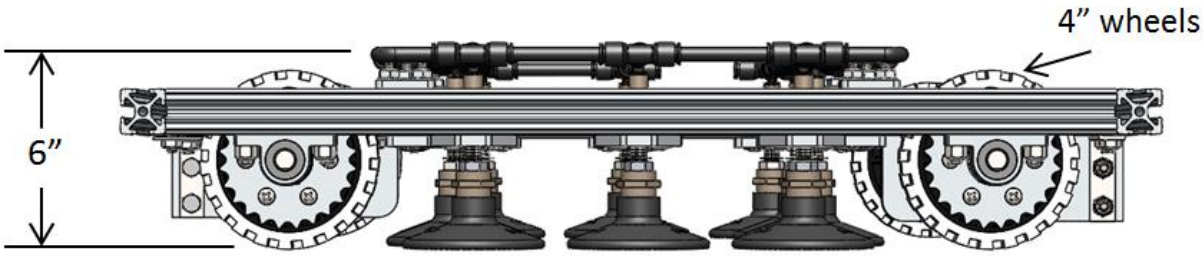

Figure 56. Side CAD view, showing basic important dimensions.

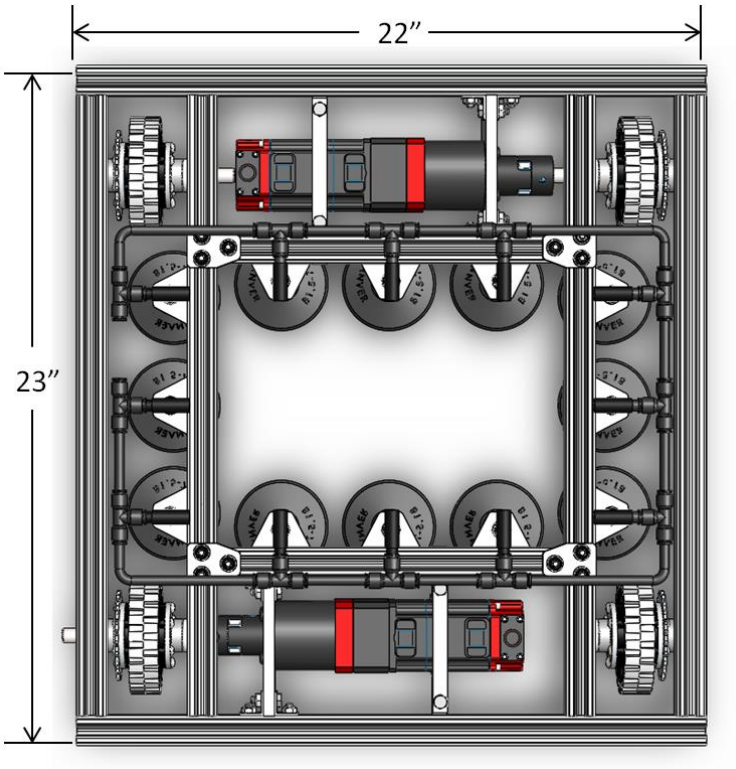

Figure 57. Top CAD view, showing basic important dimensions.

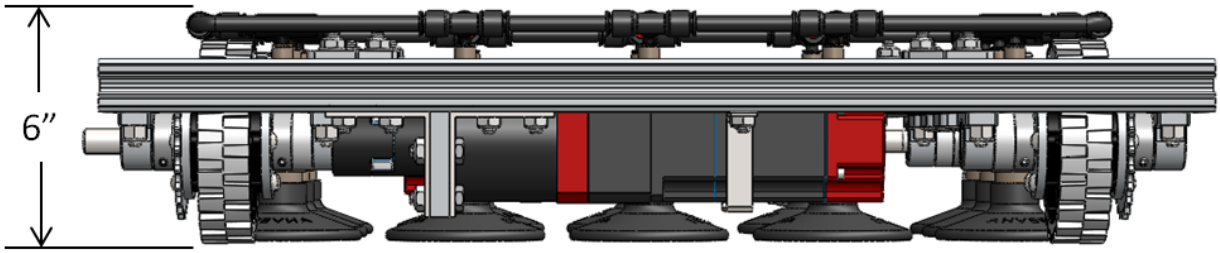

Figure 58. Front CAD view, showing basic important dimensions.

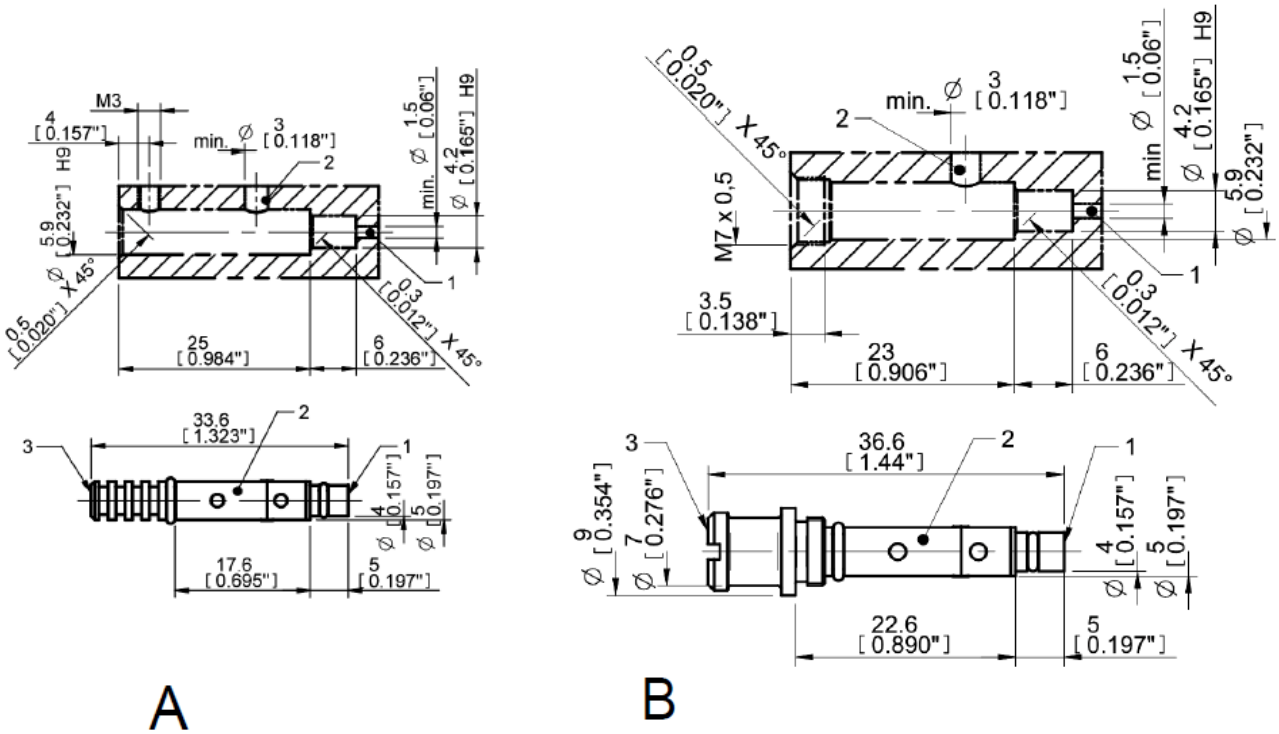

Figure 59. Piab Venturi Pump detailed drawings.

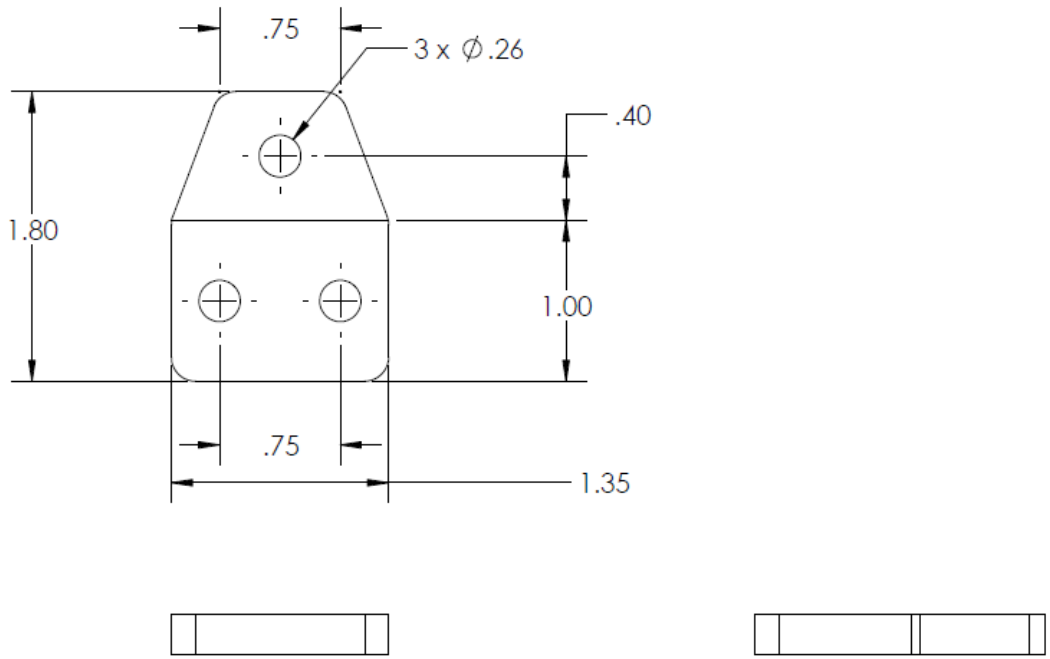

		UNLESS OTHERWISE SPECIFIED:		NAME	DATE
		DIMENSIONS ARE IN INCHES TOLERANCES: FRACTIONAL ± ANGULAR: MACH ± BEND ± TWO PLACE DECIMAL ± THREE PLACE DECIMAL ±	DRAWN		
			CHECKED		
			ENG APPR.		
			MFG APPR.		
		INTERPRET GEOMETRIC TOLERANCING PER:	Q.A.		
		MATERIAL	COMMENTS:		
NEXT ASSY	USED ON	FINISH			
APPLICATION		DO NOT SCALE DRAWING			

TITLE:

SIZE	DWG. NO.	REV
A	T-shape connectors	
SCALE: 1:1	WEIGHT:	SHEET 1 OF 1

PROPRIETARY AND CONFIDENTIAL

THE INFORMATION CONTAINED IN THIS DRAWING IS THE SOLE PROPERTY OF <INSERT COMPANY NAME HERE>. ANY REPRODUCTION IN PART OR AS A WHOLE WITHOUT THE WRITTEN PERMISSION OF

SolidWorks Student License
Academic Use Only

4 3 2 1

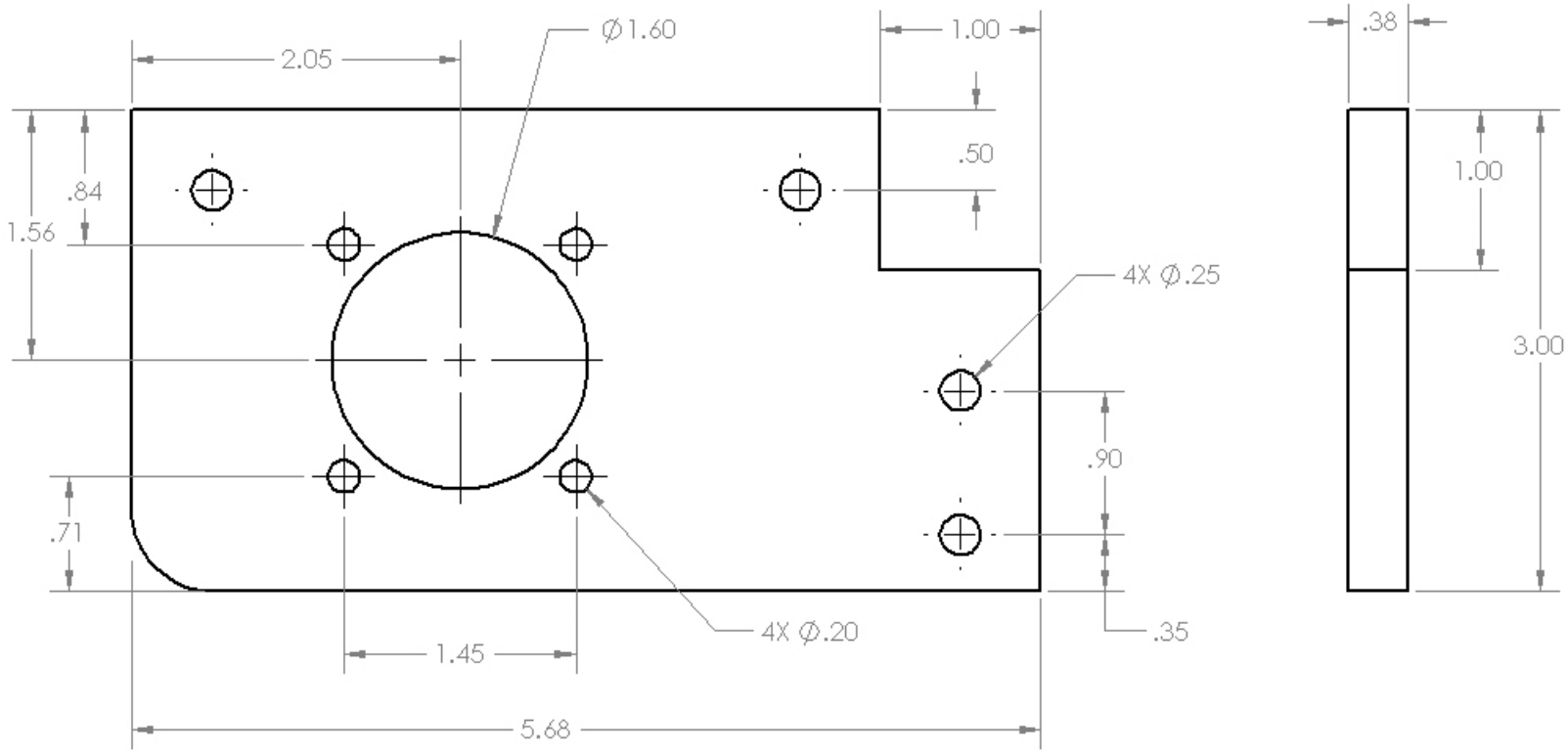

		UNLESS OTHERWISE SPECIFIED:		NAME	DATE
		DIMENSIONS ARE IN INCHES TOLERANCES: FRACTIONAL ± ANGULAR: MACH ± BEND ± TWO PLACE DECIMAL ± THREE PLACE DECIMAL ±	DRAWN		
			CHECKED		
			ENG APPR.		
			MFG APPR.		
		INTERPRET GEOMETRIC TOLERANCING PER:	Q.A.		
		MATERIAL	COMMENTS:		
NEXT ASSY	USED ON	FINISH			
APPLICATION		DO NOT SCALE DRAWING			

PROPRIETARY AND CONFIDENTIAL
THE INFORMATION CONTAINED IN THIS DRAWING IS THE SOLE PROPERTY OF <INSERT COMPANY NAME HERE>. ANY REPRODUCTION IN PART OR AS A WHOLE WITHOUT THE WRITTEN PERMISSION OF <INSERT COMPANY NAME HERE> IS PROHIBITED.

TITLE:

Motor Mounting Plate

SIZE	DWG. NO.	REV
A		
SCALE: 1:1	WEIGHT:	SHEET 1 OF 1

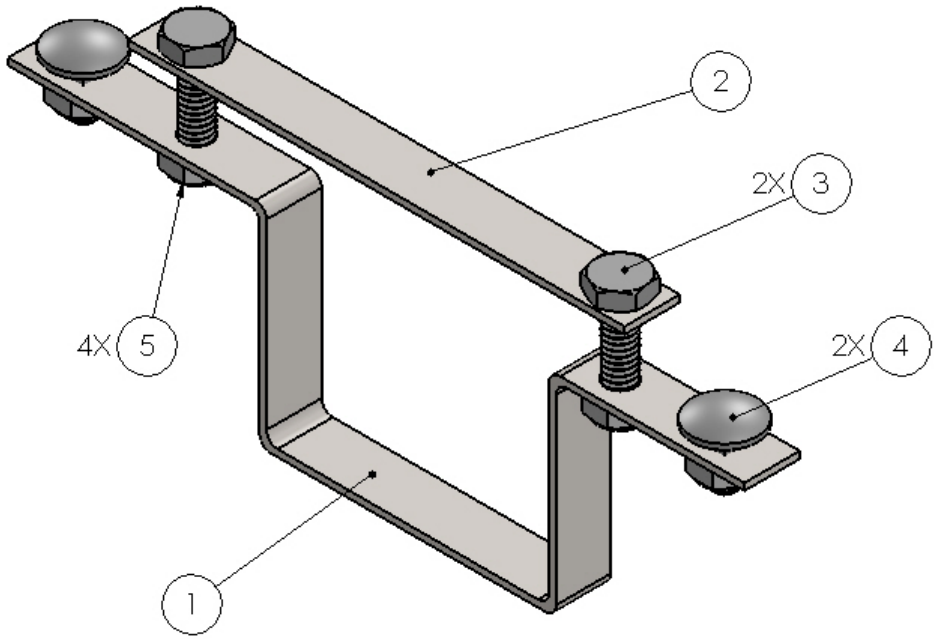

SCALE 1 : 1

ITEM NO.	PART NUMBER	QTY.
1	Rear motor support	1
2	Rear motor support2	1
3	91309A542	2
4	93180A208	2
5	94945A205	4

PROPRIETARY AND CONFIDENTIAL
THE INFORMATION CONTAINED IN THIS DRAWING IS THE SOLE PROPERTY OF <INSERT COMPANY NAME HERE>. ANY REPRODUCTION IN PART OR AS A WHOLE WITHOUT THE WRITTEN PERMISSION OF <INSERT COMPANY NAME HERE> IS PROHIBITED.

NEXT ASSY | USED ON
APPLICATION

UNLESS OTHERWISE SPECIFIED:
DIMENSIONS ARE IN INCHES
TOLERANCES:
FRACTIONAL ±
ANGULAR: MACH ± BEND ±
TWO PLACE DECIMAL ±
THREE PLACE DECIMAL ±
INTERPRET GEOMETRIC TOLERANCING PER:
MATERIAL
FINISH
DO NOT SCALE DRAWING

	NAME	DATE
DRAWN		
CHECKED		
ENG APPR.		
MFG APPR.		
Q.A.		

COMMENTS:

TITLE:
Motor Rear Mount Assembly

SIZE A | DWG. NO. | REV

SCALE: 1:2 | WEIGHT: | SHEET 1 OF 3

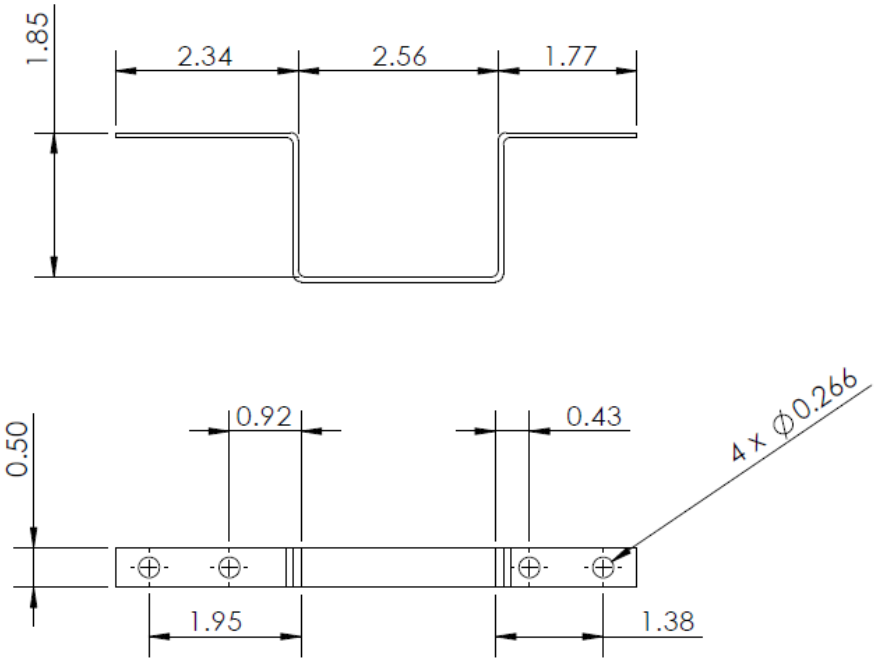

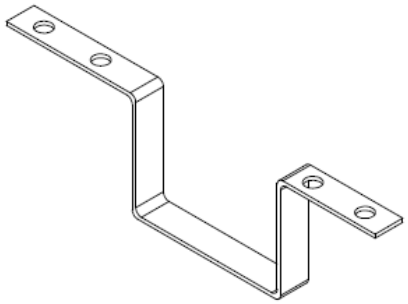

		UNLESS OTHERWISE SPECIFIED:		NAME	DATE
		DIMENSIONS ARE IN INCHES TOLERANCES: FRACTIONAL± ANGULAR: MACH± BEND ± TWO PLACE DECIMAL ± THREE PLACE DECIMAL ±	DRAWN		
			CHECKED		
			ENG APPR.		
			MFG APPR.		
		INTERPRET GEOMETRIC TOLERANCING PER:	Q.A.		
		MATERIAL	COMMENTS:		
NEXT ASSY	USED ON	FINISH			
APPLICATION		DO NOT SCALE DRAWING			

TITLE:

SIZE	DWG. NO.	REV
A	Rear motor support	
SCALE: 1:2	WEIGHT:	SHEET 1 OF 1

PROPRIETARY AND CONFIDENTIAL

THE INFORMATION CONTAINED IN THIS DRAWING IS THE SOLE PROPERTY OF <INSERT COMPANY NAME HERE>. ANY REPRODUCTION IN PART OR AS A WHOLE WITHOUT THE WRITTEN PERMISSION OF

SolidWorks Student License
Academic Use Only

4 3 2 1

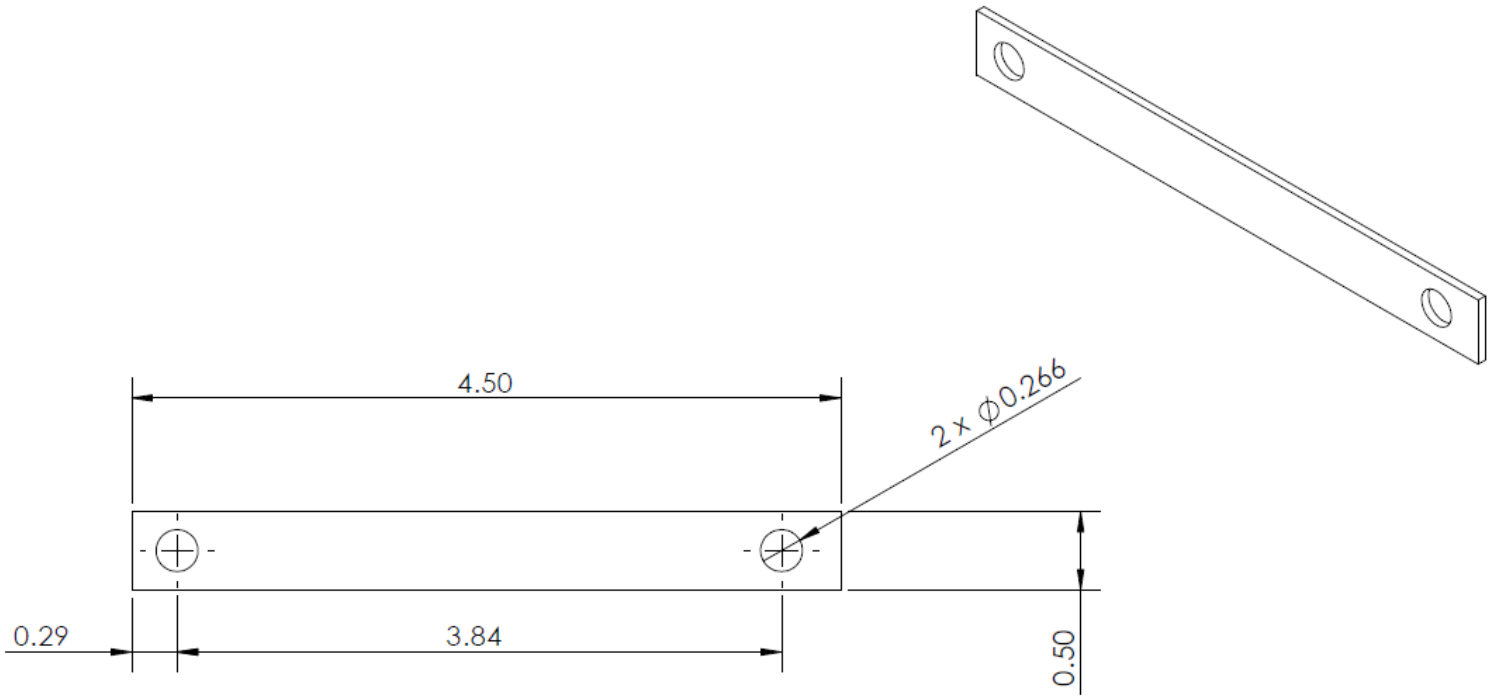

		UNLESS OTHERWISE SPECIFIED:		NAME	DATE
		DIMENSIONS ARE IN INCHES TOLERANCES: FRACTIONAL ± ANGULAR: MACH ± BEND ± TWO PLACE DECIMAL ± THREE PLACE DECIMAL ±	DRAWN		
			CHECKED		
			ENG APPR.		
			MFG APPR.		
		INTERPRET GEOMETRIC TOLERANCING PER:	Q.A.		
		MATERIAL	COMMENTS:		
NEXT ASSY	USED ON	FINISH			
APPLICATION		DO NOT SCALE DRAWING			

TITLE:

SIZE	DWG. NO.	REV
A	Rear motor support2	
SCALE: 1:1	WEIGHT:	SHEET 1 OF 1

PROPRIETARY AND CONFIDENTIAL

THE INFORMATION CONTAINED IN THIS DRAWING IS THE SOLE PROPERTY OF <INSERT COMPANY NAME HERE>. ANY REPRODUCTION IN PART OR AS A WHOLE WITHOUT THE WRITTEN PERMISSION OF

SolidWorks Student License
Academic Use Only

4 3 2 1

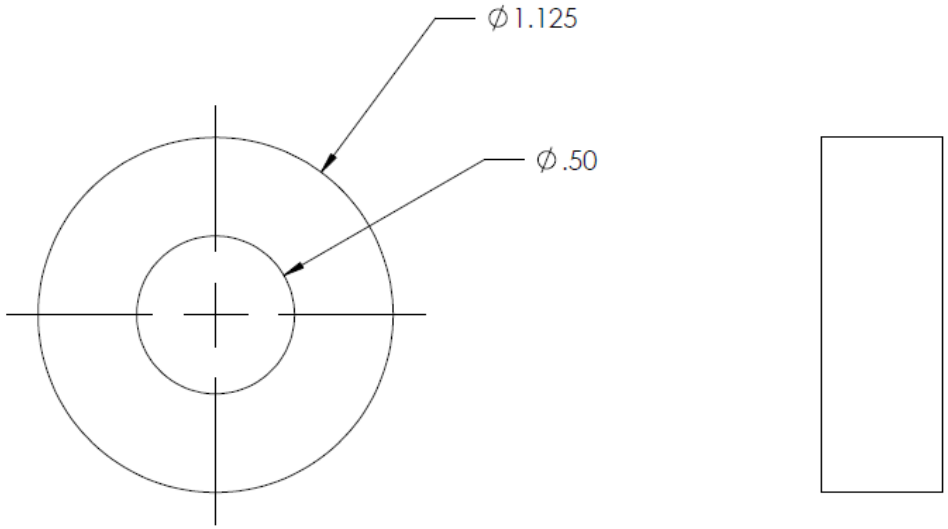

		UNLESS OTHERWISE SPECIFIED:		NAME	DATE
		DIMENSIONS ARE IN INCHES TOLERANCES: FRACTIONAL ± ANGULAR: MACH ± BEND ± TWO PLACE DECIMAL ± THREE PLACE DECIMAL ±	DRAWN		
			CHECKED		
			ENG APPR.		
			MFG APPR.		
		INTERPRET GEOMETRIC TOLERANCING PER:	Q.A.		
		MATERIAL	COMMENTS:		
NEXT ASSY	USED ON	FINISH			
APPLICATION		DO NOT SCALE DRAWING			

TITLE:

SIZE	DWG. NO.	REV
A	Shaft Bushing, Delrin	
SCALE: 2:1	WEIGHT:	SHEET 1 OF 1

PROPRIETARY AND CONFIDENTIAL
THE INFORMATION CONTAINED IN THIS DRAWING IS THE SOLE PROPERTY OF <INSERT COMPANY NAME HERE>. ANY REPRODUCTION IN PART OR AS A WHOLE WITHOUT THE WRITTEN PERMISSION OF

SolidWorks Student License
Academic Use Only

4 3 2 1

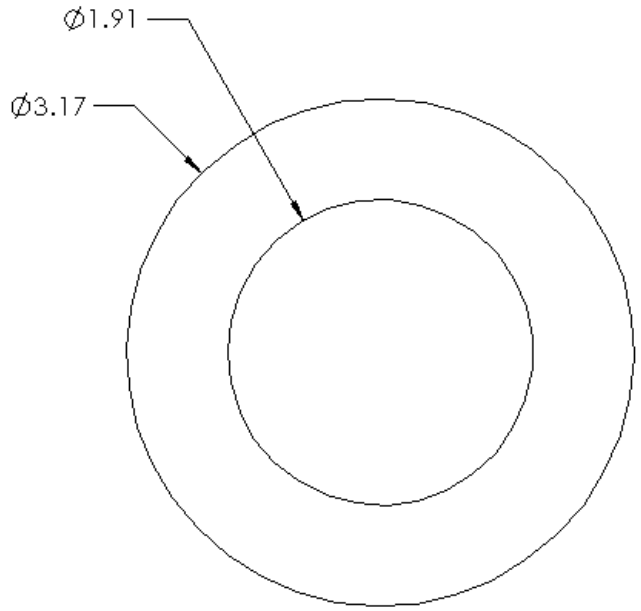

		UNLESS OTHERWISE SPECIFIED:		NAME	DATE
		DIMENSIONS ARE IN INCHES TOLERANCES: FRACTIONAL ± ANGULAR: MACH ± BEND ± TWO PLACE DECIMAL ± THREE PLACE DECIMAL ±	DRAWN		
			CHECKED		
			ENG APPR.		
			MFG APPR.		
		INTERPRET GEOMETRIC TOLERANCING PER:	Q.A.		
		MATERIAL 1/64" thick PTFE	COMMENTS:		
NEXT ASSY	USED ON	FINISH			
APPLICATION		DO NOT SCALE DRAWING			

TITLE:

PTFE Laminate

SIZE	DWG. NO.	REV
A		

SCALE: 1:1	WEIGHT:	SHEET 1 OF 1

PROPRIETARY AND CONFIDENTIAL

THE INFORMATION CONTAINED IN THIS DRAWING IS THE SOLE PROPERTY OF <INSERT COMPANY NAME HERE>. ANY REPRODUCTION IN PART OR AS A WHOLE WITHOUT THE WRITTEN PERMISSION OF <INSERT COMPANY NAME HERE> IS PROHIBITED.

PART NUMBER VERSION STATUS				

DRAWING REVISIONS		
REV	DESCRIPTION	APPROVED
0	ORIGINAL ISSUE	BLH 01-30-07

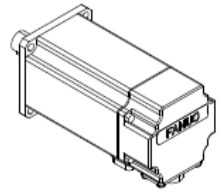

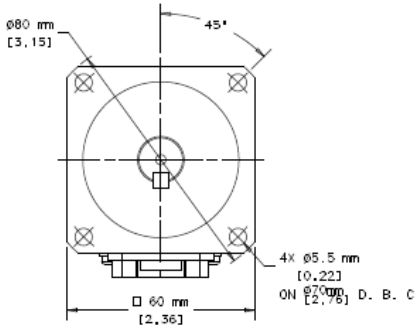

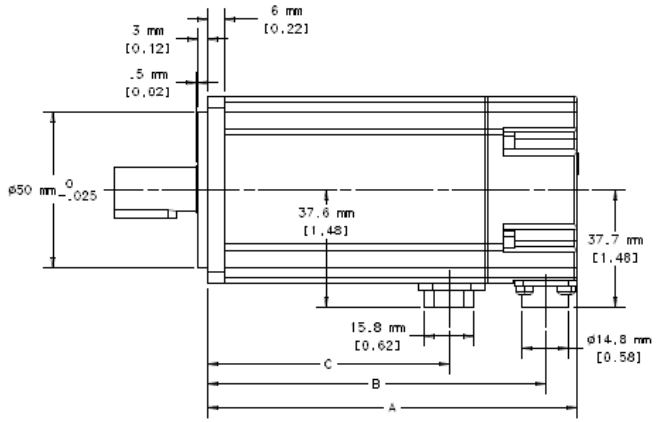

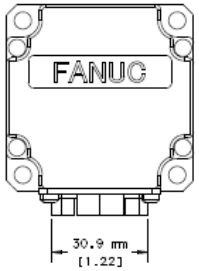

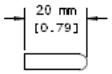

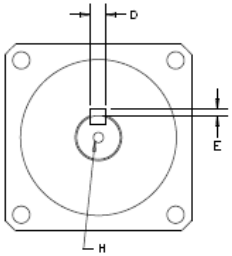

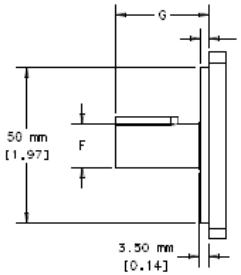

OPTION:
STRAIGHT SHAFT
WITH KEYWAY
A06B-11□-B203
-B503

NOTES:

SHAFT DIA RUNOUT	MAX 0.02mm
RABBET DIA. ECCENTRICITY	MAX 0.04mm
MOUNTING FACE RUNOUT	MAX. 0.06mm
MAXIMUM RADIAL LOAD	196N (20kgf) [44lb]

MODEL	A	B	C	D	E	F	G	H
β0.4is	75	65	34.5	$3^{0}_{-.005}$	$1.2^{0}_{-.1}$	$9^{0}_{-.009}$	25	M3X6DEPTH
β0.5is	89.5	79.5	49	$3^{0}_{-.005}$	$1.2^{0}_{-.1}$	$9^{0}_{-.009}$	25	M3X6DEPTH
β1is	118.5	108.5	78	$5^{0}_{-.05}$	$2^{0}_{-.1}$	$14^{0}_{-.011}$	30	M4X10DEPTH

GE FANUC AUTOMATION N.A. INC. CONFIDENTIAL AND PROPRIETARY INFORMATION

DESIGN BY: BOBBY L HICKS	DATE: 01-04-07	GE FANUC Automation North America, Inc. Charlottesville, Va. U.S.A.	TITLE: β0.4is, β0.5is AND β1is FANUC MOTOR DIMENSIONS CNC
APPROVED BY: S. GLENN THOMAS	DATE: 01-30-07		
ISSUED:	THIRD ANGLE PROJECTION	CAD INFORMATION: CNC MISC	DRG. NO. A06B-011□-B203
			PLOT SCALE 1.0 — SHEET NO. 1 — CONT. ON FL

621A

DIST TO

Plotted : 01-30-07 11:12:22 a.m.

APPENDIX C: VENDOR COMPONENT SPECIFICATIONS AND DATA SHEETS

VENTURI PUMP

piab

Xi2.5-2

- Two-stage COAX® cartridge - MICRO - probably the world's smallest multistage vacuum ejector.
- High vacuum flow at deep vacuum levels, to 27.2 -inHg.
- Large vacuum flow in relation to energy consumption.
- Quick response time when deep vacuum is needed.
- Good for handling sealed materials.
- Used in P2010 and VGS™2010.

Technical data

Description	Unit	Value
Feed pressure, max.	psi	101.5
Temperature range	°F	14-122
Weight	oz	0.05-0.08
Material		Al, NBR, PA, SS, TPE

Vacuum flow

Feed pressure*	Air consumption	Vacuum flow (scfm) at different vacuum levels (-inHg)									Max vacuum
psi	scfm	0	3	6	9	12	15	18	21	24	-inHg
65	0.25	0.49	0.32	0.17	0.11	0.08	0.06	0.04	0.02	0.006	26.3
72.5	0.28	0.51	0.36	0.21	0.13	0.08	0.06	0.04	0.02	0.02	27.2
87	0.32	0.51	0.34	0.19	0.11	0.08	0.06	0.04	0.02	0.01	26.9

**Feed pressure tolerance, +/- 1.45 psi*

Evacuation time

Feed pressure*	Air consumption	Evacuation time (s/cf) to reach different vacuum levels (-inHg)								Max vacuum
psi	scfm	3	6	9	12	15	18	21	24	-inHg
65	0.25	15.0	39.7	83	147	227	340	530	966	26.3
72.5	0.28	13.9	34.8	70.3	127	207	320	510	793	27.2
87	0.32	14.2	36.8	77.3	142	221	334	524	901	26.9

**Feed pressure tolerance, +/- 1.45 psi*

Blow flow

Feed pressure	Air consumption	Blow flow (scfm) at different pressure levels (psi)									Max pressure
psi	scfm	0	2	3	4	6	7	9	10	12	psi
87	0.32	0.78	0.70	0.55	0.44	0.44	0.42	0.40	0.36	0.32	13

MOTOR

Model βi S 0. 5/6000 Specification A06B-0115-B□03

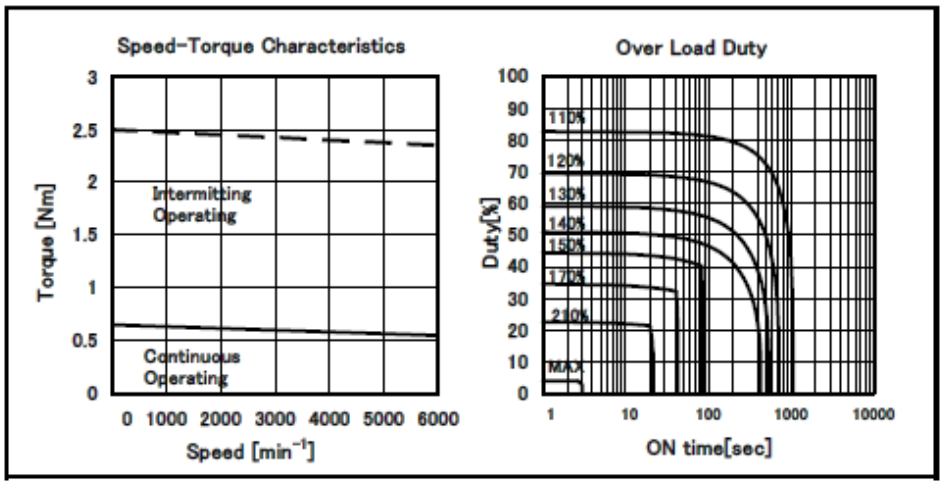

Data sheet

Parameter	Symbol	Value			Unit
Stall Torque (*)	Ts	0.65 6.6			Nm kgfcm
Stall Current (*)	Is	2.9			A (rms)
Rated Output (*)	Pr	0.35 0.47			kW HP
Rating Speed	Nr	6000			min^{-1}
Maximum Speed	Nmax	6000			min^{-1}
Maximum Torque (*)	Tmax	2.5 26			Nm kgfcm
Rotor Inertia	Jm	0.000018 0.000184			kgm^2 $kgfcms^2$
Rotor Inertia (with Brake)	Jm	0.000027 0.000276			kgm^2 $kgfcms^2$
Torque constant (*)	Kt	0.223 2.28			Nm/A (rms) kgfcm/A (rms)
Back EMF constant (1phase) (*)	Ke Kv	7.7 0.074			V (rms)/1000 min^{-1} V (rms)sec/rad
Armature Resistance (1 phase) (*)	Ra	0.85			Ω
Mechanical time constant	tm	0.0009			s
Thermal time constant	tt	10			min
Static friction	Tf	0.04 0.4			Nm kgfcm
Weight	w	1			kg
Weight (with Brake)	w	1.4			kg
Max. Current of Servo Amp.	Imax	20			A (peak)

(*) The values are the standard values at 20℃ and the tolerance is ±10%.
The speed-torque characteristics very depending on the type of software, parameter setting, and input voltage of the digital servo software. (The above figures show average values.)

MICRON

XTRUE™

True Planetary™ Gearheads

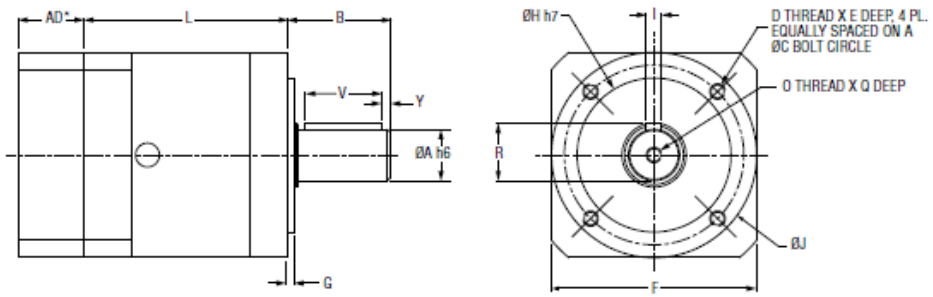

*AD = Adapter Length
Adapter Length will vary depending on motor. Consult customer service for details.

Dimensions

Part Number	A Output Shaft Diameter mm [in]	B Output Shaft Length mm [in]	Y Shaft End Distance mm [in]	V Key Length mm [in]	R Key Height mm [in]	I Key Width mm [in]	H Pilot Diameter mm [in]	J Body Diameter mm [in]	G Pilot Length mm [in]
XT040	10 [0.39]	26 [1.02]	2.5 [0.10]	18 [0.71]	11.2 [0.44]	3 [0.12]	26 [1.02]	40 [1.57]	2 [0.08]
XT060	14 [0.55]	35 [1.37]	2.5 [0.10]	25 [0.98]	16 [0.63]	5 [0.20]	40 [1.57]	60 [2.36]	3 [0.12]
XT080	20 [0.79]	40 [1.57]	4.0 [0.16]	28 [1.10]	22.5 [0.89]	6 [0.24]	60 [2.36]	80 [3.15]	3 [0.12]
XT120	25 [0.98]	55 [2.16]	5.0 [0.20]	40 [1.57]	28 [1.10]	8 [0.31]	80 [3.15]	115 [4.53]	4 [0.16]
XT160	40 [1.57]	87 [3.42]	8.0 [0.32]	65 [2.55]	43 [1.69]	12 [0.47]	130 [5.12]	160 [6.30]	5 [0.20]

Dimensions

Part Number	D Thread	E Thread Depth mm [in]	O Output Shaft Thread	Q Thread Depth mm [in]	F Flange Square mm [in]	L Length mm [in]		C Bolt Circle mm [in]
						3:1 - 10:1	15:1 - 100:1	
XT040	M4	6 [0.24]	M3	9 [0.35]	42 [1.65]	36.5 [1.43]	49.5 [1.94]	34 [1.34]
XT060	M5	8 [0.31]	M5	12 [0.47]	61 [2.40]	51 [2.00]	68 [2.67]	52 [2.05]
XT080	M6	10 [0.39]	M6	16 [0.63]	90 [3.54]	67 [2.64]	90 [3.54]	70 [2.76]
XT120	M10	16 [0.63]	M10	22 [0.87]	119 [4.53]	87.3 [3.44]	179 [4.67]	100 [3.94]
XT160	M12	20 [0.79]	M16	36 [1.42]	142 [5.59]	119.6 [4.71]	168.9 [6.65]	145 [5.71]

Specifications

Part Number	Stages	Backlash (arc-min)	Efficiency	Weight kg	Weight [lbs]	Ratio Availablility
XT040	1 2	13 15	93% 88%	0.45 0.5	[1.0] [1.1]	3:1, 5:1, 10:1 15:1; 25:1, 30:1, 50:1, 100:1
XT060	1 2	13 15	93% 88%	1.0 1.2	[2.2] [2.6]	3:1, 4:1, 5:1, 7:1; 10:1 15:1, 20:1, 25:1, 30:1, 40:1,50:1; 70:1; 100:1
XT080	1 2	13 15	93% 88%	3.0 3.7	[6.6] [8.1]	3:1, 4:1, 5:1, 7:1; 8:1; 10:1 15:1, 20:1, 25:1, 30:1, 40:1, 50:1; 70:1; 80:1; 100:1
XT120	1 2	13 15	93% 88%	5.7 7.3	[12.5] [16.1]	3:1, 4:1, 5:1, 7:1; 10:1 15:1, 20:1, 25:1, 30:1, 40:1, 50:1; 70:1; 100:1
XT160	1 2	13 15	93% 88%	12.8 17.2	[28.2] [37.8]	3:1, 4:1, 5:1, 7:1; 10:1 15:1, 20:1, 25:1, 30:1, 40:1, 50:1; 70:1; 100:1

Specifications subject to change without notice.

XTRUE™

True Planetary™ Gearheads

Performance Specifications

	Part Number	Ratio	20,000 Hour Life T_r (1000 rpm) Nm	[in-lb]	T_r (2000 rpm) Nm	[in-lb]	T_r (3000 rpm) Nm	[in-lb]	T_r (4000 rpm) Nm	[in-lb]	Tpeak Nm	[in-lb]	J kg-cm²	[in-lb-sec²*10⁻⁴]	Torsional Stiffness Nm/arc-min	[in-lb/arc-min]
XT040	XT040-003	3:1	5.2	[46]	4.2	[37]	3.7	[33]	3.4	[30]	15.6	[138]	0.013	[0.12]	0.7	[6.2]
	XT040-005	5:1	6.1	[54]	5.3	[47]	3.6	[32]	4.3	[38]	18.3	[162]	0.005	[0.04]	0.7	[6.2]
	XT040-010	10:1	5.8	[51]	4.6	[41]	4.1	[36]	3.7	[33]	17.2	[152]	0.003	[0.03]	0.7	[6.2]
	XT040-015	15:1	8.4	[74]	6.8	[60]	6.0	[53]	5.5	[49]	25.2	[223]	0.004	[0.04]	0.7	[6.2]
	XT040-025	25:1	9.3	[82]	7.6	[67]	6.7	[59]	6.1	[54]	27.8	[246]	0.004	[0.04]	0.7	[6.2]
	XT040-030	30:1	9.5	[84]	8.4	[74]	7.5	[66]	6.8	[60]	28.6	[253]	0.003	[0.03]	0.7	[6.2]
	XT040-050	50:1	11.3	[100]	9.3	[82]	8.2	[73]	7.6	[67]	33.8	[299]	0.003	[0.03]	0.7	[6.2]
	XT040-100	100:1	8.1	[72]	7.5	[66]	7.1	[63]	6.9	[61]	24.4	[216]	0.003	[0.03]	0.7	[6.2]
XT060	XT060-003	3:1	16	[139]	13	[112]	12	[102]	11	[93]	55	[483]	0.52	[4.6]	1.8	[15.9]
	XT060-004	4:1	20	[177]	17	[149]	15	[130]	14	[121]	46	[409]	0.46	[4.1]	1.8	[15.9]
	XT060-005	5:1	18	[158]	15	[130]	13	[112]	12	[102]	48	[427]	0.46	[4.1]	1.8	[15.9]
	XT060-007	7:1	17	[149]	14	[121]	12	[102]	11	[93]	43	[381]	0.46	[4.1]	1.8	[15.9]
	XT060-010	10:1	16	[139]	15	[130]	14	[121]	13	[112]	47	[418]	0.44	[3.9]	1.8	[15.9]
	XT060-015	15:1	26	[232]	21	[186]	19	[167]	17	[149]	55	[483]	0.46	[4.1]	1.8	[15.9]
	XT060-020	20:1	27	[242]	25	[223]	22	[195]	21	[186]	48	[427]	0.46	[4.1]	1.8	[15.9]
	XT060-025	25:1	25	[223]	23	[204]	20	[177]	19	[167]	55	[483]	0.46	[4.1]	1.8	[15.9]
	XT060-030	30:1	29	[260]	26	[232]	23	[204]	21	[186]	55	[483]	0.46	[4.1]	1.8	[15.9]
	XT060-040	40:1	28	[251]	27	[242]	27	[242]	25	[223]	48	[427]	0.44	[3.9]	1.8	[15.9]
	XT060-050	50:1	26	[232]	25	[223]	25	[223]	23	[204]	55	[483]	0.44	[3.9]	1.8	[15.9]
	XT060-070	70:1	25	[223]	24	[214]	24	[214]	22	[195]	48	[427]	0.44	[3.9]	1.8	[15.9]
	XT060-100	100:1	21	[186]	20	[177]	19	[167]	18	[158]	43	[381]	0.44	[3.9]	1.8	[15.9]
XT080	XT080-003	3:1	59	[520]	48	[427]	43	[381]	39	[344]	165	[1459]	2.2	[19.5]	5.4	[47.8]
	XT080-004	4:1	70	[623]	58	[511]	53	[465]	48	[427]	165	[1459]	1.8	[15.9]	5.4	[47.8]
	XT080-005	5:1	65	[576]	53	[465]	47	[418]	43	[381]	165	[1459]	1.8	[15.9]	5.4	[47.8]
	XT080-007	7:1	63	[558]	50	[446]	45	[400]	40	[353]	165	[1459]	1.7	[15.0]	5.4	[47.8]
	XT080-008	8:1	62	[549]	49	[434]	45	[398]	42	[372]	165	[1460]	1.6	[14.2]	5.4	[47.8]
	XT080-010	10:1	54	[474]	48	[427]	45	[400]	43	[381]	165	[1459]	1.8	[15.9]	5.4	[47.8]
	XT080-015	15:1	90	[799]	78	[688]	69	[613]	63	[558]	175	[1552]	1.8	[15.9]	5.4	[47.8]
	XT080-020	20:1	92	[818]	88	[781]	81	[716]	75	[660]	175	[1552]	1.5	[13.3]	5.4	[47.8]
	XT080-025	25:1	87	[771]	83	[734]	76	[669]	69	[613]	175	[1552]	1.7	[15.0]	5.4	[47.8]
	XT080-030	30:1	100	[883]	90	[799]	85	[753]	78	[688]	175	[1552]	1.7	[15.0]	5.4	[47.8]
	XT080-040	40:1	96	[846]	92	[818]	90	[799]	88	[781]	175	[1552]	1.6	[14.2]	5.4	[47.8]
	XT080-050	50:1	90	[799]	87	[771]	85	[753]	83	[734]	175	[1552]	1.6	[14.2]	5.4	[47.8]
	XT080-070	70:1	88	[781]	85	[753]	83	[734]	82	[725]	175	[1552]	1.6	[14.2]	5.4	[47.8]
	XT080-080	80:1	84	[743]	80	[708]	78	[690]	74	[655]	175	[1549]	1.6	[14.2]	5.4	[47.8]
	XT080-100	100:1	72	[641]	67	[595]	63	[558]	61	[539]	175	[1552]	1.6	[14.2]	5.4	[47.8]

T_r = Rated output torque at rated speed for specific hours of life.
T_{peak} = Allowable momentary peak torque for emergency stop or heavy shock loading.
J = Mass moment of inertia reflected to the input shaft (including pinion assembly).
Specifications subject to change without notice.

MICRON

XTRUE™

True Planetary™ Gearheads

Performance Specifications

	Part Number	Ratio	20,000 Hour Life T_r (1000 rpm) Nm [in-lb]	T_r (2000 rpm) Nm [in-lb]	T_r (3000 rpm) Nm [in-lb]	T_r (4000 rpm) Nm [in-lb]	Tpeak Nm [in-lb]	J kg-cm² [in-lb-sec²×10⁻⁶]	Torsional Stiffness Nm/arc-min [in-lb/arc-min]
XT120	XT120-003	3:1	90 [799]	74 [650]	65 [576]	59 [520]	298 [2639]	4.4 [39]	17.4 [154.0]
	XT120-004	4:1	107 [948]	89 [790]	79 [697]	74 [650]	298 [2639]	3 [27]	17.4 [154.0]
	XT120-005	5:1	99 [873]	81 [716]	71 [632]	65 [576]	298 [2639]	2.9 [26]	17.4 [154.0]
	XT120-007	7:1	97 [855]	79 [697]	68 [604]	63 [558]	298 [2639]	2.8 [25]	17.4 [154.0]
	XT120-010	10:1	87 [771]	79 [697]	74 [650]	69 [613]	298 [2639]	2.5 [22]	17.4 [154.0]
	XT120-015	15:1	146 [1292]	119 [1050]	105 [929]	96 [846]	298 [2639]	2.9 [26]	17.4 [154.0]
	XT120-020	20:1	169 [1496]	139 [1227]	124 [1097]	114 [1013]	298 [2639]	2.9 [26]	17.4 [154.0]
	XT120-025	25:1	161 [1422]	130 [1152]	116 [1022]	106 [939]	298 [2639]	2.9 [26]	17.4 [154.0]
	XT120-030	30:1	180 [1589]	146 [1292]	129 [1143]	119 [1050]	298 [2639]	2.5 [22]	17.4 [154.0]
	XT120-040	40:1	187 [1654]	169 [1496]	150 [1329]	139 [1227]	298 [2639]	2.5 [22]	17.4 [154.0]
	XT120-050	50:1	179 [1580]	161 [1422]	142 [1254]	130 [1152]	298 [2639]	2.5 [22]	17.4 [154.0]
	XT120-070	70:1	176 [1561]	159 [1403]	140 [1236]	128 [1134]	298 [2639]	2.5 [22]	17.4 [154.0]
	XT120-100	100:1	120 [1059]	109 [966]	104 [920]	100 [883]	298 [2639]	2.5 [22]	17.4 [154.0]
XT160	XT160-003	3:1	317 [2806]	257 [2277]	228 [2016]	209 [1849]	876 [7750]	23 [204]	50.5 [446.9]
	XT160-004	4:1	371 [3280]	305 [2695]	272 [2407]	251 [2221]	876 [7750]	15 [133]	50.5 [446.9]
	XT160-005	5:1	350 [3094]	284 [2509]	251 [2221]	230 [2035]	876 [7750]	14 [124]	50.5 [446.9]
	XT160-007	7:1	344 [3048]	278 [2463]	246 [2174]	225 [1989]	876 [7750]	15 [133]	50.5 [446.9]
	XT160-010	10:1	222 [1961]	198 [1756]	185 [1635]	175 [1552]	876 [7750]	12 [106]	50.5 [446.9]
	XT160-015	15:1	508 [4498]	417 [3689]	370 [3271]	339 [3001]	876 [7750]	15 [133]	50.5 [446.9]
	XT160-020	20:1	513 [4544]	481 [4256]	428 [3791]	395 [3494]	876 [7750]	15 [133]	50.5 [446.9]
	XT160-025	25:1	492 [4358]	460 [4070]	407 [3605]	374 [3308]	876 [7750]	15 [133]	50.5 [446.9]
	XT160-030	30:1	562 [4971]	508 [4498]	455 [4024]	417 [3689]	876 [7750]	12 [106]	50.5 [446.9]
	XT160-040	40:1	536 [4739]	513 [4544]	500 [4423]	481 [4256]	876 [7750]	13 [115]	50.5 [446.9]
	XT160-050	50:1	515 [4553]	492 [4358]	479 [4237]	460 [4070]	876 [7750]	12 [106]	50.5 [446.9]
	XT160-070	70:1	509 [4507]	487 [4312]	474 [4191]	455 [4024]	876 [7750]	12 [106]	50.5 [446.9]
	XT160-100	100:1	306 [2704]	279 [2472]	265 [2342]	254 [2249]	876 [7750]	12 [106]	50.5 [446.9]

T_r = Rated output torque at rated speed for specific hours of life.

T_{peak} = Allowable momentary peak torque for emergency stop or heavy shock loading.

J = Mass moment of inertia reflected to the input shaft (including pinion assembly).

Specifications subject to change without notice.

How to order

XT 040 - 005 - 0 - RM040 - 22

Series
XT = XTRUE

Frame Size
040 = Size 40
060 = Size 60
080 = Size 80
120 = Size 120
160 = Size 160

Custom Options
0 = None
S = Special

Motor Specific

Ratio
003 = 3:1
004 = 4:1
005 = 5:1
007 = 7:1
008 = 8:1
010 = 10:1
015 = 15:1
020 = 20:1
025 = 25:1
030 = 30:1
040 = 40:1
050 = 50:1
070 = 70:1
080 = 80:1
100 = 100:1

Radial and Axial Load Ratings

XT040

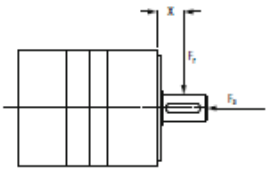

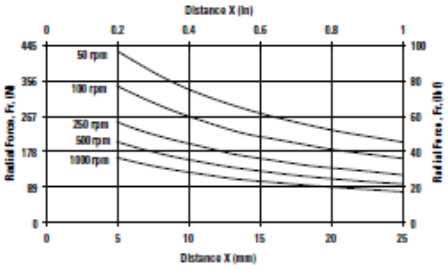

Speed rpm	Axial Load, F_a N [lb_f]
50	737 [166]
100	585 [132]
250	431 [97]
500	342 [77]
1000	272 [61]

XT060

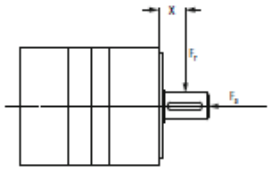

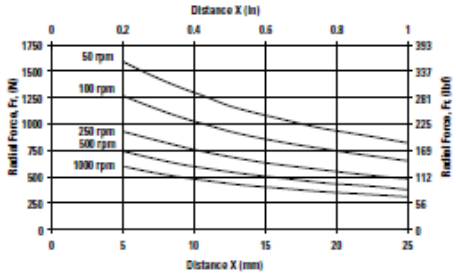

Speed rpm	Axial Load, F_a N [lb_f]
50	2542 [571]
100	2017 [454]
250	1486 [334]
500	1180 [265]
1000	936 [211]

XT080

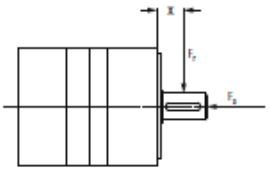

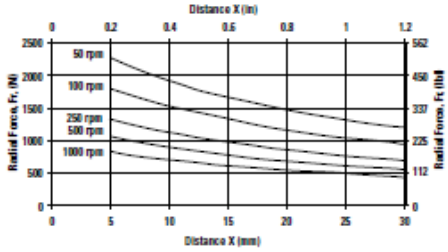

Speed rpm	Axial Load, F_a N [lb_f]
50	3780 [850]
100	3000 [675]
250	2211 [497]
500	1755 [394]
1000	1393 [313]

XT120

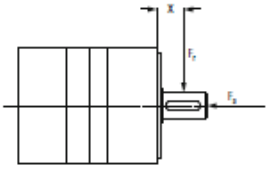

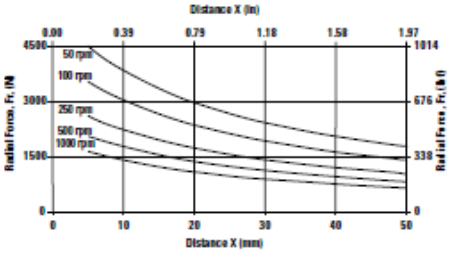

Speed rpm	Axial Load, F_a N [lb_f]
50	6894 [1550]
100	5471 [1230]
250	4034 [907]
500	3203 [720]
1000	2540 [571]

XT160

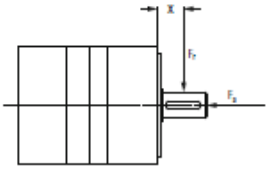

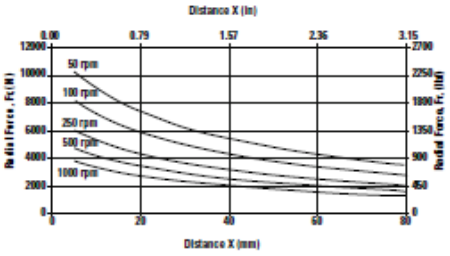

Speed rpm	Axial Load, F_a N [lb_f]
50	14,122 [3175]
100	11,209 [2520]
250	8260 [1857]
500	6556 [1474]
1000	5204 [1170]

These graphs display the allowable radial load at a given distance (X) from the mounting surface based on an L_{10} life of 20,000 hours for the mean output speed.

1010 T-Slotted Profile - 10 Series

- Compatible with all 10 Series fasteners
- Four open T-slots for mounting accessories
- 1010 is ideal for machine guards, sound enclosures, work benches, displays and panel mount racks
- Compatibility Code*: 6-10

VIBRATION PROOF™**

Part No.	1010
Material	6105-T5
Finish	Clear Anodized
Weight Per Foot	.5097 Lbs.
Stock Length (+/- .125")	97" - Part No. 1010-97 145" - Part No. 1010-145 242" - Part No. 1010-242
Moment Of Inertia	IX=.0442"⁴ IY=.0442"⁴
Estimated Area	.4379 Sq. In.

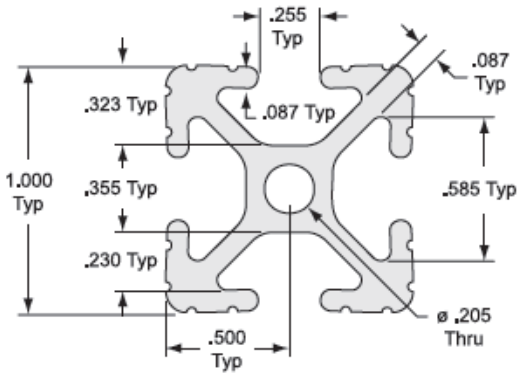

Quick Machining Reference

Machining Service	Service Number
Cut to Length	7005 (see page 563)
.218" Access Hole	7051 (see page 565)
Anchor Counterbore	7042 (see page 567)
Tap Profile End	7061 (see page 564)

Pre-Cut Lengths

48" - Part No. 1010-48	72" - Part No. 1010-72

- Pre-cut, ready to ship
- Cut to our standard tolerance of +/- .015"
- One part number, one price (includes cut charge)

Note: Look for the icon throughout the Fractional portion of this catalog. This icon points out all 10 Series compatible parts and accessories.

* See Compatibility Code information on page 152.

** See 2° Drop-Lock information on page 150.

Fractional

Torque Specifications

- **See table below for the amount of torque in foot-lbs. required to activate the 2° drop-lock feature for T-slotted profiles**
- **Nut and bolt combination is pre-loaded when tightened to the minimum torque rating**
- **When properly tightened, fasteners will not loosen even under heavy vibration**

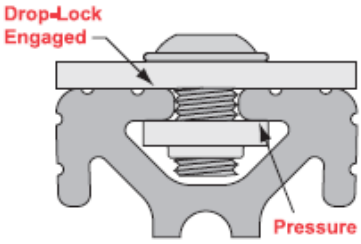

Part Number	Fastener Description	Tested Profile	Minimum Ft-lbs. Torque	Maximum Ft-lbs. Torque
3320	5/16-18 x 11/16 Flanged BHSCS & Economy T-Nut	1515	10.00	15.00
3325	5/16-18 x 3/4 Economy T-Slot Stud, Washer & Hex Nut	1515	25.00	30.00
3360	15 Series Anchor Fastener Assembly	1515-Lite	10.00	20.00
3380	15 Series End Fastener Assembly	1515-Lite	10.00	22.00
3321	1/4-20 x 1/2 Flanged BHSCS & Economy T-Nut	1010	4.00	6.00
3395	10 Series Anchor Fastener Assembly	1010	3.00	17.00
3381	10 Series End Fastener Assembly	1010	4.00	17.00

Fastener Application Tests

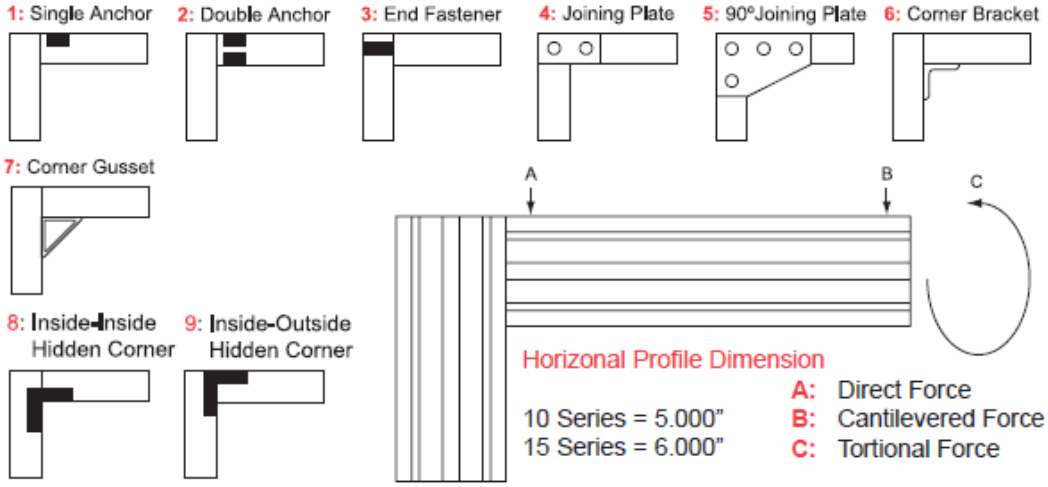

Fastener	1010 Profile			1515-Lite Profile			1515 Profile		
	A (lbs.)	B (lbs.)	C (Inch-lbs.)	A (lbs.)	B (lbs.)	C (Inch-lbs.)	A (lbs.)	B (lbs.)	C (Inch-lbs.)
1	500	250	180	950	625	540	950	1,000	700
2	900	250	260	1,200	700	1,150	1,200	1,200	2,000
3	450	200	325	1,000	500	680	1,000	820	1,150
4	175	50	400	225	200	1,000	225	200	1,100
5	175	50	500	250	200	1,120	250	200	1,260
6	325	75	180	375	225	500	575	225	500
7	325	220	260	375	750	500	575	750	500
8	N/A	N/A	N/A	50	50	50	N/A	N/A	N/A
9	N/A	N/A	N/A	240	220	240	N/A	N/A	N/A

Note: Plates, brackets and gussets were attached with 80/20® recommended bolt kits. Fasteners were tightened according to 80/20 torque specifications found at the top of the page.

Test results reflect the connection failure point. Loads at or above these points are not recommended.

80/20® Inc.
The Industrial Erector Set®
THE STANDARD

10 Series Profile Material Specifications

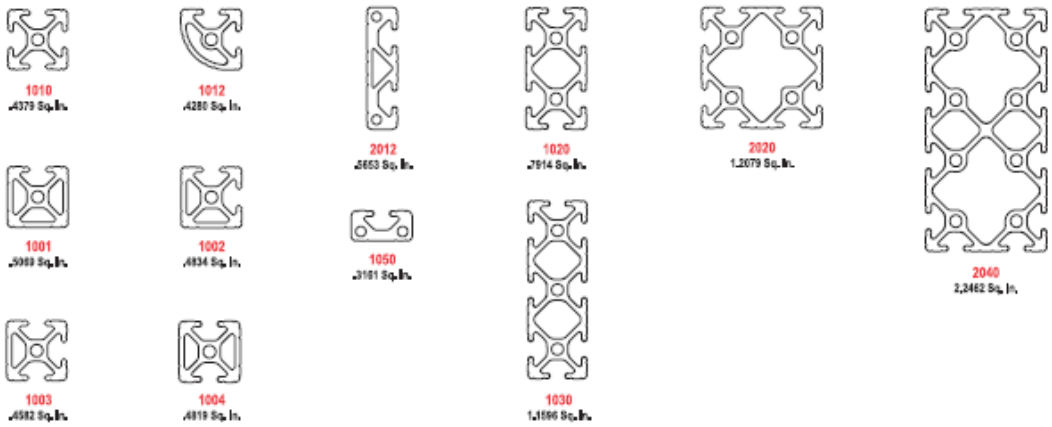

Compatibility Code*: 6-10

Part No.	1010	1001	1002	1003	1004	1012
Material	6105-T5 Aluminum					
Finish	Clear Anodize #204-R1					
Weight Per Foot	.5097 Lbs.	.5900 Lbs.	.5627 Lbs.	.5333 Lbs.	.5609 Lbs.	.4982 Lbs.
Stock Length **	97", 145", 242"	145" or 242"	145" or 242"	145" or 242"	145" or 242"	145" or 242"
Moment of Inertia	IX=.0442"⁴ IY=.0442"⁴	IX=.0493"⁴ IY=.0542"⁴	IX=.0492"⁴ IY=.0492"⁴	IX=.0441"⁴ IY=.0491"⁴	IX=.0443"⁴ IY=.0541"⁴	IX=.0400"⁴ IY=.0400"⁴
Estimated Area	.4379 Sq. In.	.5069 Sq. In.	.4834 Sq. In.	.4582 Sq. In.	.4819 Sq. In.	.4280 Sq. In.
Modulus of Elasticity	10,200,000 Lbs./Sq. In.					

Part No.	1050	2012	1020	1030	2020	2040
Material	6105-T5 Aluminum					
Finish	Clear Anodize #204-R1					
Weight Per Foot	.3679 Lbs.	.6580 Lbs.	.9212 Lbs.	1.3498 Lbs.	1.4060 Lbs.	2.6146 Lbs.
Stock Length **	145"	145"	97", 145", 242"	145" or 242"	145" or 242"	145" or 242"
Moment of Inertia	IX=.0074"⁴ IY=.0323"⁴	IX=.2253"⁴ IY=.0146"⁴	IX=.3078"⁴ IY=.0833"⁴	IX=.9711"⁴ IY=.1238"⁴	IX=.5509"⁴ IY=.5509"⁴	IX=3.5168"⁴ IY=1.0513"⁴
Estimated Area	.3161 Sq. In.	.5653 Sq. In.	.7914 Sq. In.	1.1596 Sq. In.	1.2079 Sq. In.	2.2462 Sq. In.
Modulus of Elasticity	10,200,000 Lbs./Sq. In.					

* See Compatibility Code information on page 152.
** For profile lengths other than stock length refer to page 563 for profile cut to length services.

APPENDIX D: SUPPORTING ANALYSIS AND CALCULATIONS

Aerobotik Wall Climber - FREE BODY DIAGRAM ANALYSIS

Conversion Factors

$LBFtoLBM = 32.2$ $[(lb_m \cdot ft)/(lb_f * s^2)]$ *Converts lbf to lbm*ft/s²*

Initial values

$MaxCupForce = 23$ $[lb_f]$ *At 65 psi of inlet pressure*

$Num_{cups} = 12$

$\mu_{cup} = 0.1$ *Friction coefficient of friction of the wall tread*

$\mu_{wheel} = 0.95$

$Normal_{force,bias} = 0.75$ *Percentage of Normal force on WHEELS*

$Weight = 55$ [lbf]

$Mass = 55$ [lbm]

$Wheelbase = 2$ [ft] *Wheelbase of the system*

$Height = 0.4$ [ft] *Height of the Center of Gravity relative to drive surface*

$Acceleration = 0$ $[ft/s^2]$

$Velocity = 4.5$ [ft/s] *Average human walking speed*

$Motor_{Torque,Output} = 0.5$ [N*m]

$$Wheel_{Dia} = \frac{1}{3} \text{ [ft]}$$

$Gearbox_{ratio} = 20$

Parameter Calculations

$$F_{suction,total} = MaxCupForce \cdot Num_{cups}$$

Bias Calculations

$$Normal_1 + Normal_2 = F_{suction,total} \cdot Normal_{force,bias}$$

Analysis Calculations

Sum of Moments about 1

$$\left[-F_{suction,total} + F_{cup,normal}\right] \cdot \frac{Wheelbase}{2} + Normal_2 \cdot Wheelbase - Weight \cdot Height = Mass \cdot Acceleration \cdot \frac{Height}{LBFtoLBM}$$

Sum of Moment about 2

$$\left[F_{suction,total} - F_{cup,normal}\right] \cdot \frac{Wheelbase}{2} - Normal_1 \cdot Wheelbase - Weight \cdot Height = Mass \cdot Acceleration \cdot \frac{Height}{LBFtoLBM}$$

Sum of Forces in the Y-direction

$$Force_{1,max} = Normal_1 \cdot \mu_{wheel}$$

$$Force_{2,max} = Normal_2 \cdot \mu_{wheel}$$

$$Friction_{cup} = F_{cup,normal} \cdot \mu_{cup}$$

$$Traction_{Force} - Friction_{cup} - Weight = Mass \cdot \frac{Acceleration}{LBFtoLBM}$$ *$Traction_{Force}$ is TOTAL wheel traction needed*

Design Factors

$$Traction_{Force,Wheel} = Force_{1,max} \cdot 2$$ *Max Traction Force is governed by the drive wheels with less Normal Force*

$$Traction_{Force,Motor} = Motor_{Torque,Output} \cdot Gearbox_{ratio} \cdot 0.73756 \cdot \frac{2}{\frac{Wheel_{Dia}}{2}}$$

$$Traction_{Ratio,Wheel} = \frac{Traction_{Force,Wheel}}{Traction_{Force}}$$ *Comparison of max wheel traction and actual drive traction*

$$Traction_{Ratio,Motor} = \frac{Traction_{Force,Motor}}{Traction_{Force}}$$ *Comparison of 'motor traction' and actual drive traction*

$$Torque_{perDriveset} = Traction_{Force} \cdot \frac{Wheel_{Dia}}{2 \cdot 2}$$ *Value is divided by 2 because two motors are used for driving*

$$Gear_{Ratio} = \frac{Torque_{perDriveset}}{Motor_{Torque,Output} \cdot 0.73756}$$ *0.73756 is the conversion factor from N*m to lbf*ft*

$$Motor_{RPM} = \frac{Velocity}{\pi \cdot Wheel_{Dia}} \cdot Gearbox_{ratio} \cdot 60$$ *Uses a desired walking speed and chosen gear ratio to find motor RPM*

Unit Settings: SI C kPa kJ mass deg

Acceleration = 0 [ft/s^2]
$F_{cup,normal}$ = 69 [lb_f]
$Gear_{Ratio}$ = 13.99
$Motor_{RPM}$ = 5157 [RPM]
$Normal_{force,bias}$ = 0.75
$Traction_{Force}$ = 61.9 [lb_f]
$Traction_{Force,Wheel}$ = 175.8
$Traction_{Ratio,Wheel}$ = 2.839

$Friction_{cup}$ = 6.9 [lb_f]
$F_{suction,total}$ = 276 [lb_f]
MaxCupForce = 23 [lb_f]
$Motor_{Torque,Output}$ = 0.5 [N*m]
Num_{cups} = 12
$Traction_{Force,Motor}$ = 88.51
$Traction_{Ratio,Motor}$ = 1.43
Weight = 55 [lbf]

Initial Drive Shaft Sizing

length of 6 in

$M_a = 115$ Total Moment at Bearing, lbf-in

$T_m = 300$ Torque, lbf-in

$K_f = 1.7$ Fatigue Stress Concentration Factor

$K_{f,s} = 1.4$ Factor of Safety

$S_{u,t} = 82000$ Ultimate tensile strength of 1045 steel, psi

$S_e = k_a \cdot k_b \cdot kk_f \cdot S_{u,t}$ Endurance Limit

$k_a = 2.7 \cdot 167^{-0.265}$ Surface Factor

$k_b = 0.9$ Size Factor

$kk_f = 0.5$

$n = 1.5$

$$d_2 = \left[\left(\frac{2 \cdot K_f \cdot M_a}{S_e} + \frac{(3 \cdot (K_{f,s} \cdot T_m)^2)^{0.5}}{S_{u,t}}\right) \cdot \frac{16 \cdot n}{\pi}\right]^{(1/3)}$$ Shaft Diamter, in

Unit Settings: SI C kPa kJ mass deg

$d_2 = 0.5689$ [in]	$kk_f = 0.5$	$k_a = 0.6956$	$k_b = 0.9$
$K_f = 1.7$	$K_{f,s} = 1.4$	$M_a = 115$ [lb-in]	**n = 1.5**
$S_e = 25667$	$S_{u,t} = 82000$	$T_m = 300$	

Stress Analysis on Solidworks SimulationXpress

SUCTION CUP BRACKET

25 lb was loaded onto the suction cup mounting hole and safety factor came out to be 7.

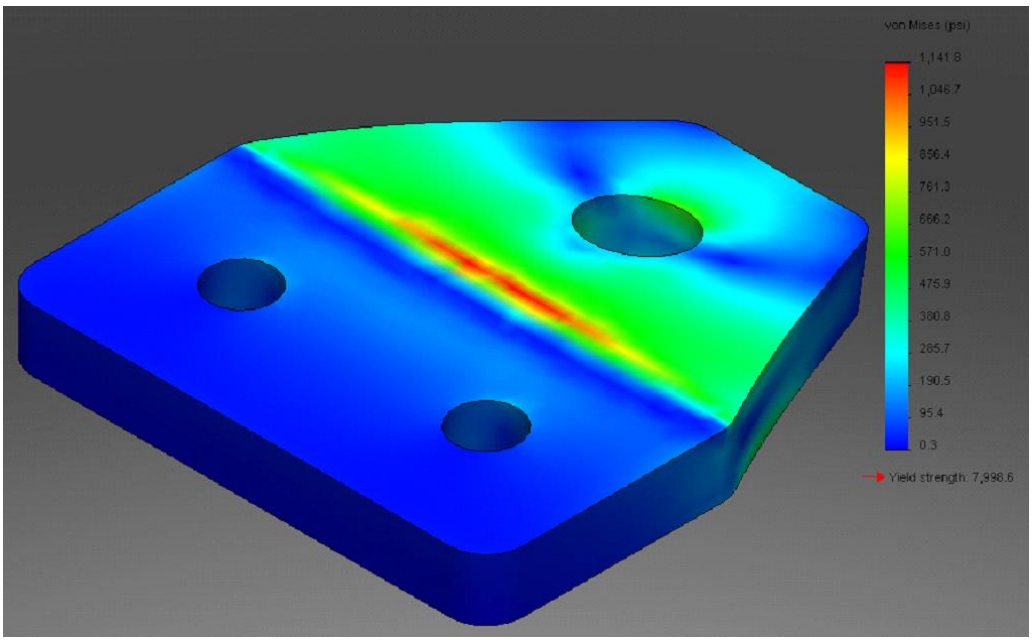

Figure 60. Von Mises stress analysis on the bracket.

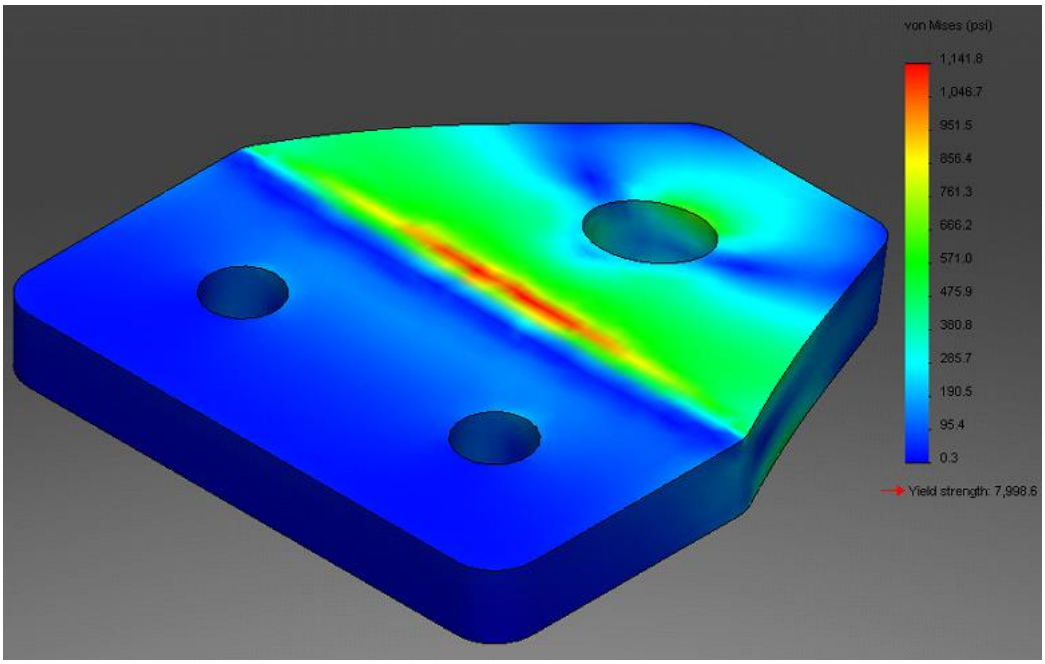

Figure 61. Displacement analysis on the bracket.

DRIVE SHAFT

136.7 lb was loaded onto the drive shaft and safety factor came out to be 5.6.

Fixture name	Fixture Image	Fixture Details
Fixed-2	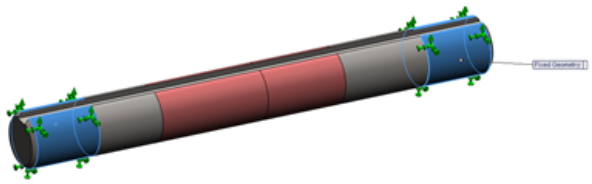	**Entities:** 2 face(s) **Type:** Fixed Geometry

Load name	Load Image	Load Details
Normal Force	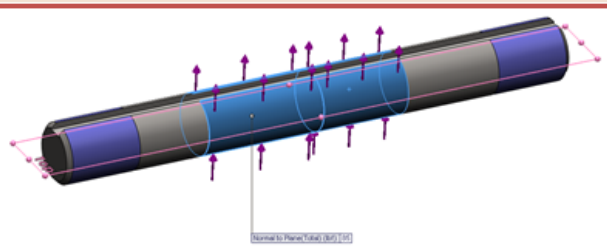	**Entities:** 2 face(s), 1 plane(s) **Reference:** Top **Type:** Apply force **Values:** **85 lbf**
Friction Force	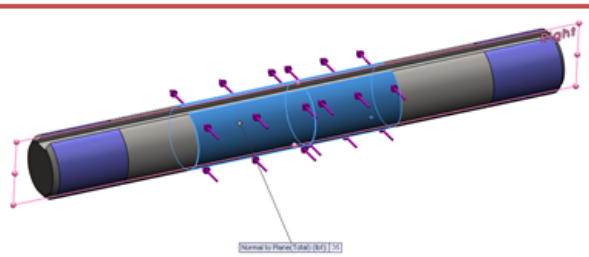	**Entities:** 2 face(s), 1 plane(s) **Reference:** Right **Type:** Apply force **Values:** **-35 lbf**
Chain Loads	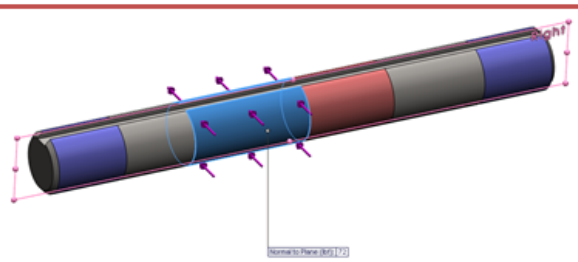	**Entities:** 1 face(s), 1 plane(s) **Reference:** Right **Type:** Apply force **Values:** **-72 lbf**

Figure 62. Loads and fixtures of the drive shaft.

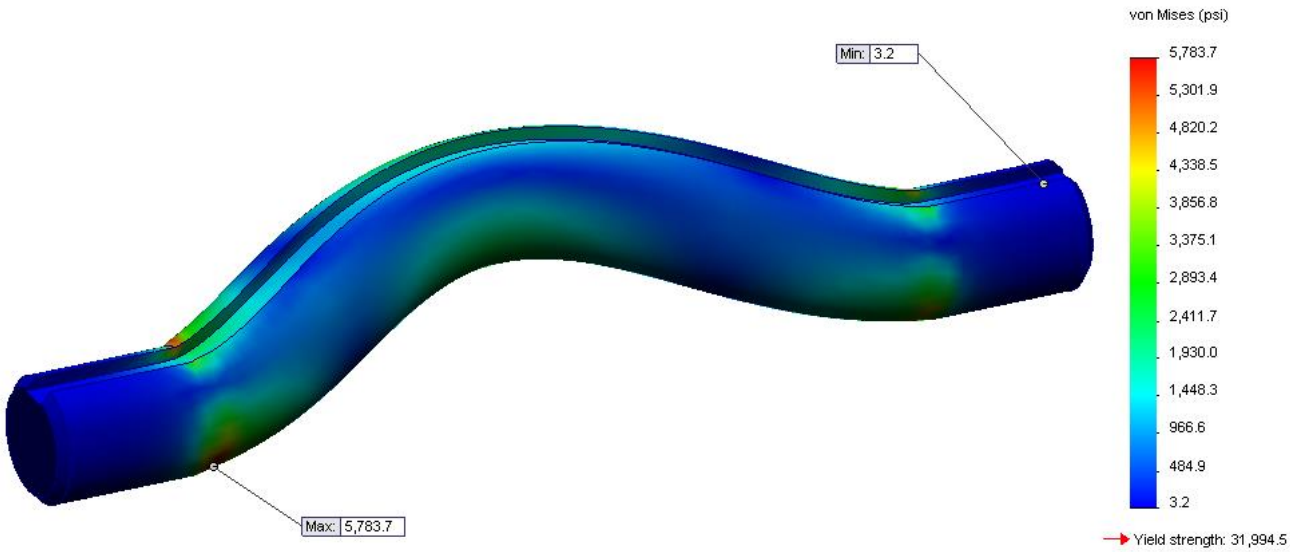

Figure 63. Von Mises stress analysis on the drive shaft.

Figure 64. Displacement analysis on the drive shaft.

Name	Type	Min	Max
Stress	VON: von Mises Stress	2.85721 psi Node: 11178	5826.58 psi Node: 10515
Keyed shaft-SimulationXpress Study-Stress-Stress			

Name	Type	Min	Max
Displacement	URES: Resultant Displacement	0 in Node: 7	0.000242974 in Node: 9594
Keyed shaft-SimulationXpress Study-Displacement-Displacement			

Name	Type
Deformation	Deformed Shape
Keyed shaft-SimulationXpress Study-Displacement-Deformation	

Name	Type	Min	Max
Factor of Safety	Max von Mises Stress	5.49112 Node: 10515	11197.8 Node: 11178
Keyed shaft-SimulationXpress Study-Factor of Safety-Factor of Safety			

Figure 65. Drive shaft SimulationXpress results.

APPENDIX E: DESIGN RESOURCES

WRITTEN REFERENCES

(2013). Retrieved from Industrial Climbing Machines: http://www.icm.cc/about.php

Creedy, A. P. (1984). Skid Steering of Wheeled and Tracked Vehicle.

MACS: Multifunction Automated Crawling System. (2013). Retrieved from JPL: http://www-robotics.jpl.nasa.gov/tasks/showTask.cfm?TaskID=114&tdaID=900001

Mel Siegel, P. G. (n.d.). Robotic Assistants for Aircraft Inspectors.

Shigley, Joseph Edward, and Charles R. Mischke. *Mechanical engineering design*. 5th ed. New York: McGraw-Hill, 1989. Print.

Solc, Frantisek, and Jaroslav Sembera. "Kinetic Model of a Skid Steered Robot." *ISPRA'08 Proceedings of the 7th WSEAS International Conference on Signal Processing, Robotics and Automation* (2008): 61-65. World Scientific and Engineering Academy and Society (WSEAS), 20 Feb. 2008. Web.

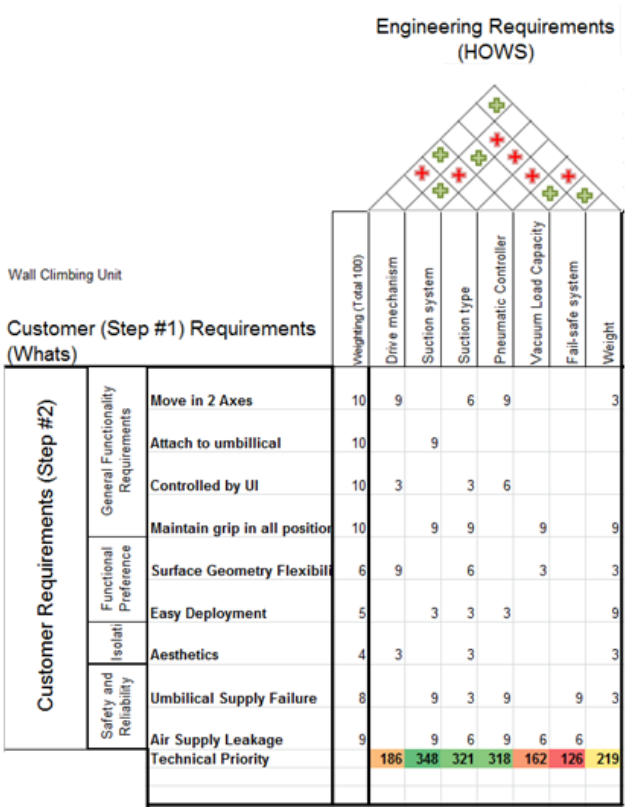

Figure 66. Quality Function Deployment chart.
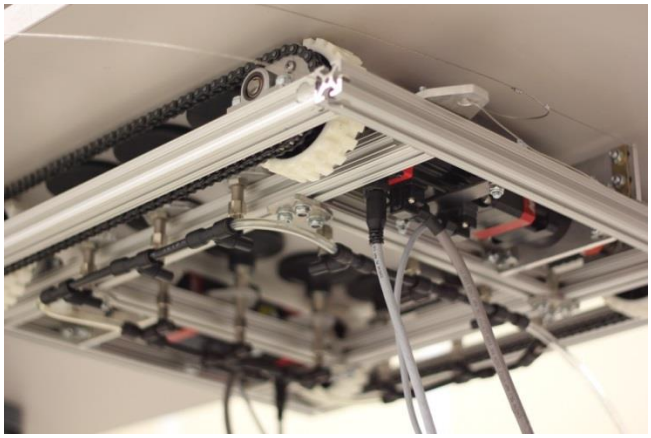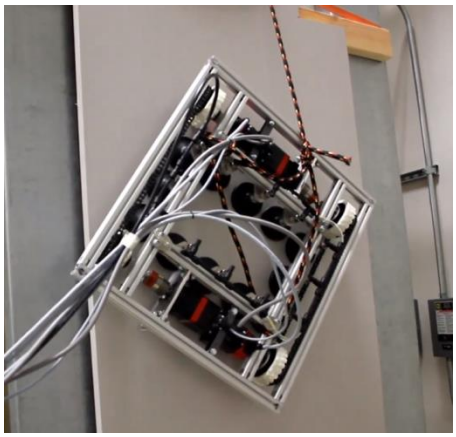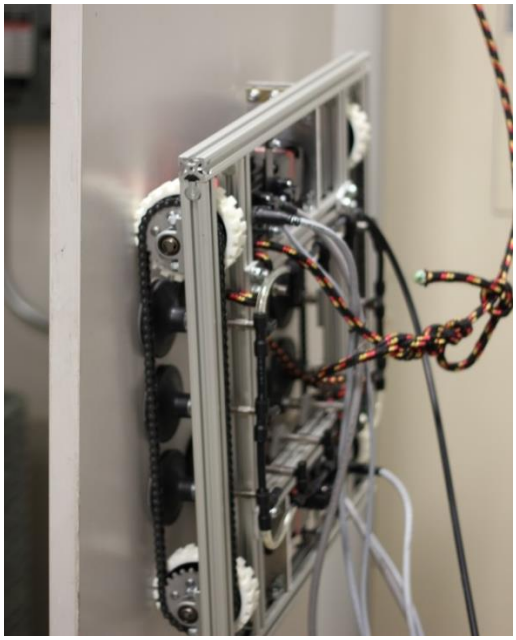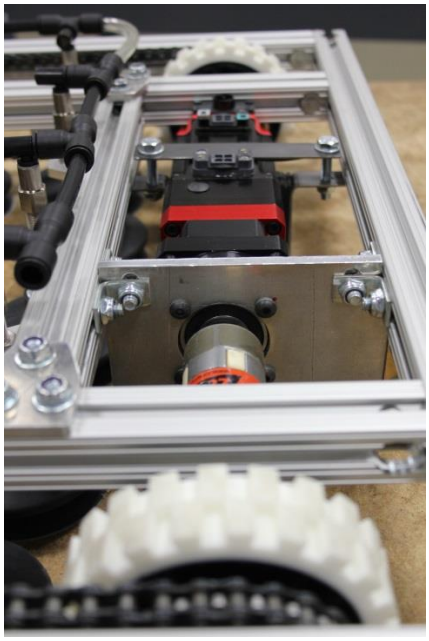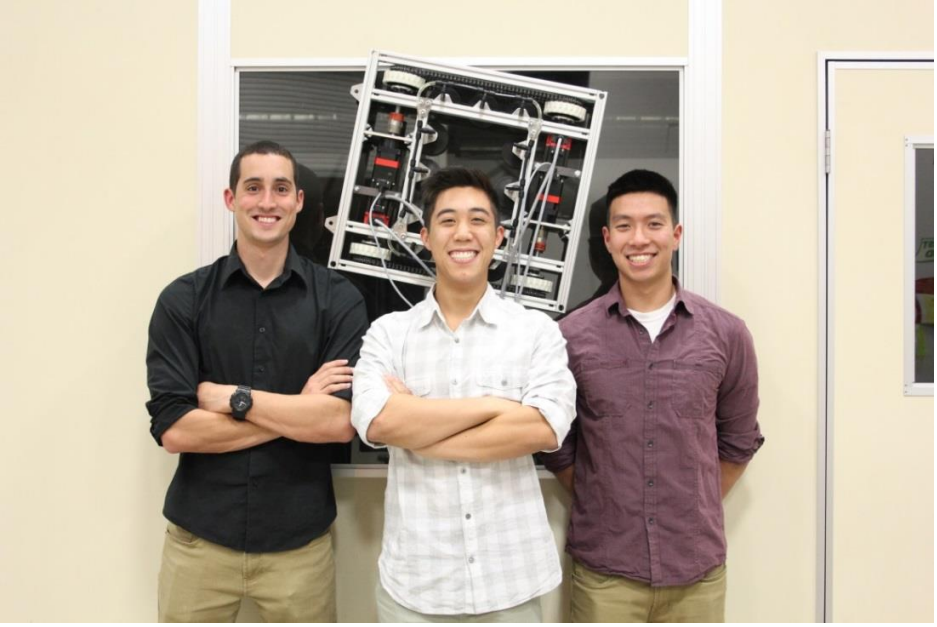
ADDITIONAL PICTURES